2022

SENSTIVE ENANTIOMERIC ANALYSIS OF N-ACYL HOMOSERINE LACTONES IN BACTERIAL MATRICES

Abiud E. Portillo

SENSTIVE ENANTIOMERIC ANALYSIS OF N-ACYL HOMOSERINE LACTONES IN BACTERIAL MATRICES

by

ABIUD E PORTILLO

Presented to the Faculty of the Graduate School of

The University of Texas at Arlington in Partial Fulfillment

of the Requirements

for the Degree of

DOCTOR OF PHILOSOPHY

THE UNIVERSITY OF TEXAS AT ARLINGTON

December 2022

Acknowledgments

I could not start this section until first mentioning my mentor, guide and professor Dr. Daniel W. Armstrong. The opportunity he gave me to work in his lab and learn from him as much as I could has undoubtedly increased the number of useful tools I have in my utility box. From making a figure in an article speak for itself, to estimating the resolution between peaks in chromatogram with pinpoint accuracy, to even being a great salesman. I owe my abilities in this field to his never-ending interest in my growth as a teacher, PhD student and hopefully an expert in this art.

I thank Dr. Kevin Schug who first introduce me the world of analytical chemistry and my first GC in his Instrumental Analysis class and for giving me the ability to work with top-of-the-line analytical equipment. To Dr. Subhrangsu Mandal I give my many thanks for it was his Metabolism and Regulation course which sparked my interest in continuing and switching my B.S. degree to Biochemistry. I am thankful to Dr. Morteza Khaledi for also taking time to become a part of my graduate committee and his support during my PhD program.

I thank Dr. Choyce Weatherly and Dr. Diego Lopez which in a difficult and undecisive time, led me towards the path of analytical chemistry and ultimately Dr. Armstrong's group. I would like to give my sincerest thanks to Dr. Jimmy Rogers, Dr. Peter Kroll and Dr Frank Foss who one day believed in my abilities to become a PhD candidate and recommended me for the chemistry graduate program at The University of Texas at Arlington. A special thanks to Anne Ellis, the best assistant that Dr. Armstrong could have, for she gave me the confidence and guidance to keep going during my final weeks in this program.

To my friends and lab-mates that I made during my years in this program, I give them my sincerest thanks. To Beth for working hard alongside me on our first project as graduate students. To Michael who was a great person to speak to when stuck on research. To Dr. Farooq Wahab for being very approachable and understanding as well as intelligent when writing alone became very difficult, with sometimes just needing to go out for lunch with him to refresh the brain. To Arzoo, Saba and Sepideh for being the nicest people to talk to when down

and believing in my abilities as a graduate student. To Dr. John Lang thanks for the very insightful questions about my research. Sincere thanks to Dr. JT Lee for our very nice conversations about life, chiral preparatory chromatography, and nice sounding speakers. I give thanks to Josh for always making the meanest and spiciest chicken to get you through an afternoon of hard writing. I greatly appreciate Ondrej, Umang and Sam for being the best team members as well as great friends when graduate life was just a bit too much to manage alone.

To my family, that always offered a plate of food, a roof and as much love necessary to get through to the next day. I greatly thank my church; The Light of the World; which endowed me with the morals and ideas I used throughout my life, with the Apostle of Jesus Christ, Naason Joaquin Garcia, showing me not only to be a good person but to always be of great help to my community. To my wife and daughter, Yared and Rachel, my life, my reason for working hard and never allowing anything to make me give up, who suffered, cried, smiled and laughed with me every step of the way here.

September 11, 2022

Abstract

SENSTIVE ENANTIOMERIC ANALYSIS OF N-ACYL HOMOSERINE LACTONES IN BACTERIAL MATRICES

Abiud Portillo, PhD

The University of Texas at Arlington, 2022

Supervising Professor: Daniel W. Armstrong

Communication between unicellular organism has long been studied with many facets yet to be discovered. A specific type of communication in gram-negative bacteria is quorum sensing (QS). *N*-acyl homoserine lactones (N-HLs) are the molecular signals in this process. At a critical concentration of N-HLs, all bacteria of the same population stop behaving like individuals and in a concerted manner induce a specific gene expression which ultimately benefits the entire population in major. This phenomenon has been coined with the term quorum sensing with the main signaling molecules dubbed L-*N*-acyl homoserine lactones (L-N-HL). Quorum sensing signaling pathways have their influence in a vast majority of realms, from nosocomial bacterial infections, to crop debilitation, from exchange of genetic code and food spoilage to microbial warfare and even symbiosis. For these reasons and more the study of bacterial signaling in quorum sensing has long been explored. It has however, long been disregarded the possibility of the production of the enantiomeric counterpart of these signaling molecules; D-*N*-acyl homoserine lactones (D-N-HL). For this reason, almost exclusively, has the analysis, detection and characterization of N-acyl homoserine lactones (N-HLs) been treated in an achiral fashion. To analyze these N-HLs *in vivo* another hurdle manifest as the complex biological and environmental matrices in which these signaling molecules are found. This dissertation aims to 1) develop proper, sensitive, selective and specific chiral chromatographic methods for the comprehensive analysis of D,L-N-HLs and their extraction from representative difficult matrices and 2) supply a myriad of studies in which these methods are a applied to bacterial matrices, displaying their efficacy the chiral analysis of both L- and D-N-HL *in vivo*.

New methods involving high performance liquid chromatography and gas chromatography coupled to mass spectrometry (MS) were developed and evaluated for the chiral analysis of the three main classes of D,L-N-acyl homoserine lactones (N-HL). A derivatization method using *N*,*O*-bis(trimethylsilyl)trifluoroacetamide (BSTFA) with 1% v/v trimethylchlorosilane (TMCS) was adapted for the analysis of the heat labile N-3-hydroxyacyl and N-3-oxoacyl homoserine lactones by gas chromatography. This method was used to analyze and detect L- and D-N-HL in bacterial cultures of *B. cepacia* and *V. fischeri* with limits of detection down to a ng/mL. CHIRALPAK IC-3s and an achiral stationary phase column were placed in tandem for the comprehensive analysis of all N-HL by LC. The first comprehensive chiral methods were developed for LC-MS/MS and GC-MS/MS for the analysis of trace-mounts of N-HL in bacterial matrices. Proper recovery studies on D,L-N-HL were performed by coupling to hydrophilic-lipophilic balanced solid phase extraction (HLB-SPE) phases. The utility of these HLB-SPE phases is their broad polarity selectivity as well as their robustness with aqueous samples. Percent recoveries for D,L-N-HL ranged from 80% to 105% recovery when using LC-MS/MS as well as obtaining method LODs to the level of a pg/mL. Using these simple, robust and comprehensive methods we were able to identify and quantify various L- and D-N-HL, that were expected as well as previously unreported, in bacterial matrices of *Pseudomonas aeruginosa*, *Burkholderia cepacia*, *Pectobacterium atroscepticum* and *Vibrio fischeri*.

Table of Contents

List of Illustrations

List of Tables

Chapter 1

Introduction

1.1 Microbial Signaling

Unicellular organisms are capable of surviving in their environment without the aid of another being. However, the benefits that come with participating in an organized, social, biological system, in most cases, greatly outweigh the costs [1]. The production of diffusible molecules allows communication of the microbe's presence it's population as well as give information about itsenvironmental conditions [2, 3]. Signaling molecules can be quite diverse, from small diffusible molecules, functionalized fatty acids as well as small to medium chain peptidesN-acyl homoserine lactones (HLs) are a particular type of diffusible signalingmolecules that have recently piqued the interest of researchers due to their intimate relationships with agriculture, symbiosis and nosocomial settings [5-8].

1.2 N-acyl Homoserine Lactones in Quorum Sensing

N-acyl homoserine lactones (N-HLs) are one of the main signaling molecules produced almost exclusively by gram-negative bacteria and are involved in a process called autoinduction [9]. In the process of autoinduction, an autoinducer (HL) signal, produced by the bacteria, allows the population to keep track of its size. As the population grows, the concentration of autoinducer increases. The moment a critical concentration of autoinducer is produced within the effective population, a concerted expression of some phenotype will occur. This process was first described in the bioluminescent bacteria, *Photobacteria fischeri* now called *Vibrio fischeri*. [10]. This phenomenon was later termed "quorum sensing" (QS) fittingly named due to the cooperative nature of the system [9]. This system has been frequently described as a two-component system due to its reliance on a pair of proteins [11, 12]. As described, there are "transmitter" or synthase proteins that produce the HL and "sensors" or receptor proteins that take the signal and induce transcription of genetic code [12]. It was first discovered in *V. fischeri* that a HL, L-*N*-3-oxo-hexanoyl homoserine lactone, was the autoinducer signal involved in regulating expression of the *lux* operon and consequently bioluminescence [11, 13]. However, it was not until 1992, in *Erwinia carotovora* that attention was given to the chirality of these

autoinducers. A purified extract from *E. carotovora* was analyzed by spectro-polarimetry, identifying that the produced HL was of the L-configuration [14].

1.2.1 The Biosynthesis and Signaling Mechanism of L-N-acyl Homoserine Lactones

In L-*N*-acyl homoserine lactones (L-N-HLs) α-amino-butyrolactone moiety is conserved with all variations occurring in the acyl chain on the lactone's α-amino group. *S*-adenosyl-L-methionine (SAM, a product of L-methionine) is the L-N-HL precursor that forms the homoserine lactone moiety. While an acyl carrier protein (ACP) charged with a fatty acid methyl ester group forms the acyl chain of the L-HLs. In most instances, the HLs produced by gram-negative bacteria have acyl chains that can vary in length from four carbon chains to 14 carbons and recently can be found unsaturated [15]. In rare cases 16 to 20 carbon lengths have been observed [16, 17]. Functionality on the third carbon of the acyl chain has also been commonly observed. Either a carbonyl group or a hydroxyl group have been found to exist on the acyl chain however an unfunctionalized acyl group is also a common form for these HLs [9]. The hydroxyl functionalized N-HLs have a second chiral center on the acyl chain thus four stereoisomers are possible. . Below are structures of the common HLs observed from bacterial matrices.

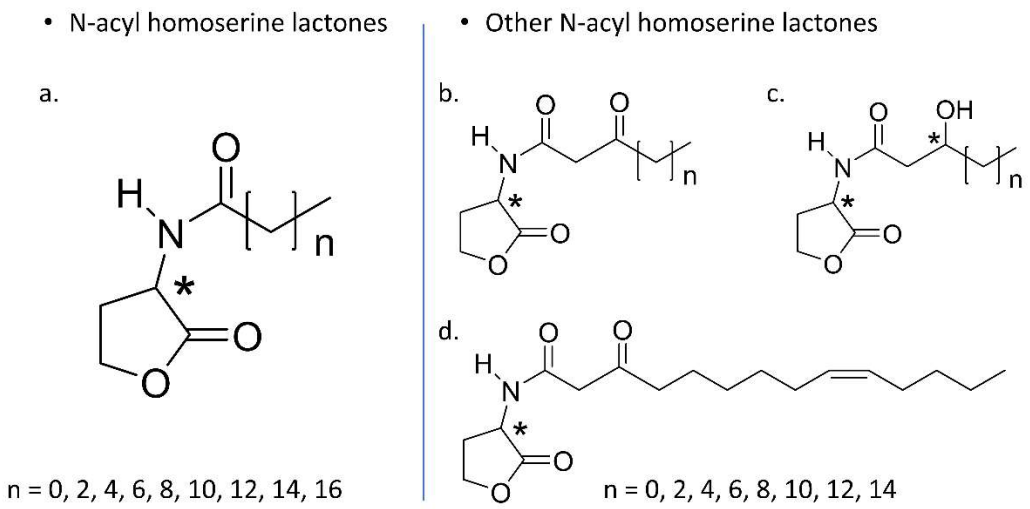

Figure 1-1. Structures of common *N*-acyl homoserine lactones; **a.** D,L-*N*-acyl homoserine lactones (DL-AHL), **b.** D,L-*N*-3-oxoacyl homoserine lactones (D,L-OHL), **c.** D,L-*N*-[(RS)-3-hydroxyacyl] homoserine lactones (D,L-HHL), **d.** D,L-*N*-3-oxoacyl homoserine lactone with unsaturated acyl chain. Asterisks (*) illustrate a center of chirality in the structure. The letter **n** denotes the number of carbons added to the base structure.

It was proposed that the majority of HLs are synthesized by LuxI-type homologue synthase proteins. Fittingly named due to its discovery from the *V. fischeri lux* operon system [11, 18]; the LuxI protein is responsible for the synthesis of *N*-3-oxohexanoyl homoserine lactone (O-C6). In the gram-negative human pathogen, *Pseudomonas aeruginosa*, there are two well-known synthase proteins that produce two distinct homoserine lactones. The LasI protein is responsible for the synthesis of *N*-3-oxododecanoyl homoserine lactone (O-C12) and the RhlI

protein responsible for the synthesis of *N*-butyryl homoserine lactone (A-C4) [11]. This species is revisited in chapter 6 for the analysis of its produced HLs. In *Agrobacterium tumefaciens* the TraI protein synthesizes *N*-3-oxooctanoyl homoserine lactone (O-C8) and is seems to be responsible for regulating conjugation (DNA transfer) between cells of *A. tumefaciens*. Interestingly the ExpI and CarI proteins found in the plant pathogen *Erwinia carotovora* both produce an identical autoinducer, O-C6. In this species O-C6 is seen to regulate virulence factors in one system and antibiotic production in another [16]. These synthesis proteins are said to belong to a single family of synthases called the LuxI family. It has been shown that they all share a conserved threonine residue at the 143 position whose role seems to stabilize ACP with carbonyls on their acyl chain. The LuxI family is not the only family of synthase proteins however that are involved in HL synthesis and by consequence QS regulation. A small family called the AinS-type proteins also direct the synthesis of N-HLs, specifically A-C8-HL. A specific characteristic of the AinS-type proteins is the ability to use both ACP (like LuxI-type proteins) and acyl-coenzyme-A groups equally. However, in both cases SAM is still the contributor of the homoserine lactone group. However, synthesis is only part of the signaling system, with most synthase proteins being part of a receptor-synthase pair. In the case of the *lux* operon system the complete QS sensor would be denoted as LuxR-LuxI, LuxR taking the role of a transcriptional activator; producing the phenotype of bioluminescence the moment it binds to its respective HL signal [19, 20]. The variety and ever-growing intricacy of bacterial internal communication involving HLs has prompted the development of various analytical methods for their analysis and quantitation from their endogenous matrices.

1.3 role of Analytical Methods in The Hunt for N-acyl Homoserine Lactones The

1.3.1 *Biological Sensors for Detection of N-acyl homoserine lactones*

N-acyl homoserine lactones are often produced at trace level amounts. This places a limitation on their detection having to rely on highly sensitive techniques for their analysis. In the advent of HLs analysis, biological sensors were developed and routinely used for observing the presence of these autoinducers [21-25]. These biosensors are commonly employed by first extracting HLs from their respective matrix and once a reasonable purification step is used, the extract is overlaid over solid growth media doped with the whole-cell bacteria sensor of choice [24]. Choosing the proper biosensor usually depends on the HL that is expected to be present in the matrix analyzed. In 1998 *luxCDABE* reporter sensors were constructed to aid in cell density studies by utilizing the HLs that activate it through bioluminescence detection [25]. These sensors were also tested with a range of N-HLs types to determine what, if any, other N-HLs also activate them apart from their native N-HL. Native N-HLs always displaythe most activity of the sensor followed by chain lengths close in length with the same functionality type. This reporter responds well to OHLs with O-C6 (the cognate) giving the most activation. Other types of biological sensors for the detection of HLs are CV026 from *Chromobacterium violaceum* that responds to small chain unfunctionalized HL by producing a violet pigment and NTL_4 from *Agrobacterium tumefaciens* which react to medium chain length HL to produce a blue pigment due to *lacZ* operon fusion [26, 27]. Using bioreporters alone is non-specific and does not give any information on how many HL are present in one matrix. For that reason, TLC is frequently coupled with bioreporter sensors allowing the possible detection of various HL homologues. It has been stated that TLC combined with bioreporters can and in many cases does lead to ambiguous results. The possibility of two very similar migrating HL that do not separate on TLC is high when analyzing bacteria that produce different HL types. Also, working with very complex matrices that have not been purified adequately can lead to unwanted coelution with target HLs giving difficult to reproduce data [28-30]. It is without question that more robust and selective methods are necessary for the analysis of HL from complex matrices.

1.3.2 *Current Chromatographic techniques for the analysis of N-acyl homoserine Lactones Do Not Consider Their Chirality*

As the study of bacterial communication and quorum sensing began to show its significance in agricultural and medical settings so did the development of more adequate analytical techniques for the analysis of N-HLs. The more modern used analytical methods that have been developed for analysis of HLs are GC, LC and SFC and coupled with various mass spectrometer detectors, from single quadrupole MS to FTICR-ESI-MS [31-37]. Chromatography allows the separation of N-HLs by chain length due to their differences in polarity. In the more common gas chromatography methods the wall coated polydimethylsiloxane stationary phases, e.g. 5% phenyl-dimethylpolysiloxane, are commonly used to achieve separation [31, 32, 38, 39]. In the case of liquid chromatography analysis, the common stationary phase used that permits adequate separation of the HL homologues are C18 functionalized silica particle columns working in the reverse phase mode [34, 40-42]. In supercritical-fluid chromatography method porous graphitic carbon was the stationary phase of choice for the separation of homologous compounds [35]. As can be seen, a disregard for the chirality of N-HLs was widespread and rarely was a chiral stationary phase used when analyzing HL from natural environments. In one study chiral GC was implemented using a heptakis-(2,3-di-*O*-acetyl-6-*O*-*t*-butyldimethyl-silyl)-β-cyclodextrin. The study was monitoring the stereoselective uptake of HLs by barley plants through artificial supplementation with racemates. Their study showed that the plants slightly favor the uptake of the L- isomer displayed by measuring peak areas of peaks on the chiral GC chromatogram [5]. Even though a chiral method was used, the production of D- and L-N-HL was not the scope of this study. It wasn't until 2009 that a chiral GC analysis was applied to a bacterial growth. In this study a broth culture of *Burholderia cepacia* was analyzed and two HLs were observed, C8 and C10-HL. Interestingly they also detected D-C10-HL at reasonable amounts. It was posited at this moment that the production of the D-HL can be due to microbial biosynthesis using D-amino acids as precursors for their synthesis [43]. It was evident that there is a need for comprehensive and sensitive chiral methods.

1.4 Research Objectives and Organization of the Dissertation

The motivation driving the research described in this dissertation is the complete lack of comprehensive chiral methods for the analysis of N-HLs. This being necessary since there is evidence that not only the naturally occurring L-N-HL is produced but also the possibility of D-HL being biosynthesized. In Chapter 2 a headspace study of chiral interconversion of *N*-acetyl-homocysteine thiolactones is evaluated. This chapter gives some insight on the thermodynamics of racemization of this similar type of compound to *N*-acyl-homoserine lactones. Chapter 3 focuses on the chiral analysis of HL standards. The two highly sensitive methods of LC-MS and GC-MS are coupled with chiral stationary phases to produce these more advanced enantiomeric methods. The focus of Chapter 4 is on the investigation of the two classical N-HL producing bacteria *Burkholderia cepacia* and *Vibrio fischeri*. A Chiral analysis is conducted for the HL produced with a biosynthetic pathway assay explored with the use of methionine supplemented minimal nutrient media. Chapter 5 outlines the development of a highly specific, highly sensitive and comprehensive method for the analysis of HL using GC-MS/MS and LC-MS/MS. Chapters 6 and 7 focus on the application of the newly developed GC-MS/MS and LC-MS/MS methods for the chiral profiling of HL from *Pseudomonas aeruginosa*, *Agrobacterium atroscepticum*, *Pseudomonas fluorescens*, *Pseudomonas putida*, *Burkholderia cepacia* and *Vibrio fischeri*.

1.5 References

[1] He, Y.-W., Deng, Y., Miao, Y., Chatterjee, S., Tran, T. M., Tian, J., Lindow, S., DSF-family quorum sensing signal-mediated intraspecies, interspecies, and inter-kingdom communication. *Trends in Microbiology*. 2022.

[2] Taga, M. E., Bassler, B. L., Chemical communication among bacteria. *Proceedings of the National Academy of Sciences*. 2003, *100*, 14549-14554.

[3] Tomasz, A., Control of the competent state in Pneumococcus by a hormone-like cell product: an example for a new type of regulatory mechanism in bacteria. *Nature*. 1965, *208*, 155-159.

[4] Yashiroda, Y., Yoshida, M., Intraspecies cell–cell communication in yeast. *FEMS Yeast Research*. 2019, *19*, foz071.

[5] Götz, C., Fekete, A., Gebefuegi, I., Forczek, S. T., Fuksová, K., Li, X., Englmann, M., Gryndler, M., Hartmann, A., Matucha, M., Uptake, degradation and chiral discrimination of N-acyl-D/L-homoserine lactones by barley (Hordeum vulgare) and yam bean (Pachyrhizus erosus) plants. *Analytical and bioanalytical chemistry*. 2007, *389*, 1447-1457.

[6] Luo, L.-m., Wu, L.-j., Xiao, Y.-l., Zhao, D., Chen, Z.-x., Kang, M., Zhang, Q., Xie, Y., Enhancing pili assembly and biofilm formation in Acinetobacter baumannii ATCC19606 using non-native acyl-homoserine lactones. *BMC microbiology*. 2015, *15*, 1-7.

[7] dos Santos Lima Fagotti, D., Abrantes, J. L. F., Cerezini, P., Fukami, J., Nogueira, M. A., Del Cerro, P., Valderrama-Fernández, R., Ollero, F. J., Megías, M., Hungria, M., Quorum sensing communication: Bradyrhizobium-Azospirillum interaction via N-acyl-homoserine lactones in the promotion of soybean symbiosis. *Journal of basic microbiology*. 2019, *59*, 38-53.

[8] Girard, L., Blanchet, E., Stien, D., Baudart, J., Suzuki, M., Lami, R., Evidence of a large diversity of N-acyl-homoserine lactones in symbiotic Vibrio fischeri strains associated with the squid Euprymna scolopes. *Microbes and environments*. 2019, ME18145.

[9] Fuqua, W. C., Winans, S. C., Greenberg, E. P., Quorum sensing in bacteria: the LuxR-LuxI family of cell density-responsive transcriptional regulators. *Journal of bacteriology*. 1994, *176*, 269-275.

[10] Nealson, K. H., Platt, T., Hastings, J. W., Cellular control of the synthesis and activity of the bacterial luminescent system. *Journal of bacteriology*. 1970, *104*, 313-322.

[11] Fuqua, C., Greenberg, E. P., Listening in on bacteria: acyl-homoserine lactone signalling. *Nature reviews Molecular cell biology*. 2002, *3*, 685-695.

[12] Parkinson, J. S., Kofoid, E. C., Communication modules in bacterial signaling proteins. *Annual review of genetics*. 1992, *26*, 71-112.

[13] Eberhard, A., Burlingame, A. L., Eberhard, C., Kenyon, G. L., Nealson, K. H., Oppenheimer, N., Structural identification of autoinducer of Photobacterium fischeri luciferase. *Biochemistry*. 1981, *20*, 2444-2449.

[14] Bainton, N. J., Stead, P., Chhabra, S. R., Bycroft, B. W., Salmond, G., Stewart, G. S., Williams, P., N-(3-oxohexanoyl)-L-homoserine lactone regulates carbapenem antibiotic production in Erwinia carotovora. *Biochemical Journal*. 1992, *288*, 997-1004.

[15] Thiel, V., Kunze, B., Verma, P., Wagner-Döbler, I., Schulz, S., New structural variants of homoserine lactones in bacteria. *ChemBioChem*. 2009, *10*, 1861-1868.

[16] Miller, M. B., Bassler, B. L., Quorum sensing in bacteria. *Annual review of microbiology*. 2001, *55*, 165-199.
[17] Ng, W.-L., Bassler, B. L., Bacterial quorum-sensing network architectures. *Annual review of genetics*. 2009, *43*, 197.
[18] Engebrecht, J., Nealson, K., Silverman, M., Bacterial bioluminescence: isolation and genetic analysis of functions from Vibrio fischeri. *Cell*. 1983, *32*, 773-781.
[19] Rutherford, S. T., Van Kessel, J. C., Shao, Y., Bassler, B. L., AphA and LuxR/HapR reciprocally control quorum sensing in vibrios. *Genes & development*. 2011, *25*, 397-408.
[20] Ball, A. S., Chaparian, R. R., van Kessel, J. C., Quorum sensing gene regulation by LuxR/HapR master regulators in vibrios. *Journal of bacteriology*. 2017, *199*, e00105-00117.
[21] Burmølle, M., Hansen, L., Oregaard, G., Sørensen, S., Presence of N-acyl homoserine lactones in soil detected by a whole-cell biosensor and flow cytometry. *Microbial ecology*. 2003, *45*, 226-236.
[22] Fuqua, C., Winans, S. C., Conserved cis-acting promoter elements are required for density-dependent transcription of Agrobacterium tumefaciens conjugal transfer genes. *Journal of Bacteriology*. 1996, *178*, 435-440.
[23] McClean, K. H., Winson, M. K., Fish, L., Taylor, A., Chhabra, S. R., Camara, M., Daykin, M., Lamb, J. H., Swift, S., Bycroft, B. W., Quorum sensing and Chromobacterium violaceum: exploitation of violacein production and inhibition for the detection of N-acylhomoserine lactones. *Microbiology*. 1997, *143*, 3703-3711.
[24] Andersen, J. B., Heydorn, A., Hentzer, M., Eberl, L., Geisenberger, O., Christensen, B. B., Molin, S. r., Givskov, M., gfp-based N-acyl homoserine-lactone sensor systems for detection of bacterial communication. *Applied and environmental microbiology*. 2001, *67*, 575-585.
[25] Winson, M. K., Swift, S., Fish, L., Throup, J. P., Jørgensen, F., Chhabra, S. R., Bycroft, B. W., Williams, P., Stewart, G. S., Construction and analysis of luxCDABE-based plasmid sensors for investigating N-acyl homoserine lactone-mediated quorum sensing. *FEMS microbiology letters*. 1998, *163*, 185-192.
[26] Tommonaro, G., Abbamondi, G. R., Iodice, C., Tait, K., De Rosa, S., Diketopiperazines produced by the halophilic archaeon, Haloterrigena hispanica, activate AHL bioreporters. *Microbial ecology*. 2012, *63*, 490-495.
[27] Damte, D., Gebru, E., Lee, S., Suh, J., Park, S., Evaluation of anti-quorum sensing activity of 97 indigenous plant extracts from Korea through bioreporter bacterial strains Chromobacterium violaceum and Pseudomonas aeruginosa. *J. Microb. Biochem. Technol*. 2013, *5*, 42-46.
[28] Shaw, P. D., Ping, G., Daly, S. L., Cha, C., Cronan Jr, J. E., Rinehart, K. L., Farrand, S. K., Detecting and characterizing N-acyl-homoserine lactone signal molecules by thin-layer chromatography. *Proceedings of the National Academy of Sciences*. 1997, *94*, 6036-6041.
[29] Liu, M., Wang, H., Griffiths, M., Regulation of alkaline metalloprotease promoter by N-acyl homoserine lactone quorum sensing in Pseudomonas fluorescens. *Journal of applied microbiology*. 2007, *103*, 2174-2184.
[30] Steindler, L., Venturi, V., Detection of quorum-sensing N-acyl homoserine lactone signal molecules by bacterial biosensors. *FEMS microbiology letters*. 2007, *266*, 1-9.

[31] Cataldi, T., Bianco, G., Frommberger, M., Schmitt-Kopplin, P., Direct analysis of selected N-acyl-L-homoserine lactones by gas chromatography/mass spectrometry. *Rapid Communications in Mass Spectrometry*. 2004, *18*, 1341-1344.
[32] Cataldi, T. R., Bianco, G., Palazzo, L., Quaranta, V., Occurrence of N-acyl-L-homoserine lactones in extracts of some Gram-negative bacteria evaluated by gas chromatography–mass spectrometry. *Analytical biochemistry*. 2007, *361*, 226-235.
[33] Cataldi, T. R., Bianco, G., Abate, S., Accurate mass analysis of N-acyl-homoserine-lactones and cognate lactone-opened compounds in bacterial isolates of Pseudomonas aeruginosa PAO1 by LC-ESI-LTQ-FTICR-MS. *Journal of mass spectrometry*. 2009, *44*, 182-192.
[34] Wang, J., Ding, L., Li, K., Schmieder, W., Geng, J., Xu, K., Zhang, Y., Ren, H., Development of an extraction method and LC–MS analysis for N-acylated-l-homoserine lactones (AHLs) in wastewater treatment biofilms. *Journal of Chromatography B*. 2017, *1041*, 37-44.
[35] Hoang, T. P. T., Barthélemy, M., Lami, R., Stien, D., Eparvier, V. r., Touboul, D., Annotation and quantification of N-acyl homoserine lactones implied in bacterial quorum sensing by supercritical-fluid chromatography coupled with high-resolution mass spectrometry. *Analytical and bioanalytical chemistry*. 2020, *412*, 2261-2276.
[36] Wang, J., Quan, C., Wang, X., Zhao, P., Fan, S., Extraction, purification and identification of bacterial signal molecules based on N-acyl homoserine lactones. *Microbial biotechnology*. 2011, *4*, 479-490.
[37] Li, X., Fekete, A., Englmann, M., Frommberger, M., Lv, S., Chen, G., Schmitt-Kopplin, P., At-line coupling of UPLC to chip-electrospray-FTICR-MS. *Analytical and bioanalytical chemistry*. 2007, *389*, 1439-1446.
[38] Charlton, T. S., De Nys, R., Netting, A., Kumar, N., Hentzer, M., Givskov, M., Kjelleberg, S., A novel and sensitive method for the quantification of N-3-oxoacyl homoserine lactones using gas chromatography–mass spectrometry: application to a model bacterial biofilm. *Environmental microbiology*. 2000, *2*, 530-541.
[39] Sheng, H., Song, Y., Bian, Y., Wu, W., Xiang, L., Liu, G., Jiang, X., Wang, F., Determination of N-acyl homoserine lactones in soil using accelerated solvent extraction combined with solid-phase extraction and gas chromatography-mass spectrometry. *Analytical Methods*. 2017, *9*, 688-696.
[40] Bruhn, J. B., Christensen, A. B., Flodgaard, L. R., Nielsen, K. F., Larsen, T. O., Givskov, M., Gram, L., Presence of acylated homoserine lactones (AHLs) and AHL-producing bacteria in meat and potential role of AHL in spoilage of meat. *Applied and Environmental Microbiology*. 2004, *70*, 4293-4302.
[41] Rothballer, M., Uhl, J., Kunze, J., Schmitt-Kopplin, P., Hartmann, A., in: Quorum Sensing. Springer, 2018, pp. 61-72.
[42] Huang, S., Zhang, H., Ng, T. C. A., Xu, B., Shi, X., Ng, H. Y., Analysis of N-Acy-L-homoserine lactones (AHLs) in wastewater treatment systems using SPE-LLE with LC-MS/MS. *Water Research*. 2020, *177*, 115756.
[43] Malik, A. K., Fekete, A., Gebefuegi, I., Rothballer, M., Schmitt-Kopplin, P., Single drop microextraction of homoserine lactones based quorum sensing signal molecules, and the separation of their enantiomers using gas chromatography mass spectrometry in the presence of biological matrices. *Microchimica Acta*. 2009, *166*, 101-107.

Chapter 2

Headspace Study of Chiral Interconversion of *N*-acyl homocysteine Thiolactones

2.1 Abstract

In this paper racemization of (L)-N-acetyl-L-homocysteine thiolactone has been studied and its kinetics described. The results show that the kinetics of racemization at 150 ^{o}C is the same for vials made of glass, silanized glass or Teflon coated glass. The temperature dependence of the kinetics has been studied and the activation Gibbs energy and activation entropy has been obtained from the transition state theory. The catalytic effect of G-DP, G-BP and B-DP GC chiral stationary phases on the racemization has been observed and quantified by the values of racemization rate constants; B-DP exhibited the greatest activity. Parameters of energy barrier calculated from experiment were compared with theoretical values acquired from quantum mechanics calculation.

Dynamic gas chromatography of racemic mixture of N-acetyl homocysteine thiolactone enantiomers on chiral B-DP, G-DP and G-BP capillary columns was used to study catalytic effect as well as kinetic and thermodynamic enantiomerization data. Comparison of enantiomerization rates at 180 ^{o}C indicated highest catalytic activity of G-BP capillary column. Finally, the mechanism of the racemization has been described by quantum chemical modelling. Agreement between the experimental and calculated values of activation Gibbs energy, activation enthalpy and activation entropy is good.

2.2 Introduction

Separation methods have become versatile tools for the determination of kinetic activation parameters and energy barriers to interconversion of isomers and enantiomers. There are several experimental configurations where gas chromatography is used for kinetic studies of chemical reactions. Combination of batch-wise kinetic studies with GC analysis is frequently employed [1-5].

The conformational and configurational lability of enantiomers can be characterized by different terms, each defining a specific process. Racemization is defined as the production of a racemate from a chiral starting material in which one enantiomer is present in excess. The resulting product is described as a racemic mixture or a racemate [6]. The term enantiomerization characterizes a process in which the enantiomers undergo inversion of their respective conformations [7].

N-acylhomocysteine thiolactones (N-AcHCTL) are chiral and have been used as acylating reagents for biological carbohydrates and proteins producing thiol-bearing moieties on the backbone of such molecules. These derivatives are studied for their changes in physiological and biochemical properties in biomedicine, industrial and pharmaceutical disciplines. [8-10]. *N*-acyl L-homocysteine thiolactones also are potent modulators of the RhlR quorum sensing receptor in *Pseudomonas aeruginosa* [11]. Further, it was found that N-AcHCTLs could restore pigment production to a mutant of the quorum sensing bacterium, C violaceurn (CV026) [12]. During a recent study, it was reported that N-AcHCLTs and some related N-acylhomoserine lactones appear to show on-column en restore pigment production to a mutant of the quorum sensing bacterium, C violaceurn (CV026) [12]. During a recent study, it was reported that N-AcHCLTs and some related N-acylhomoserine lactones appear to show on-column enantiomerization when subject to higher temperature GC separations [13]. Consequently, it is of interest to study the thermodynamics and kinetics of interconversion due to this compound's behavior and relevance in biological studies.

In this paper a combination of batch-wise headspace kinetic studies was performed for racemization of N-acetyl homocysteine thiolactone (N-AcHCTL) enantiomers. The conversion

proceeds batch-wise in isolated vials and its progress was evaluated by the enantioselective capillary gas chromatography. Kinetic and thermodynamic activation data for the racemization were obtained using the parameters that control the batch-wise reaction (reaction time, type of vials, temperature and catalysis) [1, 4, 7].

Methods in which the kinetics of chemical reactions are studied along the separation process are often called *dynamic* separation methods [1-3]. Elution profiles of binary interconversions, such as the intN-AcHCTL erconversion of thermolabile conformational isomers, and enantiomers obtained by *dynamic* chromatography, are generally characterized by transient elution profiles which are characterized by the formation of a plateau between the terminal peaks of the enantiomers. Figure S1 in the Electronic supplementary material shows interconversion of racemic mixture of 99.5% N-AHCTL on G-BP capillary column at 150 °C. Plateau formation in chromatographic separations of enantiomers represents a diagnostic tool for the recognition of the liability of stereogenic elements [1].

It has been published that a racemic mixture of enantiomers may be used for the gas chromatographic chiral on-column enantiomerization study when the considered enantiomers are separated or deconvoluted [1, 3, 14].

Peak areas and corresponding retention times determined from experimental data by Peak deconvolution method were used to calculate enantiomerization rate constants and Gibbs to determine catalytic effects of the chiral stationary phase [1, 3, 14].

2.3 Theoretical

The theoretical basis for obtaining the racemization rate constants from experimental results are described below. This procedure represents a modification of the one published previously [4].

Racemization proceeds via enantiomerisation by the opposing reaction:

$$L \underset{k_{r,-1}}{\overset{k_{r,1}}{\rightleftarrows}} D \qquad (1)$$

A racemic mixture represents the equilibrium state of enantiomerisation. In the racemic mixture, the concentrations of L and D enantiomers are equal and, therefore, the equilibrium constant of racemization is equal to one. At equilibrium, the rate of forward and reverse reaction has to be

the same so that, since the concentrations are equal, also the rate constants of forward and reverse reactions are the same, i.e. $k_{r,1}^{L\to D} = k_{r-1}^{D\to L} = k_r$ where both, the forward and reverse reactions, are the first-order reactions with the same rate constant k_r .

The rate of L racemization can be expressed as:

$$\frac{\mathrm{d}c_\mathrm{L}}{\mathrm{d}t} = -k_r c_\mathrm{L} + k_r c_\mathrm{D} \tag{2}$$

where c_L and c_D are concentrations of L and D enantiomers in the reaction mixture. The concentrations c_L and c_D obey the material balance

$$c_\mathrm{L} + c_\mathrm{D} = c_{0\mathrm{L}} + c_{0\mathrm{D}} = c_0 \tag{3}$$

where $c_{0\mathrm{L}}$, $c_{0\mathrm{D}}$ and c_0 are the concentrations of L and D form and both forms at time t = 0. Combination of Eqs. (2) and (3) gives:

$$\frac{\mathrm{d}c_\mathrm{L}}{\mathrm{d}t} = k_r \left(c_0 - 2c_\mathrm{L}\right) \tag{4}$$

After integration of Eq.(4) one can obtain:

$$c_\mathrm{L} = \frac{1}{2}\left[c_0 + \left(2c_{0\mathrm{L}} - c_0\right)e^{-2k_r t}\right] \tag{5}$$

Taking into account Eq.(3), the concentration of the D form can be expressed as:

$$c_\mathrm{D} = \frac{1}{2}\left[c_0 - \left(2c_{0\mathrm{L}} - c_0\right)e^{-2k_r t}\right] \tag{6}$$

The area of the chromatographic peak is proportional to the amount of the substance, which for the L form, is the product $c_\mathrm{L}\cdot V$ and analogically for the D form, where V is the volume of the injected reaction mixture. Since the injected volume may slightly differ for different analyses, the way to obtain reproducible results is to express the ratio of the peak areas of *D* and *L* forms, *AD*/*AL*, which should be equal to the ratio $c_\mathrm{D}/c_\mathrm{L}$. From Eqs. (5) and (6) for the ratio $c_\mathrm{D}/c_\mathrm{L}$ one can get:

$$\frac{c_{\mathrm{D}}}{c_{\mathrm{L}}} = \frac{1-\left(2\frac{c_{0\mathrm{L}}}{c_0}-1\right)e^{-2k_r t}}{1+\left(2\frac{c_{0\mathrm{L}}}{c_0}-1\right)e^{-2k_r t}} \tag{7}$$

If we denote purity of the L form as:

$$p_{\mathrm{L}} = \frac{c_{0\mathrm{L}}}{c_0} \tag{8}$$

then the ratio c_D/c_L is:

$$\frac{c_{\mathrm{D}}}{c_{\mathrm{L}}} = \frac{1-\left(2p_{\mathrm{L}}-1\right)e^{-2k_r t}}{1+\left(2p_{\mathrm{L}}-1\right)e^{-2k_r t}} \tag{9}$$

At the beginning of the experimental curve c_D/c_L there is very often seen an onset as if the heating of the reaction mixture took some time. Therefore, we introduced into Eq. (9) the time necessary for heating, t_0:

$$\frac{c_{\mathrm{D}}}{c_{\mathrm{L}}} = \frac{1-\left(2p_{\mathrm{L}}-1\right)e^{-2k_r\left(t-t_0\right)}}{1+\left(2p_{\mathrm{L}}-1\right)e^{-2k_e\left(t-t_0\right)}} \tag{10}$$

If we denote

$$a = \left(2p_{\mathrm{L}}-1\right)e^{2k_r t_0} \tag{11}$$

then Eq. (10) can be rewritten as

$$\frac{c_{\mathrm{D}}}{c_{\mathrm{L}}} = \frac{1-ae^{-2k_r t}}{1+ae^{-2k_r t}} \tag{12}$$

Eq. (12) can be rearranged as follows:

$$\ln\frac{1+\frac{c_{\mathrm{D}}}{c_{\mathrm{L}}}}{1-\frac{c_{\mathrm{D}}}{c_{\mathrm{L}}}} = 2k_r t - \ln a \tag{13}$$

Eq.(13) is formally the same as the equation derived in [4].

When plotting the term on the left side of Eq. (13) as a function of time, one should obtain a straight line with the slope $2k_r$ and the intercept (-ln a). However, as seen from Eq. (11), the slope in Eq.(13) has a more complex meaning than that in [4]. The linearization in Eq. (13) might

lead to a bias in optimized parameters. Hence, the racemization rate constants k and the parameters a were obtained from the experimental c_D/c_L curves by the non-linear least-squares method using the program Origin Pro 9 (OriginLab, Northampton,MA).

2.4 Experimental

2.4.1 Synthesis of N-AcHCTL

Single enantiomers and racemic compounds were synthesized with a single step synthesis as reported previously [13]. A 1:2 molar ratio equivalent homocysteine thiolactone and triethylamine (Sigma-Aldrich) were placed in a 50 mL round-bottom flask and the mixture suspended in 10 mL of acetonitrile and the flask brought to 0°C in an ice bath. A 1 mole equivalent of acyl-chloride in 10 mL of acetonitrile was added dropwise to the stirring mixture for 30 minutes. The reaction was then brought to room temperature while stirring for 1.5 hours. Acetonitrile was removed by rotary evaporation in a 40 °C water bath at a pressure of 226 mbar until a white residual precipitate was observed, indicating product.

2.4.2 Headspace Teflon coating glass vials

For the Teflon coating, 10 mL headspace vials were filled with colloidal suspension of Teflon PTFE DISP 30 up to the top, making sure are internal surfaces are in contact with the suspension. The suspension is then removed and vials are allowed to dry until a dry white film is observed. The vials are further dried in oven at 120 °C for 30 minutes. Once they are dried, the vials were sintered at a temperature of 380 °C for 10 minutes producing a smooth, even, and durable film on the inner walls of the headspace vials.

2.4.3 Headspace method for heated racemization of enantiomers.

The oven of Agilent Technologies 6890N GC system was used to heat samples during the racemization procedure at several temperatures. A sand bath, constructed from a 250 mL beaker with 150 mL of sand was used to insulate the headspace vials. Headspace vials were purchased from Supelco (Bellefonte, Pennsylvania, USA) and silanized headspace vials were purchased from Analytical sales & services, Inc. (Flanders, New Jersey, USA). Teflon PTFE DISP 30 (Sigma-Aldrich, St. Louis, USA) was used to coat the glass vials because there was a small increase in the racemization rate constants in the untreated glass vials and the silanized ones during sampling to keep the sample temperature constant. The sand bath was placed in the oven at the required temperature to allow the temperature of the sand to equilibrate with the oven temperature. 10-mL vials from Teflon coated glass and silanized glass vials. Three basic sets of experiments were performed during this study:

1. Set of 10-mL of Teflon coated glass, glass and silanized glass vials were used as reaction vials. Each vial was loaded with 2 mg of 99.5% (L)-N-AcHCTL and placed in the sand bath inside the oven and heated at 150 ^{o}C at various time of racemization.
2. Set of 10 mL silanized glass vials were filled with 2 mg of 91.5 % (L)-N-AcHCTL and placed in a sand bath inside the oven. Time dependence of racemization at selected temperature was followed as a function of time.
3. Three sets of silanized glass vials were filled with 2mg of 8.5% (D)-N-AHCTL and 10-mg of either G-DP (2,3-di-O-propionyl-6-O-tert-butyldimethylsilyl-□-cyclodextrin), B-DP (2,3-di-O-propionyl-6-O-tert-butyldimethylsilyl-β-cyclodextrin) or G-BP (2,6-di-O-pentyl-3-butyryl-□-cyclodextrin) chiral GC stationary phases were added. Racemization of the contents of each set of vials at 150 ^{o}C was followed as a function of time.

The reaction vial headspace vapors were sampled with a Hamilton 1701 10-µL gastight syringe at chosen times. Each vapor sample was analyzed by capillary GC.

2.4.4 Combination of chiral separation with batch-wise headspace kinetic method

In this method, the racemization of an enantiomer is performed outside the separation system (off-line) at certain temperatures for the required time similarly as it has been described by Canoira et al. [5]. Samples of gradual racemization were separated by enantioselective methods at temperatures where separation condition quenches the interconversion. Table S1 in the Electronic supplementary material shows data obtained by thermal racemization of 99.5% of N-AcHCTL using batch-vise head space kinetic method on Teflon coated glass vials at 150^{o}C.

2.4.5 Headspace method for thermal and catalytic on column interconversion of (L, D) (N)-AcHCTL) racemate

In this chapter, the deconvolution process was used to study configuration inversion of the racemic mixture of 99.5% (L) N-acetyl homocysteine thiolactone during gas chromatographic separation of enantiomers on chiral capillary columns. For on column enantiomerization of racemates of N-AcHCTL the following capillary columns were used: G-DP (2,3-di-O-propionyl-6-O-tert-butyldimethylsilyl-γ-cyclodextrin), 30-m x 0.25-mm x 0.12-µm film thickness, B-DP (2,3-di-O-propionyl-6-O-tert-butyldimethylsilyl-β-cyclodextrin), 30-m x 0.25-mm x 0.12-µm film thickness, and G-BP (2,6-di-O-pentyl-3-butyryl-γ-cyclodextrin), 30-m x 0.25-mm x 0.12-µm film thickness. All columns were Supelco, Bellefonte, USA).

Chromatograms obtained by the gas chromatographic separation of racemic mixture of N-AcHCTL on G-DP, B-DP or G-BP chiral capillary GC columns at different temperatures were used to determine the kinetic and thermodynamic data corresponding to inversion of the L and D enantiomers. Corresponding peak areas and retention times were determined by computer-assisted deconvolution of chromatograms [14].

2.4.6 Capillary gas chromatography

Samples of vial headspace vapors in gradually increasing racemization times were analyzed with Agilent technologies 6850 GC-FID capillary GC using Beta DEX 225 (Supelco, Bellefonte, USA**) (**25% 2.3-di-O-acetyl-6-O-TBDMS-β-cyclodextrin in SPB 20 (20% phenyl-80%-dimethylsiloxane) fused silica capillary column (30-m x 0.25-mm x 0.25-µm film thickness) at 150 °C. Conditions of GC-FID analysis were at 170 °C, helium carrier flow of average velocity 40 cm s^{-1}, split ratio of 50:1 with 3-µL injections, temperatures of injection port 220 °C and FID detector 250 °C.

2.5 Results and Discussion

Here we describe the effects of the purity of enantiomer of (L) N-AcHCTL, used vial material, temperature and catalysts on the racemization of N-AcHCTL as well as enantiomerization rate constants, temperature dependences of apparent enantiomerization rate constants ($k_{e,L\to D}$ and $k_{e,D\to L}$) and Gibbs free energy barriers ($\Delta G_{L\to D}$ and $\Delta G_{D\to L}$) obtained by catalytic inversion of N-AcHCTL enantiomers during gas chromatographic separation on B-DP, G-DP and G-BP chiral capillary columns. Finally, quantum-chemical calculations are carried out in order to elucidate the mechanism of racemization.

The scheme for the interconversion of the enantiomers of (L)-N-AcHCTL is shown in Fig.2.1.

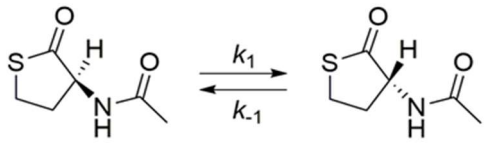

L D

Figure 2-1. Scheme of interconversion of enantiomers of N-acetyl homoscysteine thiolactone. In racemic mixture forward and reverse reactions has the same rate constant, k_r

2.5.1 Thermal racemization of 99.5% of (L)-N-(AcHCTL)

As already written in Introduction, racemization is defined as the production of a racemate from a chiral starting material in which one enantiomer is present in excess [6]. Kinetic and thermodynamic activation data for the racemization may be obtained using the parameters that control the batch-wise reaction (reaction time, type of vials, temperature and catalysis).
Tab. 2.S2 listed in the Electronic supplementary material shows data obtained by the capillary GC separation of *AL%* and *AD%* enantiomers, as well as dependence of relative peak areas of *AL%* and *AD%* enantiomers on racemization time obtained by head space method of 99.5% (L)-N-AcHCTL in Teflon coated glass vials at 150 °C. Chromatograms and data listed in Tab. 2.S2 were obtained by processing of chromatographic experimental data by Excel and Origin software.

2.5.2 Effect of vial material on the thermal racemization of (L)- N-AcHCTL

Three sets of vials made of Teflon coated glass, glass and silanized glass were employed for the racemization studies. For the experiments, 99.5% (*L*)-N-AcHCTL (p_L = 0.995) was used at a temperature of 150 °C. The raw experimental data are listed in Table S3 in the Electronic supplementary material. The agreement between experimental and calculated curves of the dependence of c_D/c_L vs. time is shown in Fig.2.2 and the resulting values of the racemization rate constant k_r and the parameter a in Eq. (12) are summarized in Table 2.1.
The agreement between experimental and calculated curves of the dependence of c_D/c_L *vs*. time is shown in Fig.2.2 and the resulting values of the racemization rate constant k and the parameter a in Eq. (12) are summarized in Table 2.1.

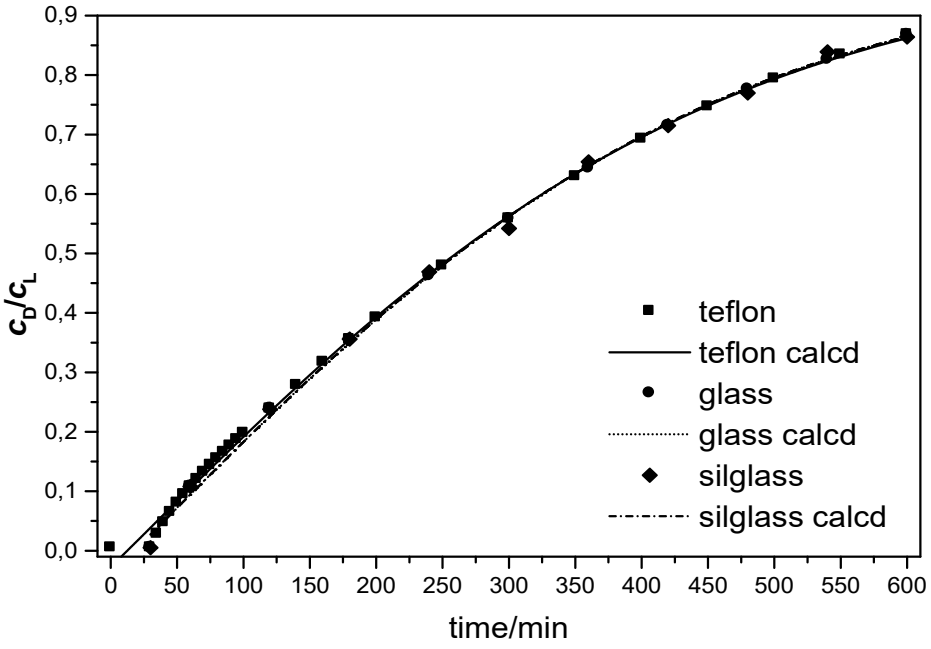

Figure 2-2. Experimental points and calculated curves of the dependence of c_D/c_L *vs*. racemization time for vials made of Teflon coated glass, glass and silanized glass (silglass) at 150 ^oC.

Table 2-1: Values of rate constants k_r and parameter a with their standard deviations for various vial materials.

material	$10^5 \cdot k_r$ / s^{-1}	a
Teflon coated glass	3.70 $\pm$ 0.03	1.057 $\pm$ 0.008
glass	3.75 $\pm$ 0.05	1.083 $\pm$ 0.015
silanized glass	3.77 $\pm$ 0.07	1.085 $\pm$ 0.020

As seen from Fig.2.2, the agreement between experimental and calculated values is very good so that the theory describes satisfactorily the experimental findings. The resulting values of k_r and a are listed in Table 2.1. As seen from Fig.2.2, the kinetic curves are practically identical for all the vials employed for racemization. Also, there is no statistically significant difference among the racemization rate constants as seen from Table 1. The material of vials has no influence on the kinetics of racemization.

2.5.3 Effect of temperature

The experiments were carried out in Teflon coated glass vials at temperatures of 150, 160 and 170 ^{o}C. The raw experimental data are shown in Table 2.S3 in the Supplemental Information.

Fig.2.3 shows experimental points and calculated curves of the dependence of cD/cL vs. racemization time for % 99.5% (L)-N-AcHCTL for various temperatures in silanized glass vials.

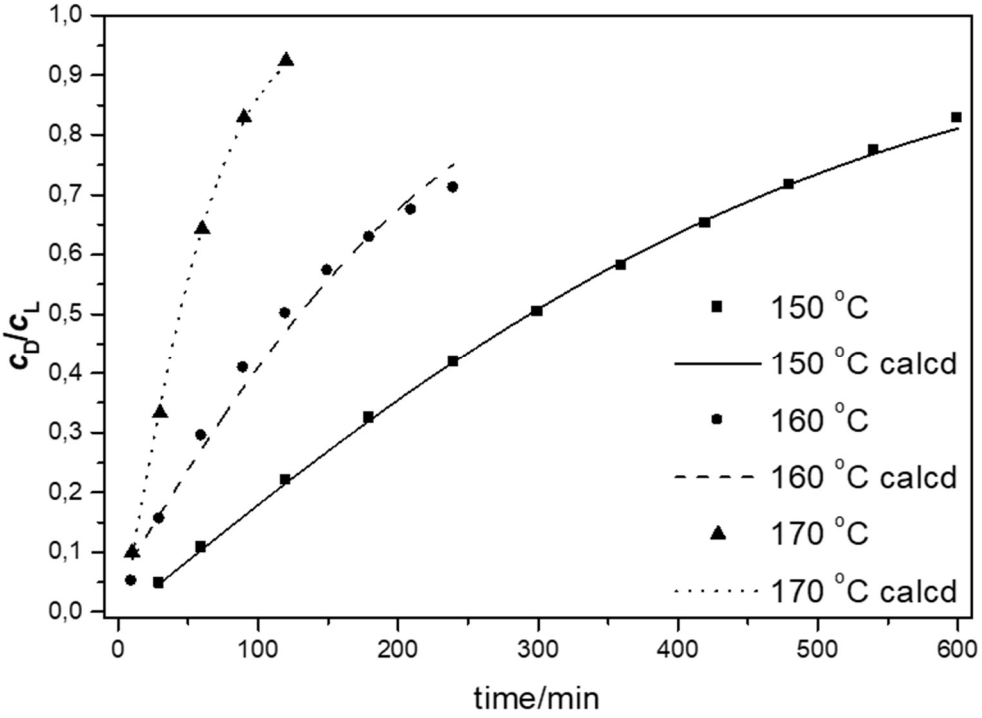

Figure 2-3 Experimental points and calculated curves of the dependence of cD/cL vs. racemization time for % 99.5% (L)-N-AcHCTL for various temperatures in silanized glass vials.

As seen from Fig.2.3, the agreement between experimental and calculated values is again very good so that the theory describes satisfactorily the experimental findings. The resulting values of k_r and t_0 are listed in Table 2.1. As seen from Fig.2.3, the kinetic curves are practically identical for all the vials employed for racemization. Also, there is no statistically significant difference among the racemization rate constants as seen from Table 2.2. The material of vials has no influence on the kinetics of racemization.

Table 2-2: Values of racemization rate constants k_r and parameter a with their standard deviations for various temperatures.

temperature	$10^5 \cdot k_r$ / s^{-1}	a / min	$\Delta G^{\#}$/, kJ mol^{-1}
150 °C	3.17 ± 0.03	1.017 ± 0.009	143.76 ± 0.03
160 °C	6.43 ± 0.32	0.905 ± 0.037	144.69 ± 0.18
170 °C	22.45 ± 0.48	1.091 ± 0.024	143.51 ± 0.08

As expected, temperature has a significant effect on the rate of racemization. From the temperature dependence of the rate constant, the activation parameters can be evaluated. Applying the theory of activated complex, the activation Gibbs energy has been calculated using the following formula:

$$\Delta G^{\neq} = R\,T \ln\left(\frac{h\,k_r}{\kappa\,k_B T}\right) \tag{14}$$

where k_r is the racemization rate constant, k_B is the Boltzmann constant, κ is the transmission coefficient and h is Planck's constant, T is the absolute temperature and R is the gas constant. [15]

The values of $\Delta G^{\#}$ have been calculated for κ=0.5 and are listed in Table 2.2. Values for the enthalpy of activation $\Delta H^{\neq}$ and entropy of activation, $\Delta S^{\neq}$ were obtained from the linear dependence of $\Delta G^{\#}$ on T as the intercept and slope [15]:

$$\Delta G^{\neq} = \Delta H^{\neq} - T\,\Delta S^{\neq} \tag{15}$$

The resulting values are: $\Delta H^{\neq}$ = (149 ± 26) kJ mol^{-1}, $\Delta S^{\neq}$ = (-13 ± 61) J $K^{-1}mol^{-1}$.

2.5.3 Effect of catalytic activity of G-DP, G-BP and B-DP GC stationary phases

Hence, to study quantitatively this phenomenon, in this paragraph we studied racemization kinetics of 91.5% (L)-N-AcHCTL with addition of G-DP (2,3-di-O-propionyl-6-O-tert-butyldimethylsilyl-γ-cyclodextrin), G-BP (2,6-di-O-pentyl-3-butyryl-γ-cyclodextrin) or B-DP (2,3-

di-O-propionyl-6-O-tert-butyldimethylsilyl-β-cyclodextrin) chiral GC stationary phases were added. Homogenized contents of headspace vials were racemized up to 6 hours at 150 °C.

Agreement between the experimental points and calculated curves is demonstrated in Fig.2.4, and this agreement between experiment and theory is very good. The resulting values of *k* and *a* are summarized in Table 2.3.

From Table 2.3 it is seen that the racemization rate constants are significantly higher for the mixtures of 91.5% N-AcHCTL with the various chiral stationary phases than for the 91.5% N-AcHCTL alone. The difference between the catalytic effect of two of the stationary phases, G-DP and G-BP, is statistically insignificant. The highest catalytic effect was found for the B-DP stationary phase.

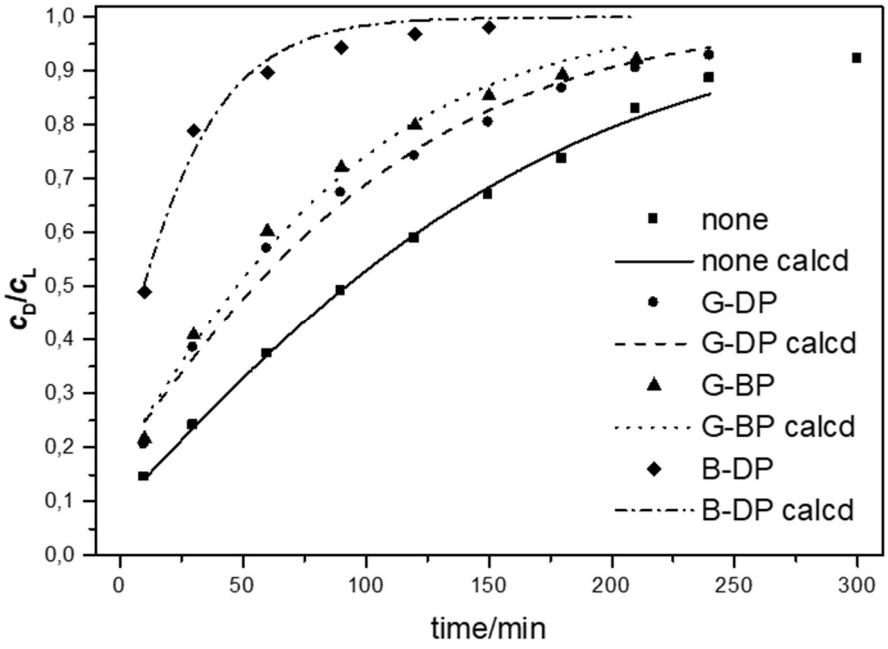

Figure 2-4. Experimental points and calculated curves of the dependence of c_D/c_L *vs*. racemization time for % 91.5% (*L*)-N-AcHCTL in silanized glass vials with addition of various stationary phases at 150 °C, purity of (L)-N-AcHCTL was p_L=91.5%.

Table 2-3. Values of racemization rate constants k_r and the parameter a with their standard deviations for silanized glass vials and for various stationary phases at 150 °C, purity of (L)-N-AcHCTL was p_L = 91.5%.

catalyst	$10^5 \cdot k_r$ s^{-1}	a
none	8.27 ± 0.20	0.830 ± 0.018
G-DP	11.02 ± 0.62	0.688 ± 0.035
G-BP	12.95 ± 0.75	0.698 ± 0.037
B-DP	34.7 ± 5.2	0.498 ± 0.064

2.5.4 Enantiomerization of N-AcHCTL

2.5.4.1. Determination of kinetic and thermodynamic data

In contrast to racemization, the term enantiomerization characterizes the process by which the individual enantiomers of chiral molecules undergo inversion of their respective stereogenic elements. Enantiomerization is a microscopic process describing the reversible conversion of one enantiomer (*L*) into the enantiomer (*D*):

$$L \xrightarrow{k^{app}_{e,,L\to D}} D$$

or (*D*) into the enantiomer (*L*)

$$D \xrightarrow{k^{app}_{e,D\to L}} L$$

where $k^{app}_{e,\,L\to D}$ and $k^{app}_{e,\,D\to L}$ are apparent enantiomerization rate constants defined in Supplementary Text 2.S1.

The apparent rate constant $k^{app}_{e,\,L\to D}$ of enantiomerization *L* to *D* was calculated from peak areas *A* to *B* using the equation:

$$k^{app}_{e,\,L\to D} = \frac{1}{2t}\ln\frac{A_{L,0}}{2A_L - A_{L,0}} \qquad (16)$$

Similar equation was used for the calculation of the apparent rate constant ($k_{e,\,D\to L}^{app}$) for enantiomerization *D* to *L:*

$$k_{e,\,D\to L}^{app}=\frac{1}{2t}\ln\frac{A_{D,0}}{2A_D-A_{D,0}} \qquad (17)$$

where A_0 and A are the peak areas of the enantiomer prior to and after the chromatographic separation and, t is enantiomerization time.

The enantiomer peak areas and corresponding retention times for peaks *L* and *D* and the peak clusters *L*+D** and *D*L** shown in Fig.2.S1 in the electronic supplementary material show a peak areas obtained by deconvolution method using published procedure [14]. The electronic versions of chromatograms listed in Figs.2.5-2.7 were exported into a Microcal Origin (RiginLab, Northampton, MA) software where the Peak Fitting program was used to get the deconvoluted peak data and retention times of the enantiomers [14].

Fig.2.5-2.7 illustrates a deconvolution of peak clusters of N-AcHCTL enantiomers separated by dynamic gas chromatography of racemic mixture of N-acetyl homocysteine thiolactone enantiomers on chiral B-DP, G-DP and G-BP capillary columns at various temperatures. Peak clusters and peaks found by a computer assisted deconvolution of these clusters obtained by chromatographic separation of racemic mixture of N-AcHCTL enantiomers are depicted in Fig.2.5 for G-DP capillary column at 160, 170 and 180 °C, in Fig.6 for B-DP capillary column at 180, 190 and 200 °C and in Fig.2.7 for G-BP capillary column at 180, 190 and 200 °C. The outer solid line in these figures shows original peak clusters (i.e. chromatograms). Dashed lines (1 and 4) show *L* and *D* enantiomers and short-dashed lines (2 and 3) deconvoluted peaks of enantiomers L* and D*.

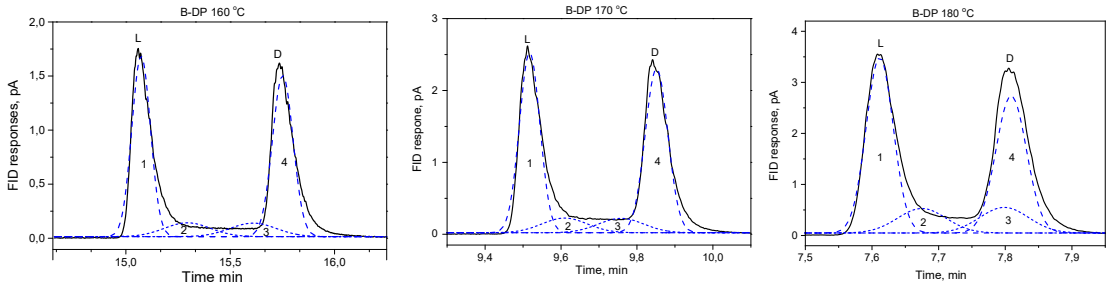

Figure 2-5. Gas chromatographic separation and deconvolution of racemic mixture of N-acetyl homocysteine thiolactone enantiomers on G-DP capillary column at 160, 170 and 180 °C.

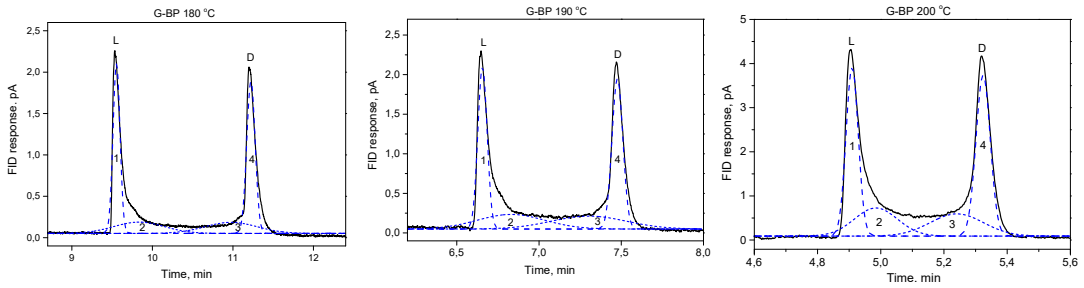

Figure 2-6. Gas chromatographic separation and deconvolution of racemic mixture of N-acetyl homocysteine thiolactone enantiomers on B-DP capillary column at 180, 190 and 200 °C.

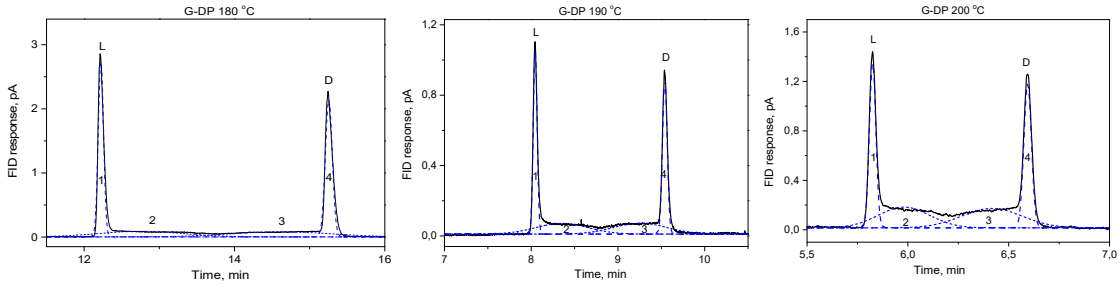

Figure 2-7. Gas chromatographic separation and deconvolution of racemic mixture of N-acetyl homocysteine thiolactone enantiomers on G-BP capillary column at 180, 190 and 200 °C.

2.5.4.2. Determination of kinetic and thermodynamic data for enantiomerization activation parameters

Table 2.4 shows apparent enantiomerization rate constants $k_{e,L\to D}^{app}$ and $k_{e,D\to L}^{app}$ calculated from deconvolution data using logarithmic form of Arrhenius equation for *L* and *D* enantiomer:

$$\ln k_{e,\,L\to D}^{app} = -\frac{E_{a,\,L\to D}}{RT} + \ln A \tag{18}$$

$$\ln k_{e,\,D\to L}^{app} = -\frac{E_{a,\,D\to L}}{RT} + \ln A \tag{19}$$

where E_a is activation energy.

Gibbs energy barriers $\Delta G_{L\to D}^{\neq}$ and $\Delta G_{D\to L}^{\neq}$ were calculated by Eyring equation for L and D enantiomer:

$$-\Delta G_{L\to D}^{\neq} = R\,T \ln\left(-\frac{h\,k_{e,\,L\to D}^{app}}{\kappa\,k_B T}\right) \tag{20}$$

$$-\Delta G_{D\to L}^{\neq} = R\,T \ln\left(-\frac{h\,k_{e,\,D\to L}^{app}}{\kappa\,k_B T}\right) \tag{21}$$

Table 2-4. Temperature dependences of apparent enantiomerization rate constants ($k_{e,\,L\to D}^{app}$ and $k_{e,\,D\to L}^{app}$) and Gibbs free energy barriers ($-\Delta G_{L\to D}^{\neq}$ and $-\Delta G_{D\to L}^{\neq}$) obtained by catalytic inversion of N-AcHCTL enantiomers during gas chromatographic separation on B-DP, G-DP and G-BP chiral capillary columns.

Column	Temperature °C	$10^4 \cdot k_{e,L\to D}^{app}$ s^{-1}	$-\Delta G_{L\to D}^{\neq}$ kJ mol^{-1}	$10^4 \cdot k_{e,D\to L}^{app}$ s^{-1}	$-\Delta G_{D\to L}^{\neq}$ kJ mol^{-1}
B-DP	160	1.85	135.9	1.90	135.8
	170	2.95	137.4	2.69	137.7
	180	3.54	139.9	3.19	140.3
G-DP	180	6.00	137.9	4.59	138.9
	190	12.2	138.3	9.99	139.1
	200	20.7	139.3	1.94	139.5
G-BP	170	2.45	138.1	1.16	140.8
	180	7.39	137.1	5.19	138.4
	190	14.5	137.6	9.43	139.3

Comparison of data in Table 2.4 for apparent rate constants $k_{e,L\to D}^{app}$ at 180 °C shows higher catalytic effect for G-BP column. Gibbs free energy barriers $-\Delta G_{L\to D}^{\neq}$ in Table 4 at 180 °C decrease from 139.9 kJ mol^{-1} for B-DP, to 137.9 kJ mol^{-1} for G-DP and to 137.1 kJ mol^{-1} for G-BP. Gibbs free energy barrier $-\Delta G_{D\to L}^{\neq}$ are slightly higher than that of $-\Delta G_{L\to D}^{\neq}$ at corresponding temperature due to longer interaction of the second eluted enantiomer with the chiral stationary phase, which corresponds with the conclusions found by Gasparrini et al. [16].

Text 2.S2 in Supplementary material describes procedures how temperature dependences of apparent rate constants, k_e^{app} and energy barriers $\Delta G^{\neq}$, listed in Table 2.4, were used to determine the activation energy. E_a activation enthalpy H and entropy ΔS for catalytic inversion of N-AcHCTL enantiomers during its gas chromatographic separation on B-DP, G-DP and G-BP chiral capillary columns.

Data of $\Delta H_{L\to D}$ and $\Delta H_{D\to L}$ as well as $\Delta S_{a,L\to D}$ and $\Delta S_{a,D\to L}$ listed in Table 2.5 were determined from the slopes of and the intercepts on Y axis using the equations listed in Text 2.S2 Supplementary material.

Table 2-5. Eyring activation parameters and Arhenius activation energies for inversion of enantiomers in racemic mixture of N-AcHCTL by the catalytic action of chiral columns.

Column	$\Delta H_{L\rightarrow D}$ kJ mol^{-1}	$\Delta H_{D\rightarrow L}$ kJ mol^{-1}	$\Delta S_{a,L\rightarrow D}$ J mol^{-1} K^{-1}	$\Delta S_{a,D\rightarrow L}$ J mol^{-1} K^{-1}	$\Delta E_{a,D\rightarrow L}$ kJ mol^{-1}	$\Delta E_{a,D\rightarrow L}$ kJ mol^{-1}
B-DP	49.28	38.34	-205.33	-230.50	52.96	42.02
G-DP	85.74	99.77	-119.34	-90.47	89.55	103.57
G-BP	129.06	157.32	-24.33	33.79	132.78	161.04

2.5.5. Catalytic influences of chiral stationary phases and chiral capillary columns on the racemization and enantiomerization of N-AcHCTL enantiomers

Table 2.6. shows dependence of racemization rate constants $k_{e,L\rightarrow D}$ obtained by heating of (L)-N-AcHCTL enantiomers in silanized glass vials filled with the B-DP, G-DP B-DP gas chromatographic stationary phases as well as the apparent enantiomerization rate $k_{r,L\rightarrow D}^{app}$ constants obtained by gas chromatographic separation of (L)-N-AcHCTL on B-DP, G-DP and B-DP capillary columns at 150 ^{o}C.

Table 2-6. Catalytic influence of (a) chiral capillary columns (B-DP, G-DP and G-BP) on enantiomerization apparent rate constants $k_{e,L\rightarrow D}^{app}$ as well as (b) catalytic influence of B-DP, G-DP and G-BP chiral stationary phases on racemization rate constants $k_{e,L\rightarrow D}$ in silanized glass vials at 150 ^{o}C for (L)-N-AcHCTL enantiomers.

Stationary Phase	T, °C	$10^4 \cdot k_{r,L\to D}, s^{-1}$	$10^4 \cdot k^{app}_{e,L\to D}, s^{-1}$
B-DP	150	1.10	1.360
G-DP	150	1.29	0.760
G-BP	150	3.47	0.372

Racemization rate constants $k_{r,\,L\to D}$ and apparent enantiomerization rate constants $k^{app}_{e,\,L\to D}$ were used to describe interconversion of N-AcHCTL enantiomers at 150 °C.

Tab.6 demonstrates that the catalytic effect of chiral stationary phases increases racemization rate constants $k_{e,L\to D}$ in the order of B-DP, G-DP and G-BP. The apparent enantiomerization rate constants $k^{app}_{e,\,L\to D}$ increase in reverse order of chiral capillary columns: G-BP, G-DP and B-DP.

The text listed in this section will result from racemization and enantiomerization (L)-N- AcHCTL enantiomers is a composite and requires a further study.

2.6 Quantum-chemical calculations

(L)- N-AcHCTL is a configurational isomer that cannot be converted into (D) N-AcHCTL by rotating the molecule around a single bond. To change the configuration, cleavage of the covalent bond and formation of a new one is needed. To elucidate the mechanism, quantum-chemical calculations were carried out. The determination of the inversion barrier for conversion of the L enantiomer (i.e., the S absolute configuration) of N-AcHCT to the D-form (i.e., the R absolute configuration) was performed on the basis of the reaction pathway depicted in Fig.2.9:

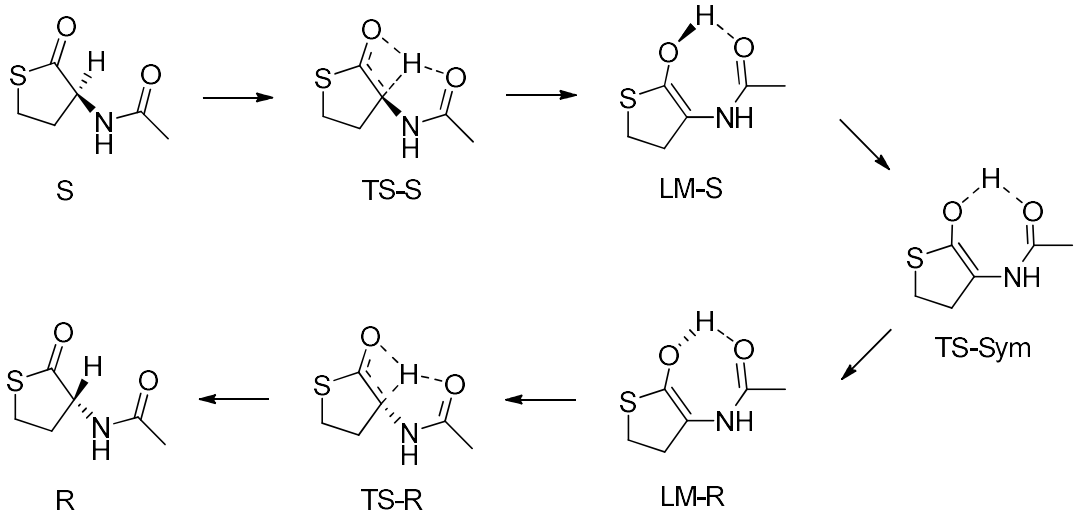

Figure 2-8: Reaction scheme of the enantiomerization from the *S*-conformer of N-acetyl-L-homocysteine thiolactone to the D-enantiomer or R-conformer, Transition states: TS-S, TS-Sym, TS-R; local minima: LM-S, LM-R,

Conformation analysis was performed using Spartan program package [21] and quantum chemical calculations were performed using Gaussian 16 software package [22]. Geometry optimization of minima and the transition states involved in Fig.2.9 were performed at M062X level of theory and 6-31+G(d,p) basis set. All the calculations were carried out *in vacuo*. Frequency calculations were done on the minima in order to ascertain the type of stationary point as well as to obtain zero-point vibrational energies. Thermodynamic properties were calculated at a temperature 433 Kelvin. A quasi-harmonic correction was applied during the entropy calculation by setting all positive frequencies that are less than 100 cm^{-1} [23]. Transition state geometries were optimized using the same method, verifying each time that only one imaginary vibrational frequency is present in the transition state. Intrinsic Reaction Coordinate (IRC) calculations were performed to determine the connections between stationary points. Single point energy calculations were done using M062X level of theory and 6-311++G(2df,2pd) basis set Fig.2.10.

By comparing experimental and theoretical values of the thermodynamic properties of inversion barrier it can be concluded that the $\Delta H^{\neq}$ and $\Delta S^{\neq}$ values coincide within the 'experimental error' caused by calculation, only the value of $\Delta G^{\neq}$ is a little larger (theory reproduces all known heats of formation to the root-mean-square accuracy of 2 kcal/mol [24],

which indicates that probably conditions of individual experiments in 'heating experiment' were probably differed very slightly.

Table 2-7. Experimental and theoretical values of thermodynamic properties of the inversion barrier for the conversion of L enantiomer of AcHCT to the D-form at temperature 433 K.

	Experimental value	*Theoretical value*
$\Delta G_e^{\ddagger}$, kJ mol^{-1}	144.7 ± 0.2	161.11
$\Delta H_e^{\ddagger}$, kJ mol^{-1}	149 ± 26	152.00
$\Delta S_e^{\ddagger}$, J mol^{-1}K^{-1}	-13 ± 61	-21.06

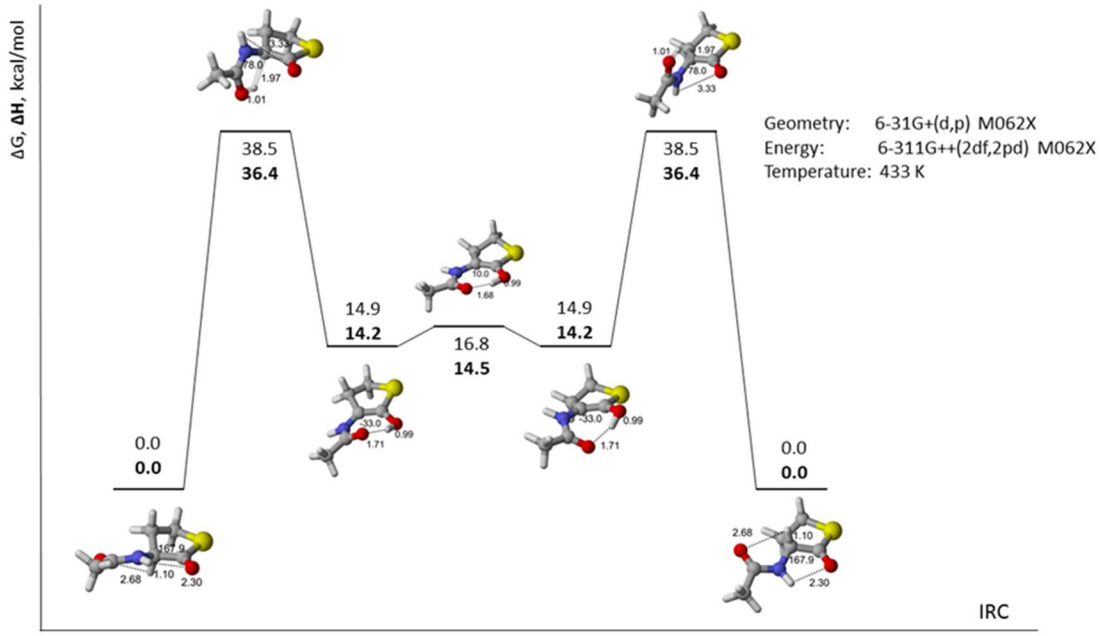

Figure 2-9: Reaction energy profile of the enatiomerization from N-acetyl-L-homocysteine thiolactone to D-enantiomer,

2.7 Conclusions

In this paper racemization of N-acetyl-L-homocysteine thiolactone has been studied and its kinetics has been described. A method for obtaining the racemization constants from the experimental data has been suggested. The results show that the kinetics of racemization at 150 ^{o}C is not affected by the material of the vial. The temperature dependence of the kinetics has been studied and the activation Gibbs energy and activation entropy has been obtained from the transition state theory. Catalytic effect of G-DP, G-BP and B-DP GC stationary phases on the racemization has been observed and quantified by the values of racemization rate constants. B-DP exhibited the greatest activity. Dynamic gas chromatography of racemic mixture of N-acetyl homocysteine thiolactone enantiomers on chiral B-DP, G-DP and G-BP capillary columns was used to study kinetic and thermodynamic enantiomerization data.

Finally, the mechanism of the racemization has been described by quantum chemical modelling. Agreement between the experimental and calculated values of activation Gibbs energy, activation enthalpy and activation entropy is good which supports the proposed mechanism.

2.8 Supplemental Materials

Table 2-S1. Relative peak areas A_L and A_D in % determined by the headspace method, detected with flame ionization detector, for the racemization of 99.5% N-Ac-L-HCTL in Teflon coated glass, glass and silanized glass vials at 150 ^{o}C.

Time	Teflon			Glass			Silanized glass		
min	A_L[%]	A_D[%]	c_D/c_L	A_L[%]	A_D[%]	c_D/c_L	A_L[%]	A_D[%]	c_D/c_L
30	95.28	4.72	0.050	95.48	0.52	0.005	95.48	0.52	0.005
60	91.09	8.91	0.098	90.28	9.72	0.108	90.27	9.73	0.108
120	82.22	17.78	0.216	80.74	19.26	0.239	80.78	19.22	0.238
180	74.57	25.43	0.341	73.79	26.21	0.355	73.77	26.23	0.356
240	69.91	30.09	0.430	68.38	31.62	0.462	68.09	31.91	0.469
300	66.88	33.12	0.495	64.17	35.83	0.558	64.83	35.17	0.542
360	64.36	35.64	0.554	60.88	39.12	0.643	60.47	39.53	0.654
420	60.60	39.40	0.650	58.31	41.69	0.715	58.31	41.69	0.715

480	58.33	41.67	0.714	56.31	43.69	0.776	56.49	43.51	0.770
540	55.86	44.14	0.790	54.75	45.25	0.826	54.39	45.61	0.839
600	54.60	45.40	0.832	53.53	46.47	0.868	53.64	46.36	0.864

Relative peak areas of A_L and A_D in % were calculated from FID responses of L and D enantiomers, *AL* and *AD*, using equations: $A_L = 100 * AL/(AL + AD)$ and $A_D = 100 * AD/(AL + AD)$.

Table 2-S2. Relative peak areas in % for racemization of 99.5% N-AcL-HCTL by batch-wise method for various temperatures in silanized glass vials.

150 °C				160 °C				170 °C			
Time min	A_L[%]	A_D[%]	c_D/c_L	Time min	A_L[%]	A_D[%]	c_D/c_L	Time min	A_L[%]	A_D[%]	c_D/c_L
30	95.51	4.49	0.047	10	95.17	4.83	0.051	10	90.95	9.05	0.100
60	90.32	9.68	0.107	30	86.58	13.42	0.155	30	75.00	25.00	0.333
120	81.94	18.06	0.220	60	77.31	22.69	0.294	60	60.87	39.13	0.643
180	75.53	24.47	0.324	90	71.02	28.98	0.408	90	54.66	45.34	0.829
240	70.52	29.49	0.418	120	66.69	33.31	0.500	120	51.97	48.03	0.924
300	66.52	33.49	0.503	150	63.63	36.37	0.572				
360	63.26	36.74	0.581	180	61.42	38.58	0.628				
420	60.57	39.43	0.651	210	59.75	40.25	0.674				
480	58.31	41.69	0.715	240	58.44	41.55	0.711				
540	56.39	43.61	0.773								
600	54.74	45.25	0.827								

Table 2-S3. Relative content of A_L and A_D enantiomers in % after thermal and catalytic racemization of 91.5% of Ac-L-HCTL and its mixture with chiral G-DP. G-BP and B-DP GC stationary phases in silanized glass head space vials at 150 °C.

Catalyst	none			+G-DP			+G-BP			+B-DP		
Time Min	A_L [%]	A_D [%]	c_D/c_L	A_L [%]	A_D [%]	c_D/c_L	A_L [%]	A_D [%]	c_D/c_L	A_L [%]	A_D [%]	c_D/c_L
10	87.3	12.66	0.145	83.0	16.99	0.205	82.15	17.85	0.217	67.12	32.88	0.49
30	80.5	19.42	0.241	72.2	27.79	0.385	70.95	29.05	0.409	55.86	44.14	0.79
60	72.7	27.22	0.374	63.6	36.31	0.57	62.40	37.60	0.603	52.68	47.32	0.898
90	67.0	32.93	0.491	59.7	40.28	0.674	58.10	41.90	0.721	51.46	48.54	0.943
120	62.9	37.07	0.589	57.3	42.61	0.742	55.58	44.42	0.799	50.82	49.18	0.968
150	59.8	40.12	0.670	55.4	44.58	0.804	53.94	46.06	0.854	50.48	49.52	0.981
180	57.6	42.40	0.736	53.5	46.43	0.867	52.82	47.18	0.893			
210	54.6	45.33	0.829	52.5	47.50	0.905	52.04	47.96	0.922			
240	53.0	46.98	0.886	51.8	48.14	0.928						
300	52.0	47.97	0.922									

Kinetic treatment of the enantiomerization of the racemic mixture

Example of enantiomerization of a racemic mixture of N-AcHCTL on G-BP capillary column at 150 °C is demonstrated below:

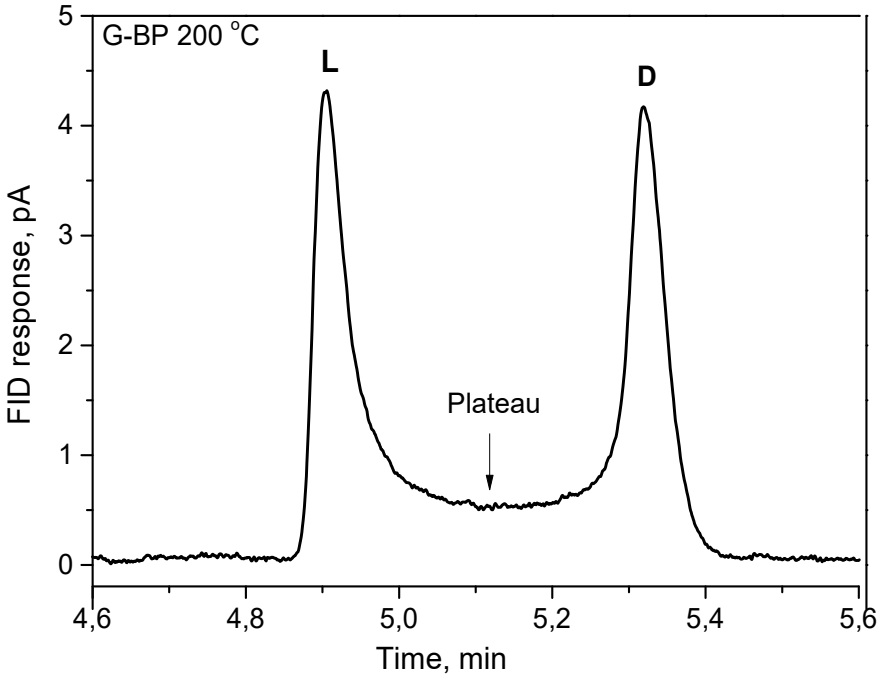

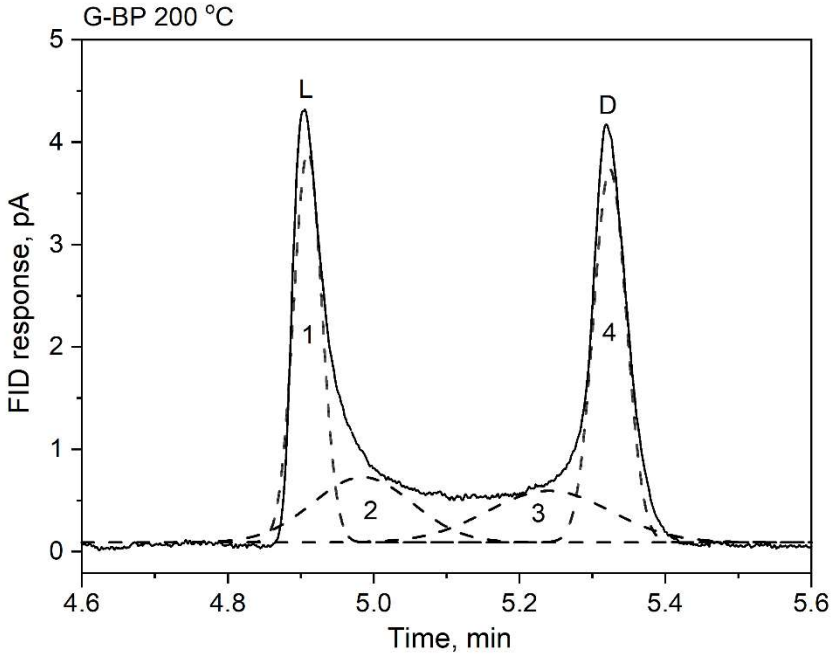

The upper Figure shows a part of the chromatogram. The bottom Figure illustrates the deconvolution procedure where there are two peaks on the non-converted enantiomers, (L and D), and two peaks (L*D* and D*L*) originated in the interconversion process.

The direct chromatographic separation of a racemic mixture of thermolabile enantiomers is known as the dynamic enantioselective chromatography. Peak areas of enantiomers determined by this method were used to calculate the apparent rate constants. Enantiomerization is the conversion of one enantiomer (L) into the enantiomer (D)

$$\mathrm{L} \xrightarrow{k^{app}_{\mathrm{L}\to\mathrm{D}}} \mathrm{D}$$

or (D) into the enantiomer (L)

$$\mathrm{D} \xrightarrow{k^{app}_{\mathrm{D}\to\mathrm{L}}} \mathrm{L}$$

where $k^{app}_{\mathrm{L}\to\mathrm{D}}$ and $k^{app}_{\mathrm{D}\to\mathrm{L}}$ are apparent enantiomerization rate constants. The apparent rate constants represent composite values of the kinetic and thermodynamic parameters of reaction paths taking place in the dynamic enantioselective chromatography, such as enantiomerization rate constants in mobile and stationary phases, distribution coefficients, etc.

In the dynamic enantioselective chromatography, the converted enantiomer is continuously separated from the original enantiomer. Hence, the pure enantiomers are converted via first-order reaction. The intermixed peaks L*D* and D*L* arise from the conversion of L and D enantiomers. Hence, the apparent rate constants are determined from the peak areas corresponding to L and D enantiomes. Foe the first-order kinetics, the rate constant can be calculated as

$$k^{app} = \frac{1}{t} \ln \frac{c_0}{c}$$

Taking into account that the enantiomerization occurs in a constant volume and that the peak area is ptoportional to the mass of the sample, the apparent rate constant of enantiomerization L to D ($k^{app}_{\mathrm{L}\rightarrow\mathrm{D}}$) can be calculated from as

$$k^{app}_{\mathrm{L}\rightarrow\mathrm{D}} = \frac{1}{t} \ln \frac{A_{\mathrm{L}0}}{A_{\mathrm{L}}}$$

An analogical equation can be used for the calculation of apparent rate constant ($k^{app}_{D\rightarrow L}$) of enantiomerization D to L

$$k^{app}_{\mathrm{D}\rightarrow\mathrm{L}} = \frac{1}{t} \ln \frac{A_{\mathrm{D}0}}{A_{\mathrm{D}}}$$

where A_0 and A are the peak areas of the enantiomer prior to and after the chromatographic separation and, t is enantiomerization time, i.e. the retention time of the enantiomer. The values of A_0 could not be measured directly and they were calculated as a half of the total peak area:

$$A_{\mathrm{L}0} = A_{\mathrm{D}0} = \left(A_{\mathrm{L}} + A_{\mathrm{LD}} + A_{\mathrm{DL}} + A_{\mathrm{D}} \right) / 2$$

The total peak area is determined experimentally, A_{L} and A_{D} are determined from the deconvolution procedure.

2.9 References

[1] J. Krupčík, P. Oswald, P. Májek, P. Sandra, D.W. Armstrong, Determination of the interconversion energy barier of enantiomers by separation methods. J. Chromatogr. A 1000 (2003) 779-800.

[2] M. Reist, B. Testa, P.A. Carrupt, M. Jung, V. Schurig, Racemization, enantiomerization, diastereomerization, and epimerization: Their meaning and pharmacological significance, Chirality 7 (1995) 396–400.

[3] J. Krupčík, J. Mydlová, P. Májek, P. Šimon, D.W. Armstrong. Methods for studying reaction kinetics in gas chromatography. Exemplified by using the 1-chloro-2,2-dimethylaziridine interconversion reaction, J. Chromatogr. A. 1186 (2008) 144-160.

[4] J. L. Bada, R. A. Schroeder, Racemization of isoleucine in calcareous marine sediments: Kinetics and mechanis. Earth and planetary science letters 15 (1972) 1-11.

[5] L. Canoira, M.J. Garcia-Martinez, J. Llamas, J. Ortiz, T.Torres, Kinetics of Amino Acid Racemization (Epimerization) in the Dentine of Fossil and Modern Bear Teeth, Int. J. Chem. Kinet., 35 (2003) 576-591.

[6] Racemization (R05030) - Gold Book – IUPAC.

[7] G.P.Moss et al., Pure Appl.Chem. 68 (1996) 2193. (Basic terminology of stereochemistry (*IUPAC* Recommendations 1996)).

[8} D. M. Abadi and P. E. Wilcox, Chemical derivatives of α-chymotrypsinogen III, reaction with N-acetyl-DL-homocysteine thiolactone, J. Biol. Chem. 235(2) (1960) 396-404.

[9] T. K. Virupaksha and H. Tarver, The reaction of insulin with N-acetyl-DL-homocysteine thiolactone: some chemical and biological properties of the products, Biochem3(10) (1964) 1507-1511.

[10] C. Ferris, M. Casas, M.J. Lucero, M.V. de Paz, M.R. Jimenez-Castellanos, Synthesis and characterization of a novel chitosan-N-acetyl-homocysteine thiolactone polymer using MES buffer, Carbohydr. Polym 111 (2014) 125-132.

[11] M.E. Boursier, J.B. Combs and H.E. Blackwell, N-acyl L-homocysteine thiolactones are potent and stable synthetic modulators of the RhlR quorum sensing receptor in Pseudomonas aeruginosa, ACS Chem. Biol. 14 (2019) 186-191.

[12] K.H. McClean, M.K. Winson, L. Fish, A. Taylor, S.R. Chhabra, M. Camara, M. Daykin, J. H. Lamb, S. Swift, B. W. Bycroft, G.S.A.B. Stewart and P. Williams, Quorum sensing and Chrornobacterium violaceurn: exploitation of violacein production and inhibition for the detection of N-acyl homoserine lactones, Microbiology 143 (1997) 3703-3711.

[13] E. Readel, A. Portillo, M. Talebi and D. W. Armstrong, Enantiomeric separation of quorum sensing autoinducer homoserine lactones using GC-MS and LC-MS, Anal. Bioanal. Chem. 412 (2020) 2927-2937.

[14] J .Krupčík, P. Oswald, I. Špánik, P. Májek, M. Bajdichová, P. Sandra, D. W. Armstrong, The Use of Computerized Peak Deconvolution for Determination of Energy Barrier to Enantiomerization in Dynamic Gas Chromatography. J. Microcol. Sep. 12 (12) (2000) 630-636.

[15] P.W.Atkins, Physical Chemistry, 6th ed., Oxford University Press. Oxford. 1998, p. 775 and p. 830.

[16] F. Gasparini, D. Misiti, M. Pierini, C. Villani. Enantiomerization barriers by dynamic HPLC. Stationary phase effect. Tetrahedron: Assymetry, 8 (1997) 2069-2073

[17] C. Ferris, M. Casas, M.J. Lucero, M.V. de Paz, M.R. Jimenez-Castellanos, Synthesis and characterization of a novel chitosan-N-acetyl-homocysteine thiolactone polymer using MES buffer, Carbohydr. Polym 111 (2014) 125 -132.

[18] M.E. Boursier, J.B. Combs and H.E. Blackwell, *N*-acyl L-homocysteine thiolactones are potent and stable synthetic modulators of the RhlR quorum sensing receptor in *Pseudomonas aeruginosa*, ACS Chem. Biol. 14 (2019) 186-191.

[19] K.H. McClean, M.K. Winson, L. Fish, A. Taylor, S.R. Chhabra, M. Camara, M. Daykin, J. H. Lamb, S. Swift, B. W. Bycroft, G.S.A.B. Stewart and P. Williams, Quorum sensing and *Chrornobacterium violaceurn*: exploitation of violacein production and inhibition for the detection of N-acyl homoserine lactones, Microbiology 143 (1997) 3703-3711.

[20] E. Readel, A. Portillo, M. Talebi and D. W. Armstrong, Enantiomeric separation of quorum sensing autoinducer homoserine lactones using GC-MS and LC-MS, Anal. Bioanal. Chem. 412 (2020) 2927-2937

[21] Spartan 14v114 (2014) Wavefunction, Inc., Irvine,

[22] Gaussian 16, Revision C,01, M.J. Frisch, G.W. Trucks, H.B, Schlegel, at al., Gaussian, Inc., Wallingford CT, 2016.

[23] a) Y. Zhao, *D.G.* Truhlar, The M06 suite of density functionals for main group thermochemistry, thermochemical kinetics, noncovalent interactions, excited states, and transition elements: two new functionals and systematic testing of four M06-class functionals and 12 other functionals, Theor. Chem. Account 120 (2008) 215–241, b) R,F. Ribeiro, A.V, Marenich, C.J,Cramer, D.G.Truhlar: Use of solution-phase vibrational frequencies in continuum models for the free energy of solvation, J. Phys. Chem. B., 115(49) (2011) 14556-4562.

[24] I. Hargittai, John A. Pople. In: Hargittai M (ed.) Candid science: conversations with famous chemists, Imperial College Press, London, 2000, p. 178–189.

Chapter 3

Enantiomeric separation of quorum sensing autoinducer homoserine lactones using GC-MS and LC-MS

3.1 Abstract

Homoserine lactones (HSLs) are signaling molecules synthesized by Gram-negative bacteria in order to communicate in a process termed “quorum sensing.” Until recently, only the L-stereoisomers of HSLs were thought to be produced and able to incite quorum sensing. However, recent studies have shown that select Gram-negative bacteria additionally produce non-trivial amounts of D-HSLs which may also play a role in quorum sensing. Current methods for the separation of HSL enantiomers cannot effectively separate all classes of HSLs and its enantiomers. More robust methods of separation and detection of D-HSLs are necessary. We have developed rapid and selective methods using liquid chromatography (LC) and gas chromatography (GC) coupled with mass spectrometry (MS) which can simultaneously enantiomerically separate all classes of HSLs. The advantages of these methods are in the MS compatibility as well as the ability to enantiomerically separate all classes of HSLs in a single run. The first enantiomeric separations of oxo- and hydroxy-HSLs by GC-MS, through the use of *N*,*O*-bis(trimethylsilyl)trifluoroacetamide–derivatizing reagents are discussed.

3.2 Introduction

Homoserine lactones (HSLs) are biologically important signaling molecules in Gram-negative bacteria [1,2,3]. When an extracellular threshold concentration is achieved, the HSLs diffuse and actively transport into the bacteria and interact with a receptor protein which initiates a communal, concerted behavior [4, 5]. Such behaviors include antibiotic production, conjugation, enzyme secretion, virulence factors, and biofilm formation [6,7,8,9,10,11,12,13,14,15,16,17,18,19]. This process has been termed “quorum sensing” (QS), as a sizeable colony is needed to achieve such collective behaviors [3]. Different types of HSLs

induce specific behaviors in various microorganisms. The HSL structure controls its function and specificity. Figure 1 shows six variants of HSLs. Note that they can be classified according to the type of alkyl side chain appended to the homoserine lactone "head group." In all cases, the alkyl portion of the side chain can vary greatly in length, typically from C4 to C18. All HSLs share a chiral center (indicated by an asterisk in Fig. 3.1) located at the alpha position of the γ-butyrolactone ring. The stereochemical nomenclature associated with this chiral center is L/D as the lactone ring is a product of an amino acid. The L/D-(hydroxy)-HSLs have an additional chiral center resulting from a hydroxy group, located at the β-position carbon of the alkyl chain (Fig. 1E). Note that the L/D-(oxo)-HSLs contain a ketone functional group at the β-position carbon of the alkyl chain. Each distinct HSL is characteristic to specific microorganisms and is used to signal for different phenotypic expressions [20].

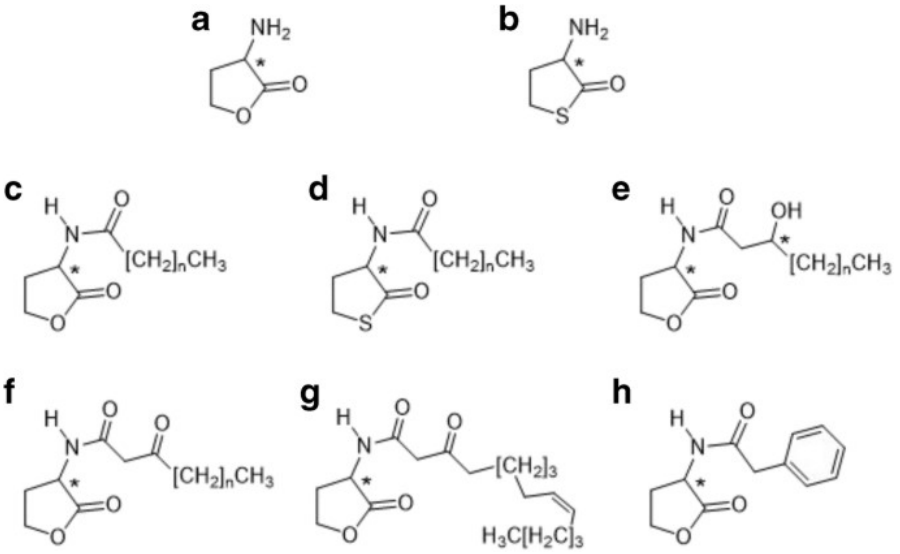

Figure 3-1 Structures of the chiral homoserine lactones and homocysteine thiolactones analyzed in this studying including (**a**) homoserine lactone moiety, (**b**) homocysteine thiolactone moiety, (**c**) L/D-(acyl)-HSL, (**d**) L/D-(acyl)-HCT, (**e**) L/D-(3-hydroxyacyl)-HSL, (**f**) L/D-(3-oxoacyl)-HSL, (**g**) L/D-(3-oxotetradec-7Z-enoyl)-HSL, and (**h**) L/D-(phenylacetyl)-HSL. Chiral centers are specified with an asterisk

The phenotypic expressions signaled by homoserine lactones during QS are exhibited by all species of Gram-negative bacteria. Colonies of Gram-negative bacteria rely on QS as a means of communication and to interact with their environment and thrive. While the phenotypes expressed through QS can be a means of survival for Gram-negative bacteria, the expression of

these phenotypes can be perilous to human health. This is especially true of opportunistic bacteria which reside within humans and thrive once conditions are suitable. One extensively studied and medically important example of this behavior involves biofilm formation. A well-known illness particularly susceptible to infection caused by Gram-negative bacteria is cystic fibrosis (CF) [21]. CF patients have increased levels of mucus within their lungs that can support colonies of Gram-negative bacteria [21,22,23]. These colonies of bacteria use QS to create a biofilm, thereby creating impenetrable mucus deposits. Consequentially, these infections are more difficult to treat using antibiotics and potential treatment options are easily exhausted [23,24,25,26].

While the exact HSL molecules and phenotypes will differ from species to species of Gram-negative bacteria, the commonality for QS is the use of HSLs as the signaling molecule [20]. It is necessary to stress that the behavior exhibited by bacteria involved in CF is not unique. In general, any opportunistic Gram-negative bacteria that have reached a high enough population density can exhibit QS [3]. Therefore, highly specific and practical chromatographic methods are necessary to analyze a broad range of HSLs.

HSLs are customarily analyzed using achiral GC-MS, LC-MS, and more recently, supercritical fluid mass spectrometry (SFC-MS) methods, because it is assumed the L-configuration is the only active stereoisomer [27,28,29,30,31]. This is the traditional assumption for many biological systems that include amino acids, which primarily exist as L-enantiomers [32, 33]. Nonetheless, a few chiral GC analyses had been developed to identify L/D-(acyl)-HSLs with chain lengths of six to twelve carbons in length [34,35,36]. In one study, Malik et al. [37] identified D-(acyl-decanoyl)-HSL in addition to the L-(acyl-decanoyl)-HSL from an extract of the Gram-negative species *Burkholderia cepacia* (*B. cepacia*). This was the first and only report of the D-stereoisomer found in *B. cepacia* but was not further pursued. A chiral LC analysis was also developed for the determination of synthetic purity of L/D-(acyl)-HSLs and L/D-(acyl)-homocysteine thiolactones (HCTs) with chain lengths of four and six carbons [38]. These chiral GC and LC methods were exclusively developed for only a few L/D-(acyl)-HSLs. Enantioselective methods have not been reported for other longer acyl chain lengths nor for other classes of

HSLs. Herein, we report the most exhaustive and complete enantiomeric separations of HSLs using new methods developed for GC-MS and LC-MS.

3.3 Experimental

3.3.1 Chemicals and Materials

Cellulose tris(3,5-dichlorophenylcarbamate) immobilized (Chiralpak IC-3) was obtained as 3-µm silica gel 250 × 4.6 mm (i.d.) column from Chiral Technologies, Inc. (West Chester, PA, USA). ZORBAX Eclipse XDB-C18 was obtained as 5-µm 150 × 4.6 mm (i.d.) column from Agilent Technologies, Inc. (Santa Clara, CA, USA). β-DEX™ 225 L × I.D. 30 m × 0.25 mm (film thickness 0.25 µm) and B-DP L × I.D. 30 m × 0.25 mm (film thickness 0.12 µm) columns were kindly provided by MilliporeSigma (Supelco, Bellefonte, PA, USA). Analytes were purchased from Sigma-Aldrich (St. Louis, MO, USA); Cayman Chemical Company (Ann Arbor, MI, USA); Chemodex (St. Gallen, Switzerland); Ark Pharm, Inc. (Arlington Heights, IL, USA); and Toronto Research Chemicals (Toronto, Canada). Standards were prepared in methanol or ethanol at 1 mg/mL for analysis. Solvents including HPLC grade ethanol (EtOH), methanol (MeOH), heptane (HEP), and all remaining reaction reagents were obtained from Sigma-Aldrich (St. Louis, MO, USA). Deionized (DI) water was obtained from a Millipore Synergy 185 water purification system (Burlington, MA, USA).

3.3.2 Chromatographic Conditions

An Agilent 1220 (Agilent Technologies, Palo Alto, CA, USA) HPLC was used to optimize all separations. It consisted of a 1200 diode array detector, autosampler, and quaternary pump. Detection was primarily analyzed at 230 nm in addition to 254 nm and 280 nm for the identification of enantiomers. A Shimadzu LC-10AT liquid chromatograph coupled to a Finnigan LXQ electrospray ionization mass spectrometry (ESI-MS) instrument was used in this study in positive ion mode. The electrospray ionization parameters were set as follows: capillary temp, 350 °C; capillary voltage, 6 V; tube lens, 65 V; and sheath gas flow rate, 15 arbitrary units. Each

analyte was screened in polar ionic mode, polar organic mode (POM), and normal phase (NP). The optimized condition for HPLC and LC-MS analysis using Chiralpak IC is 100%:0.3% ethanol:formic acid. The optimized conditions for the modified LC-MS analyses use the ZORBAX column connected to the Chiralpak IC. Analyses include a column temperature of 40 °C with an isocratic hold of either 100% acetonitrile or 85:15 methanol:water, depending on the class of HSL, until the run completed.

An Agilent 6890N (Agilent Technologies, Palo Alto, CA, USA) GC equipped with a 5975 MSD was used to carry out all separations. The optimized conditions for the *N*-(acyl)-DL, *N*-(3-oxoacyl)-DL, and *N*-(3-hydroxyacyl)-DL HSLs were done on a β-DEX™ 225 column. The oven temperature program for the *N*-(acyl)-DL, *N*-(3-oxoacyl)-DL, and *N*-(3-hydroxy)-DL HSLs is as follows: 160 °C (5 min hold) to 230 °C (90 min hold), ramp at 1 °C/min with helium at a constant flow rate of 1.1 mL/min (40 cm/s), injector temperature of 300 °C, transfer line temperature of 280 °C, MS quad temperature of 150 °C, MS source temperature of 230 °C, and electron energy of 70 eV. The separations were done in selected ion monitoring (SIM) mode at 143 m/z for the *N*-(acyl)-DL HSLs; 157, 185, 213, 241, 269, and 297 m/z for the *N*-(3-oxoacyl)-DL HSLs; and 244, 272, 300, 328, 356, and 384 m/z for the *N*-(3-hydroxyacyl)-DL HSLs.

3.3.3 Sample purification and preparation: Preparation of L/D-(acyl/3-oxoacyl/3-hydroxyacyl)-HSL and L/D-(acyl)-HCT enantiomers

A previously reported method was adapted to prepare HSL and HCT enantiomers [39]. It included a 2.0 mmol suspension of L/D-homoserine lactone moiety, or L/D-homocysteine thiolactone moiety was prepared in 10 mL acetonitrile at 0 °C. Next, 2.0 mmol of triethylamine was added and stirred into the chilled mixture for 30 min. A 2.0 mmol amount of the acyl chloride was added dropwise to the mixture and stirred for 1.5 h. The acetonitrile was rotary evaporated in a water bath of 40 °C at a pressure of 226 mbar. Residue was reconstituted in 10 mL of dichloromethane. The dissolved analyte was washed with 2× 20 mL of concentrated sodium bicarbonate solution. The organic layer was collected and dried with 2 g of magnesium

sulfate. Magnesium sulfate was removed by gravity filtration. Dichloromethane was then evaporated by blowing nitrogen to obtain the final pure synthetic product. The reaction yields for the L- and D-HCTs were 88% and 94%, respectively, while the reaction yields for L- and D-HSLs were both 95%. The starting materials for both HCTs and HSLs were enantiomerically impure and therefore influenced final yields [40]. A representative example of detection by circular dichroism to confirm the purification of the synthesized enantiomers can be found in Electronic Supplementary Material (ESM) Fig. 3.S1. Circular dichroism was performed on a Jasco CD 2095 Plus (Easton, MD, USA) chiral detector under chromatographic conditions outlined in the proceeding section "Purification of synthetic products." Confirmation of purification of the synthesized enantiomers by nuclear magnetic resonance (NMR) using the above method has been previously cited [35, 39, 41].

3.3.4 Purification of synthetic products

In efforts to obtain enantiomerically pure standards, the previous synthetic method was modified by using enantiomerically pure starting material. To increase purity, the synthesis was followed by a sample purification method: A preparatory LC method was created using the Chiralpak IC column to yield enantiomerically pure standards. Approximately 150 mg of crude synthetic product was dissolved in 1 mL of 70:30 heptane:ethanol. A series of 10 µL injection were done until enough product was collected. The modified methods were done with the Chiralpak IC and 70:30 heptane:ethanol mobile phase at a flow rate of 1 mL/min, with UV detection at 230 nm and 254 nm. The pure enantiomer was collected in a separate vessel. The mobile phase was evaporated, and the product was analyzed by LC and GC to yield an enantiomeric product of 99.5% purity.

*3.3.5 Derivatization procedure of the **L/D**-(3-oxoacyl)-HSLs and **L/D**-(3-hydroxyacyl)-HSLs*

Following the previously developed derivatization by Ruysbergh et al. [42], both the (3-oxoacyl)-HSLs and (3-hydroxyacyl)-HSLs were derivatized using *N*,*O*-bis(trimethylsilyl)trifluoroacetamide (BSTFA) and *N*,*O*-bis(trimethylsilyl) trifluoroacetamide with

trimethylchlorosilane (TMCS). This method derivatizes the oxidized group on the β-carbon with a trimethylsilyl functional group. To prepare volatile and thermally stable derivatives, 1 mL of BSTFA + 1% TMCS was added to 1 mL solution of *N*-(3-hydroxyacyl)-DL-HSLs (0.1% in DCM) and the mixture was allowed to stand for 10 min at room temperature prior to injection.

3.3.6 Quantitative evaluation of LC-MS and GC-MS methods

Representative standards, L/D-(acyl-decanoyl)-HSL, L/D-(3-oxoacyl-decanoyl)-HSL, and L/D-(3-hydroxyacyl-decanoyl)-HSL, were chosen to determine the linearity, limit of detection (LOD), and limit of quantification (LOQ) for the LC-MS and GC-MS methods. Standards for the calibration curves ranged from 0.5 ppb to 10 ppm. Quantitative evaluation for the LC-MS was performed on LCMS-8040 (Shimadzu Scientific Instruments, Columbia, MD, USA), a triple quadrupole spectrometer with electrospray ionization (ESI). LC-MS/MS was operated in the multiple reaction monitoring (MRM) mode with a positive ESI source to improve detection sensitivity. Collision energies and MRM transitions were optimized for each representative standard, and the results are summarized in ESM Table 3.S1. Quantitative evaluation for the GC-MS was performed on the previously mentioned Agilent 6890N GC-MS. Results of linearity, LODs, and LOQs are summarized in Table 3.1.

Table 3-1 Quantitative evaluation for GC-MS and LC-MS methods for select homoserine lactones

Standard[1]	**Instrument**[1]	**LOD**[2] **(nM)**	**LOQ**[2] **(nM)**	***R***[2][3]	**RSD**[4]
(Acyl-decanoyl)-HSL	LC	18	54	0.999	6.76
(3-Oxoacyl-decanoyl)-HSL	LC	8.5	25	0.999	4.86
(3-Hydroxyacyl-decanoyl)-HSL	LC	10.	30.	0.999	4.00
(Acyl-decanoyl)-HSL	GC	2.5	7.4	0.997	3.94
(3-Oxoacyl-decanoyl)-HSL	GC	180	540	0.991	3.98
(3-Hydroxyacyl-decanoyl)-HSL	GC	46	140	0.998	3.09

[(1)]Homoserine lactone name and instrument used to calculate quantitative values. All LC separations were completed using the Chiralpak IC column with an isocratic program of 100%:0.3% ethanol:formic acid and with a splitless, 1 µL injection. All GC separations were completed using a β-DEX 225 column with 1 µL injection and oven temperature program including a 5 min hold at 160 °C followed by a ramp at 1 °C/min up to 230 °C with a 90 min hold. A constant flow rate of 1.1 mL/min was maintained with helium. See "Experimental" for information regarding instrumentation [(2)]Limit of detection (LOD) was calculated as the signal-to-noise ratio is equal to 3.3 (S/N = 3), and the limit of quantitation was calculated as the signal-to-noise ratio is equal to 10 (S/N = 10). The LOD and LOQ were calculated for the L-enantiomer, and first L-enantiomer for the (3-hydroxyacyl-decanoyl)-HSL[(3)]R squared (R^2) is the correlation coefficient [(4)]Residual standard deviation (RSD) is the standard deviation of points about the fitted calibration curve

3.3.7 Data processing

Retention factors (k), selectivity (α), and resolution (R_s) were calculated for all compounds analyzed by LC-MS and GC-MS. Retention factor was calculated using $k = (t_R - t_0) / t_0$, where t_R is the retention time of the peak of interest and t_0 is the dead time of the column. Selectivity was calculated using $\alpha = k_2 / k_1$, where k_1 and k_2 refer to the retention factors of the first and second peaks, respectively. Resolution was calculated using $R_s = 2(t_{R2} - t_{R1}) / (w_1 + w_2)$, where w_1 and w_2 are the widths of the first and second peaks, respectively. Figure 3.4 has been processed by a power of 2 as previously reported [43, 44].

3.4 Results and discussion

3.4.1 GC-MS

The most complete GC-MS separation of all classes of HSLs is shown in Fig. 3.2. Most stereoisomers are baseline separated ($R_s > 1.5$) with this single method. Previously reported enantioselective methods typically had longer retention times and/or were exclusively developed for only a few (acyl)-HSLs [34,35,36]. Note that Fig. 3.2 includes the first reported separation of (3-oxoacyl)-HSL enantiomers and the first separation of (3-hydroxyacyl)-HSL stereoisomers. These β-carbon–substituted HSLs are particularly challenging to analyze due to their low volatility. The inadequate thermal stability of some chiral stationary phases designed for GC applications cannot achieve high enough temperatures to analyze these compounds. To overcome this, (3-oxoacyl)-HSLs as well as (3-hydroxyacyl)-HSLs can be derivatized with BSTFA,

thereby enhancing their volatility while maintaining thermal stability (see "Experimental"). With derivatization, the (3-oxoacyl)-HSLs with chain lengths of four to ten carbons are baseline separated and the (3-hydroxyacyl)-HSLs with chains four to fourteen carbons in length are separated using the β-DEX™ 225 column. Even with derivatization, there is a limit as retention increases to over 60 min for compounds having alkyl chains of chain lengths ten carbons or greater, and the selectivity and resolution decrease overall. One virtue of derivatization using BSTFA is the expeditious reaction, which takes less than 10 min, and appears to be universal for HSLs.

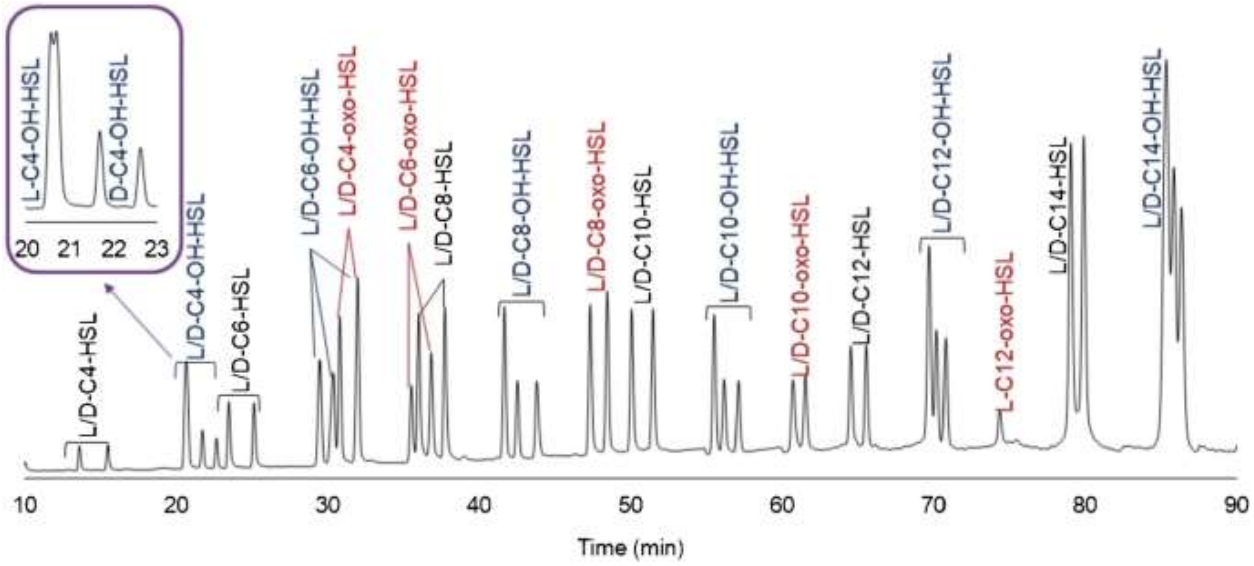

Figure 3-2 Simultaneous enantiomeric separation of sixteen racemic L/D-(acyl)-HSLs (identified in black font and as L/D-C(*n*)-HSL, where *n* denotes the number of carbons in the alkyl chain), derivatized L/D-(3-oxoacyl)-HSLs (identified in red font and as L/D-C(*n*)-oxo-HSL, where *n* denotes the number of carbons in the alkyl chain), and derivatized L/D-(3-hydroxyacyl)-HSLs (identified in blue font and as L/D-C(*n*)-hydroxy-HSL, where *n* denotes the number of carbons in the alkyl chain) using gas chromatography mass spectrometry (GC-MS). Note the L/D-(3-hydroxyacyl)-HSLs appear to have three peaks. For all L/D-(3-hydroxyacyl)-HSLs, the first peak contains both L-enantiomers while the second and third peaks are the D-enantiomers. The separations were completed using a β-DEX 225 column with oven temperature program including a 5 min hold at 160 °C followed by a ramp at 1 °C/min up to 230 °C with a 90 min hold. A constant flow rate of 1.1 mL/min was maintained with helium. See "Experimental" for more information regarding chromatographic conditions

Unlike the (acyl)-HSLs, where the MS product ion analyzed is always 143 m/z, the base peak for the derivatized HSLs changes with increasing alkyl chain length. Therefore, each

derivatized HSL will have a unique m/z that needs to be monitored using the SIM mode. Fortunately, (3-oxoacyl)-HSLs and (3-hydroxyacyl)-HSLs consistently increase by 28 m/z as the acyl chain lengthens by two carbons, making analysis not overly burdensome. This method appears to be advantageous and broadly applicable when compared to previously reported methods that analyze HSLs [34,35,36]. Overall, the method has high selectivity for the lactone ring structure and alkyl chain as displayed by the varying retention factors and selectivity (see Table 3.2).

Table 3-2 Optimized enantiomeric separations of **L**/**D**-homoserine lactones by GC-MS

Name[1]	**No. of isomers**[1]	k_1[2a]	k_2[2a]	α_2[2b]	α_3[2b]	$R_{s,2}$[2c]	$R_{s,3}$[2c]
Homoserine lactone moiety	2	8		1.13		6.9	
Homocysteine thiolactone moiety	2	10		1.06		3.7	
L/D-(Acyl-butanoyl)-HSL	2	14		1.15		15.2	
L/D-(Acyl-hexanoyl)-HSL	2	25		1.08		11.7	
L/D-(Acyl-octanoyl)-HSL	2	39		1.05		10.3	
L/D-(Acyl-decanoyl)-HSL	2	55		1.03		7.8	
L/D-(Acyl-dodecanoyl)-HSL	2	71		1.02		5.3	
L/D-(Acyl-tetradecanoyl)-HSL	2	87		1.01		3.7	
L/D-(3-Oxo-butanoyl)-HSL	2	33		1.04		7.1	
L/D-(3-Oxo-hexanoyl)-HSL	2	39		1.04		7.4	
L/D-(3-Oxo-octanoyl)-HSL	2	52		1.02		5.8	
L/D-(3-Oxo-decanoyl)-HSL	2	66		1.01		4.0	
L-(3-Oxo-dodecanoyl)-HSL	2	81		–		–	
L/D-(3-Hydroxy-butanoyl)-HSL	4	22	23	1.06	1.05	5.0	5.9
L/D-(3-Hydroxy-hexanoyl)-HSL	4	32	33	1.03	1.05	3.2	9.4
L/D-(3-Hydroxy-octanoyl)-HSL	4	45	46	1.02	1.03	3.0	7.9
L/D-(3-Hydroxy-decanoyl)-HSL	4	61	62	1.01	1.02	1.4	4.7
L/D-(3-Hydroxy-dodecanoyl)-HSL	4	77	77	1.01	1.01	1.3	1.4

Name[1]	No. of isomers[1]	k_1[2a]		α_1[2b]		$R_{s,1}$[2c]	
L/D-(3-Hydroxy-tetradecanoyl)-HSL	4	94	94	1.01	1.01	0.9	1.1

[1]Homoserine lactone name and number of isomers. All separations were completed using a β-DEX 225 column with oven temperature program including a 5 min hold at 160 °C followed by a ramp at 1 °C/min up to 230 °C with a 90 min hold. A constant flow rate of 1.1 mL/min was maintained with helium. See "Experimental" for more information regarding chromatographic conditions [2a]Calculated chromatographic parameters of the retention factor of the first peak (k_1) and of the third stereoisomer (k_2) where applicable [2b]Calculated chromatographic parameters of the selectivity of enantiomers (α_1), first and third eluting stereoisomers (α_2), and third and fourth eluting stereoisomers (α_3) [2c]Calculated chromatographic parameters of the resolution of first eluting enantiomers ($R_{s,1}$), first and third eluting stereoisomers ($R_{s,2}$), and third and fourth eluting stereoisomers ($R_{s,3}$)

The homoserine lactone and homocysteine thiolactone enantiomeric starting materials also were separated. It was found that they could be resolved on the same β-DEX™ 225 column as the alkyl-substituted HSLs, with the L-enantiomers eluting first in both cases. It should also be noted that the first eluting peak(s) for all HSL separations is the L-stereoisomer as determined by synthetically prepared L or D standards (see "Experimental"). This includes the (3-hydroxyacyl)-HSLs that have two stereogenic centers. The first two peaks are the L-stereoisomers, and the latter two peaks are the D-stereoisomers, with the L and D nomenclature referring to the chiral center of the lactone ring.

3.4.2 Interconversion of longer-chained HSLs

As the acyl chain length of substituted homoserine lactones increases, higher column temperatures are needed to elute the compounds. It was noted that compounds eluted at the highest temperatures appeared to show on-column enantiomerization of the acyl-HSLs with alkyl chain lengths greater than twelve carbons as indicated by the raised baseline between peaks (see L/D-C14-HSL in Figure 3.2). Temperature and time spent on-column play the most significant roles in on-column enantiomerization, but the stationary phase can play an additional role (data not shown). These effects are currently being studied in detail and will be reported in the future.

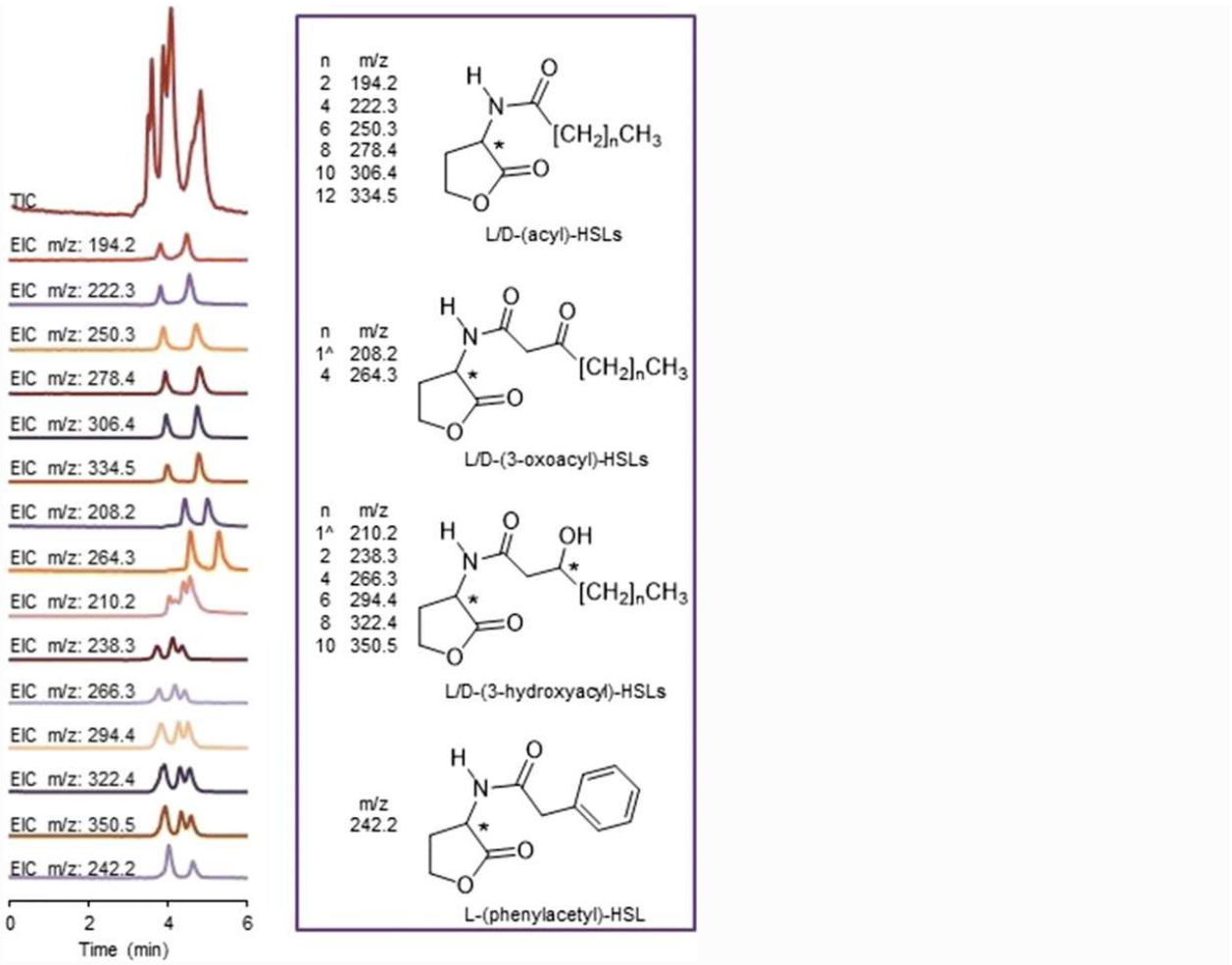

Figure 3-3 Simultaneous enantiomeric separation of a mixture containing fourteen racemic L/D-(acyl)-HSLs, L/D-(3-oxoacyl)-HSLs, and L/D-(3-hydroxyacyl)-HSLs and enantiomerically impure L-(phenylacetyl)-HSL using liquid chromatography electrospray ionization mass spectrometry (LC-ESI-MS). The top chromatogram is the total ion chromatogram (TIC), and below are the deconvoluted extracted ion chromatograms (EICs). See to the right of the chromatograms for individual structures and distinct m/z of the homoserine lactones within the mixture. Chiral centers are specified with an asterisk, and compounds that contain a CH_3 functional group only are specified with a carrot. Note the L/D-(3-hydroxyacyl)-HSLs appear to have three peaks. For all L/D-(3-hydroxyacyl)-HSLs, the first peak contains both L-enantiomers while the second and third peaks are the D-enantiomers. Note that the mixture of homoserine lactones, regardless of functional group and alkyl tail length, coelutes and has overlapping peaks. This results in ionization suppression when analyzing multiple analytes that elute at the same time. However, ionization suppression is not observed when looking at one compound. The separations were completed using a Chiralpak IC column with an isocratic program of 100%:0.3% ethanol:formic acid with a flow rate of 1.0 mL/min and split injection prior to electrospray ionization. See "Experimental" for more information regarding chromatographic conditions.

3.4.3 LC-MS

The first reported LC-MS compatible method for all classes of HSLs is shown in Figure 3.3. The HSLs analyzed are all sodium ion adducts as these produced the strongest m/z response. As previously reported for two *n*-alkyl HSLs, other types of HSLs can be separated using a cellulose-based chiral stationary phase [38]. However, the previous separations were exclusively done in the normal phase mode. The proposed method herein uses the polar organic mode, making it amenable to electrospray ionization mass spectrometry detection. The method was subsequently applied to a more sensitive triple quadrupole MS/MS technique (see ESM Table 3.S1) as HSLs have been previously profiled by a linear ion trap quadrupole and Fourier transform ion cyclotron resonance mass spectrometer (LTQ-FTICR) [29, 30]. Further, it is extended to include many alkyl chain lengths of (acyl)-HSLs in addition to (3-oxoacyl)-HSLs and (3-hydroxyacyl)-HSLs (see Table 3.3). The developed LC-MS method analyzes (3-oxoacyl)-HSLs with acyl chain lengths from four to sixteen carbons in length with excellent baseline resolution and (3-hydroxyacyl)-HSLs with acyl chain lengths from four to fourteen carbons in length in under 6 min without derivatization (see Table 3.3 and Figure 3.3). While other chain lengths were not screened, as they were not available, the method suggests high specificity of HSLs as long as they have an appended alkyl chain.

Table 3-3 Optimized enantiomeric separations of L/D-homoserine lactones by LC-MS

Name[1]	**No. of isomers**[1]	k_1[2a]	α_1[2b]	$R_{s,1}$[2c]
L/D-(Acyl-butanoyl)-HSL	2	0.20	2.10	6.23
L/D-(Acyl-hexanoyl)-HSL	2	0.20	2.32	6.67
L/D-(Acyl-heptanoyl)-HSL	2	0.21	2.22	6.70
L/D-(Acyl-octanoyl)-HSL	2	0.23	2.24	6.95
L/D-(Acyl-decanoyl)-HSL	2	0.25	2.18	6.86
L/D-(Acyl-dodecanoyl)-HSL	2	0.26	2.04	6.05
L/D-(Acyl-tetradecanoyl)-HSL	2	0.27	2.01	5.98
L/D-(Acyl-hexadecanoyl)-HSL	2	0.24	2.01	4.01

Name[1]	No. of isomers[1]	k_1[2a]		α_1[2b]		$R_{s,1}$[2c]	
L/D-(Acyl-octadecanoyl)-HSL	2	0.24		2.01		3.57	
L/D-(3-Oxoacyl-butanoyl)-HSL	2	0.42		1.45		2.88	
L/D-(3-Oxoacyl-hexanoyl)-HSL	2	0.43		1.51		3.24	
L/D-(3-Oxoacyl-octanoyl)-HSL	2	0.44		1.54		3.51	
L/D-(3-Oxoacyl-decanoyl)-HSL	2	0.46		1.53		3.49	
L/D-3-(Oxoacyl-dodecanoyl)-HSL	2	0.47		1.51		3.45	
L-3-(Oxoacyl-tetradecanoyl)-HSL	2	0.48		–		–	
L/D-(3-Oxoacyl-hexadecanoyl)-HSL	2	0.49		1.48		3.39	
L/D-(Oxo-tetradec-7Z-enoyl)-HSL	2	0.23		2.00		3.45	
L-(Phenylacetyl)-HSL	2	0.23		1.84		2.34	
		k_1[2a]	k_2[2a]	α_2[2b]	α_3[2b]	$R_{s,2}$[2c]	$R_{s,3}$[2c]
L/D-(3-Hydroxyacyl-butanoyl)-HSL	4	0.14	0.24	1.56	1.21	1.06	0.70
L/D-(3-Hydroxyacyl-hexanoyl)-HSL	4	0.16	0.26	1.76	1.27	0.76	0.36
L/D-(3-Hydroxyacyl-octanoyl)-HSL	4	0.17	0.28	1.65	1.27	0.90	0.54
L/D-(3-Hydroxyacyl-decanoyl)-HSL	4	0.18	0.31	1.67	1.27	0.94	0.51
L/D-(3-Hydroxyacyl-dodecanoyl)-HSL	4	0.19	0.34	1.70	1.25	1.07	0.54
L/D-(3-Hydroxyacyl-tetradecanoyl)-HSL	4	0.20	0.34	1.62	1.24	1.13	0.60

[1]Homoserine lactone name and number of isomers. All separations were completed using a Chiralpak IC column with an isocratic program of 100%:0.3% ethanol:formic acid with a flow rate of 1.0 mL/min and split injection prior to electrospray ionization. See "Experimental" for more information regarding chromatographic conditions [2a]Calculated chromatographic parameters of the retention factor of the first peak (k_1) and of the third stereoisomer (k_2) where applicable [2b]Calculated chromatographic parameters of the selectivity of enantiomers (α_1), first and third eluting stereoisomers (α_2), and third and fourth eluting stereoisomers (α_3) [2c]Calculated chromatographic parameters of the resolution of first eluting enantiomers ($R_{s,1}$), first and third eluting stereoisomers ($R_{s,2}$), and third and fourth eluting stereoisomers ($R_{s,3}$)

The separations of unsubstituted homoserine lactone and homocysteine thiolactone enantiomers were previously reported by our group [40]. Unlike the alkyl-substituted HSLs and HCTs, they were separated and best optimized on the LarihcShell-P and NicoShell chiral stationary phases. The moieties were screened on the Chiralpak IC column but did not show selectivity. Likewise, the alkyl chain HSLs did not have selectivity for the macrocyclic glycopeptide chiral stationary phases, indicating the importance of the alkyl chain to chiral recognition, or the lack thereof, on different chiral stationary phases.

Individual L or D standards were made to determine the elution order of the alkyl HSLs. It was found that the L-enantiomers eluted first in all cases. The retention factors for all L-stereoisomers, regardless of alkyl chain length, were similar (Figure 4.3). Likewise, all the D-stereoisomers had similar retention behaviors. Effectively, the short retention factors allow for quick analyses of individual compounds. However, there is an undesirable effect when analyzing multiple compounds in a single run, which is ionization suppression due to coelution. In Figure 4.3, it appears that the ionization suppression is greatest for the L-stereoisomer peak(s); however, the D-stereoisomer peaks are also affected. Ionization suppression is the direct result of partitioning of the surfactant-like HSLs to the solvent-air interface during electrospray ionization processes [45, 46]. Effectively, this could limit the application of the developed LC-MS method as a tool for quantitative analysis of HSLs. Fortunately, it was found that achiral separation of all homologues of acyl-HSLs could be achieved on a short reversed-phase precolumn using 100% acetonitrile mobile phase for the chiral separation. This result is shown in Figure 4.4. Likewise, the (3-oxoacyl)-HSLs and (3-hydroxyacyl)-HSLs achieve chiral separation with the same dual-column configuration. Instead, they best resolve using a modified polar organic mobile phase. These results are shown in ESM Figs. 3.S2 and 3.S3. Retentions can be adjusted by adding very small amounts of water to the mobile phase. For all discussed modified methods, resolution is minimally sacrificed when using this achiral-chiral–coupled column approach.

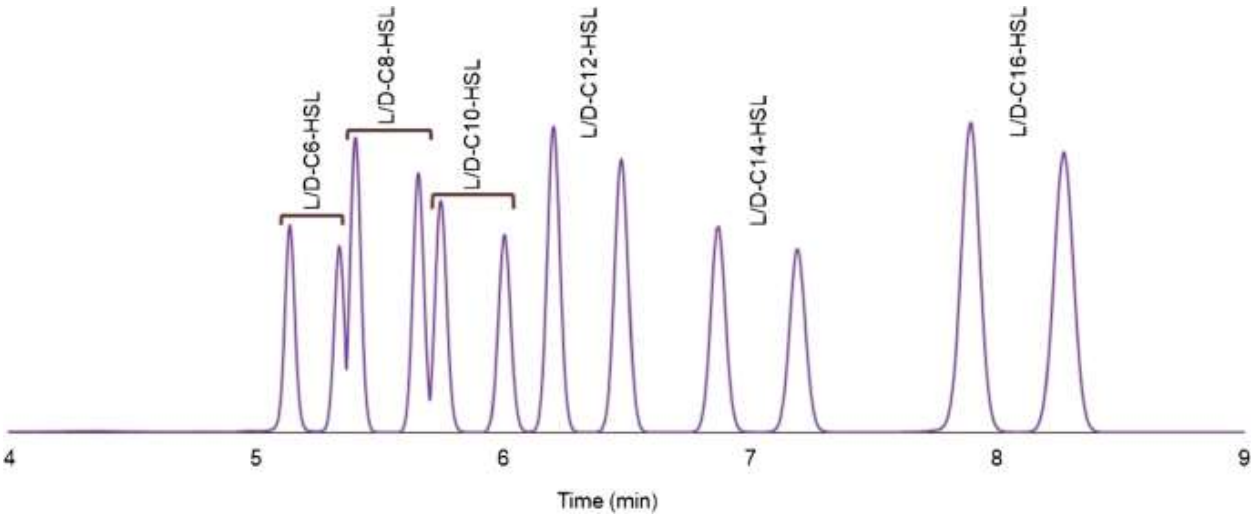

Figure 3-4 Simultaneous enantiomeric separation of six racemic L/D-(acyl)-HSLs (identified as L/D-C(*n*)-HSL, where *n* denotes the number of carbons in the alkyl chain) on the 15-cm ZORBAX C18 reversed-phase column coupled to the Chiralpak IC with a modified mobile phase conditions using high-performance liquid chromatography (HPLC). The isocratic program includes 100% acetonitrile for 10 min with a flow rate of 1.0 mL/min analyzed at 230 nm. See "Experimental" for more information regarding chromatographic conditions

3.5 Further application of developed LC and GC methods

3.5.1 Separation of (acyl)-HCTs

To further demonstrate the high selectivity of each method for the lactone functional group of the (acyl)-homoserine lactones, a relevant separation for a similar class of compounds, the (acyl)-homocysteine thiolactones, was considered. The (acyl)-HCTs are analogous in structure to the (acyl)-HSLs but instead contain a sulfur in the lactone ring in place of oxygen. The racemic HCTs were synthesized using the HCT moiety as starting material to which different substituents were added (see "Experimental"). As with the (acyl)-HSLs, there is retention, selectivity, and high resolution for all enantiomers using the aforementioned developed LC-MS and GC-MS methods (Table 3.4). Similar to the LC-MS separations of the (acyl)-HSLs, the (acyl)-HCT's homologs have similar retention behavior with increasing enantioselectivity for mid-chain length homologues and decreasing selectivity as the chain lengthens. Overall, GC-MS and LC-

MS methods have high selectivity for both HSLs and HCTs and are promising methods for other compounds that contain lactone-related functional groups.

Table 3-4 Optimized enantiomeric separations of **L/D**-(acyl)-homocysteine thiolactones by GC-MS and LC-MS

Name[1]	Instrument[1]	k_1[2a]	α[2b]	R_s[2c]
L/D-(Acyl-ethanoyl)-HCT	LC	0.15	1.22	1.0
	GC	15.3	1.10	15.7
L/D-(Acyl-butanoyl)-HCT	LC	0.15	1.07	1.6
	GC	18.8	1.11	20.5
L/D-(Acyl-hexanoyl)-HCT	LC	0.14	1.05	1.8
	GC	28.6	1.05	14.7
L/D-(Acyl-octanoyl)-HCT	LC	0.14	1.56	2.1
	GC	38.1	1.03	9.8
L/D-(Acyl-decanoyl)-HCT	LC	0.13	1.65	2.4
	GC	47.2	1.01	6.5

[1]Homocysteine thiolactone name and instrument. GC-MS separations were completed using a β-DEX 225 column with oven temperature program including a 5 min hold at 160 °C followed by a ramp at 1 °C/min up to 230 °C with a 90 min hold. A constant flow rate of 1.1 mL/min was maintained with helium. The LC-MS separations were completed using a Chiralpak IC column with an isocratic program of 100%:0.3% ethanol:formic acid with a flow rate of 1.0 mL/min and split injection prior to electrospray ionization. See "Experimental" for more information regarding chromatographic conditions [2a]Calculated chromatographic parameters of the retention factor of the first peak (k_1) [2b]Calculated chromatographic parameters of the selectivity of enantiomer pair (α) [2c]Calculated chromatographic parameters of the resolution of enantiomer pair (R_s)

3.6 Conclusions

Analysis by gas and liquid chromatography mass spectrometry is clearly applicable for the enantiomeric analysis of a broad range of acyl homoserine lactones and homocysteine thiolactones. Previous LC methods for the separation of HSLs were not MS compatible and thus were unable to simultaneously identify all classes of HSLs in a single run. The rapid analysis time of this method and its ability to separate HSLs using a single, highly selective chiral stationary phase makes it suitable for quick screening procedures. Previously reported GC methods published had selectivity only for the (acyl)-HSLs and were unable to resolve the (3-oxoacyl)- and (3-hydroxyacyl)-HSLs. With an expeditious reaction using BSTFA and TMCS, all β-substituted HSLs can also be separated using the developed method. In total, the LC method separated twenty-nine HSLs and HCTs while the GC method separated twenty-three HSLs and HCTs. The GC and LC methods are complimentary to one another and can be used for the effective analysis of a broad range of HSLs.

3.7 Supplemental Materials

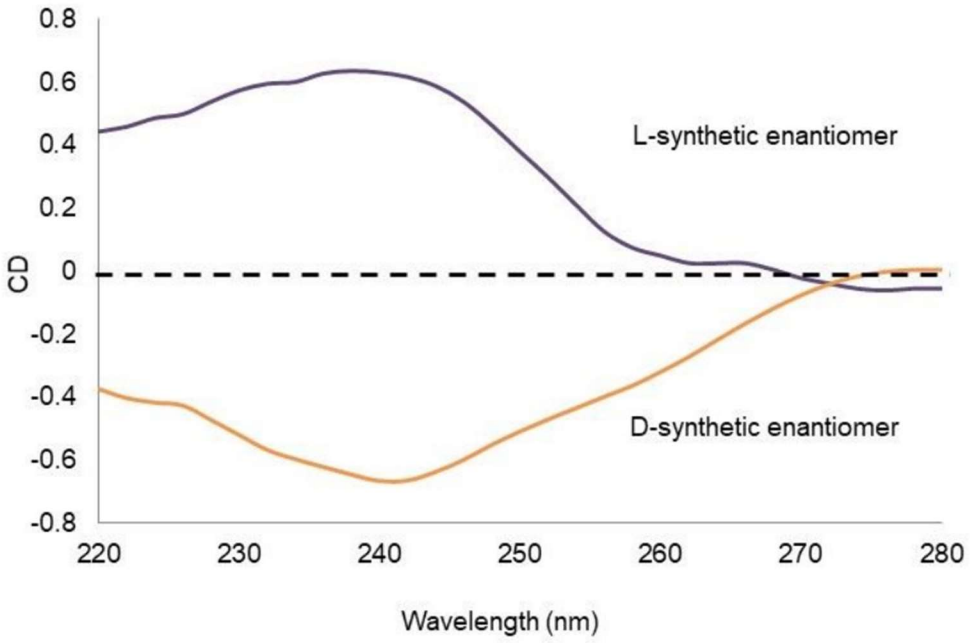

Figure 3-S1 Circular dichroism spectra for L/D-(acyl-ethanoyl)-HCT [(L) synthetic enantiomer indicated in purple and (D) synthetic enantiomer indicated in yellow]

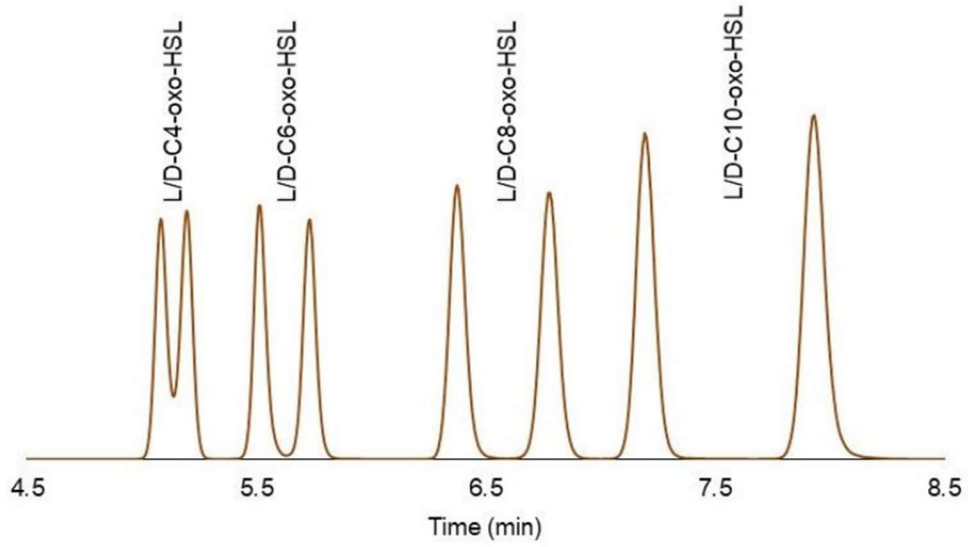

Figure 3-S2 Simultaneous enantiomeric separation of four racemic L/D-(3-oxoacyl)-HSLs (identified as L/D-C(n)-oxo-HSL, where n denotes the number of carbons in the alkyl chain) on the reverse phase column coupled to the Chiralpak IC with a modified mobile phase conditions using high performance liquid chromatography (HPLC). The isocratic program includes 85:15 methanol:water for 10 minutes with a flow rate of 1.0 mL/minute analyzed at 230 nm. See "Experimental" for more information regarding chromatographic conditions

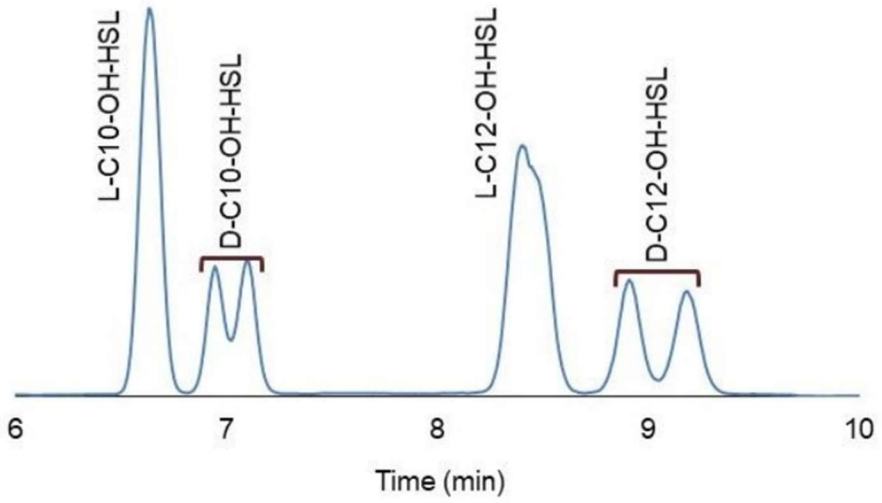

Figure 3-S3 Simultaneous enantiomeric separation of four racemic L/D-(3-hydroxyacyl)-HSLs (identified as L/D-C(n)-OH-HSL, where n denotes the number of carbons in the alkyl chain) on the reverse phase column coupled to the Chiralpak IC with a modified mobile phase conditions using high performance liquid chromatography (HPLC). The isocratic program includes 85:15 methanol:water for 10 minutes with a flow rate of 1.0 mL/minute analyzed at 230 nm. Note the L/D-(3-hydroxyacyl)-HSLs appear to have three peaks. For all L/D-(3-hydroxyacyl)- HSLs the first peak contains both L enantiomers while the second and third peaks are the D enantiomers. See "Experimental" for more information regarding chromatographic conditions

Table 3-S1 Results of MRM optimization on Shimadzu LCMS-8040

Standard[1]	Precursor (m/z)	Product (m/z)	Q1[2] (V)	CE[2]	Q3[2] (V)
(acyl-decanoyl)-HSL	256.05 [M^{+1}]	102.05 [M + H – 154.00]	-29	-12	-28
(3-oxoacyl-decanoyl)-HSL	269.85 [M^{+1}]	102.00 [M + H – 167.85]	-28	-11	-14
(3-hydroxyacyl-decanoyl)-HSL	272.05 [M^{+1}]	101.95 [M + H – 170.10]	-14	-13	-15

[1]Homoserine lactones subject to HPLC-MS/MS on LCMS-8040 (Shimadzu Scientific Instruments, Columbia, MD) triple quadrupole spectrometer with electrospray ionization (ESI). The drying gas and nebulizing gas flow rate were 15 L/min and 2 L/min, respectively; the desolvation line temperature and heat block temperature were 250 °C and 400 °C, respectively. HPLC-MS/MS was operated in multiple reaction monitoring (MRM) mode with a positive ESI source.

[2]Mass spectrometry parameters for quadrupoles 1 and 3 (Q1 and Q3, respectively) and collision energy (CE).

3.8 References

1. Joint I, Allan Downie J, Williams P. Bacterial conversations: talking, listening and eavesdropping. An introduction. Philos Trans R Soc Lond Ser B Biol Sci. 2007;362(1483):1115–7. https://doi.org/10.1098/rstb.2007.2038.

2. Ng WL, Bassler BL. Bacterial quorum-sensing network architectures. Annu Rev Genet. 2009;43:197–222. https://doi.org/10.1146/ annurev-genet-102108-134304.

3. Turovskiy Y, Kashtanov D, Paskhover B, Chikindas ML. Quorum sensing: fact, fiction, and everything in between. Adv Appl Microbiol. 2007;62:191–234. https://doi.org/10.1016/S0065-2164(07)62007-3.

4. Fuqua C, Greenberg EP. Listening in on bacteria: acyl-homoserine lactone signalling. Nat Rev Mol Cell Biol. 2002;3(9):685–95. https://doi.org/10.1038/nrm907.

5. Henke JM, Bassler BL. Bacterial social engagements. Trends Cell Biol. 2004;14(11):648–56. https://doi.org/10.1016/j.tcb.2004.09. 012.

6. Swift S, Throup JP, Williams P, Salmond GP, Stewart GS. Quorum sensing: a population-density component in the determination of bacterial phenotype. Trends Biochem Sci. 1996;21(6):214–9.

7. Atkinson S, Chang CY, Sockett RE, Camara M, Williams P. Quorum sensing in Yersinia enterocolitica controls swimming and swarming motility. J Bacteriol. 2006;188(4):1451–61. https://doi. org/10.1128/JB.188.4.1451-1461.2006.

8. Nicas TI, Iglewski BH. The contribution of exoproducts to virulence of Pseudomonas aeruginosa. Can J Microbiol. 1985;31(4): 387–92. https://doi.org/10.1139/m85-074.

9. Van Delden C, Iglewski BH. Cell-to-cell signaling and Pseudomonas aeruginosa infections. Emerg Infect Dis. 1998;4(4): 551–60. https://doi.org/10.3201/eid0404.980405.

10. Ochsner UA, Koch AK, Fiechter A, Reiser J. Isolation and characterization of a regulatory gene affecting rhamnolipid biosurfactant synthesis in Pseudomonas aeruginosa. J Bacteriol. 1994;176(7): 2044–54. https://doi.org/10.1128/jb.176.7.2044-2054.1994

11. Kohler T, Curty LK, Barja F, van Delden C, Pechere JC. Swarming of Pseudomonas aeruginosa is dependent on cell-to-cell signaling and requires flagella and pili. J Bacteriol. 2000;182(21):5990–6. https://doi.org/10.1128/jb.182.21.5990-5996.2000.

12. Stickler DJ, Morris NS, McLean RJ, Fuqua C. Biofilms on indwelling urethral catheters produce quorum-sensing signal molecules in situ and in vitro. Appl Environ Microbiol. 1998;64(9):3486–90.

13. McLean RJ, Whiteley M, Stickler DJ, Fuqua WC. Evidence of autoinducer activity in naturally occurring biofilms. FEMS Microbiol Lett. 1997;154(2):259–63. https://doi.org/10.1111/j. 1574-6968.1997.tb12653.x.

14. Bachofen R, Schenk A. Quorum sensing autoinducers: do they play a role in natural microbial habitats? Microbiol Res. 1998;153(1): 61–3.

15. Parker WL, Rathnum ML, Wells JS, Trejo WH, Principe PA, Sykes RB. Sq 27,860, a simple carbapenem produced by species of Serratia and Erwinia. J Antibiot. 1982;35(6):653–60. https://doi. org/10.7164/antibiotics.35.653.

16. Axelrood PE, Rella M, Schroth MN. Role of antibiosis in competition of Erwinia strains in potato infection courts. Appl Environ Microbiol. 1988;54(5):1222–9.

17. Hines DA, Saurugger PN, Ihler GM, Benedik MJ. Genetic-analysis of extracellular proteins of Serratia marcescens. J Bacteriol. 1988;170(9):4141–6. https://doi.org/10.1128/jb.170.9.4141-4146. 1988.

18. Givskov M, Eberl L, Molin S. Control of exoenzyme production, motility and cell differentiation in Serratia liquefaciens. FEMS Microbiol Lett. 1997;148(2):115–22. https://doi.org/10.1016/ S0378-1097(96)00530-7.

19. Givskov M, Olsen L, Molin S. Cloning and expression in Escherichia coli of the gene for extracellular phospholipase A1 from Serratia liquefaciens. J Bacteriol. 1988;170(12):5855–62. https://doi.org/10.1128/jb.170.12.5855-5862.1988.

20. Miller MB, Bassler BL. Quorum sensing in bacteria. Annu Rev Microbiol. 2001;55:165–99.

21. Lyczak JB, Cannon CL, Pier GB. Lung infections associated with cystic fibrosis. Clin Microbiol Rev. 2002;15(2):194–222. https:// doi.org/10.1128/Cmr.15.2.194-222.2002.

22. Worlitzsch D, Tarran R, Ulrich M, Schwab U, Cekici A, Meyer KC, et al. Effects of reduced mucus oxygen concentration in airway Pseudomonas infections of cystic fibrosis patients. J Clin Invest. 2002;109(3):–317, 325. https://doi.org/10.1172/Jci200213870.

23. Hoiby N, Ciofu O, Bjarnsholt T. Pseudomonas aeruginosa biofilms in cystic fibrosis. Future Microbiol. 2010;5(11):1663–74. https:// doi.org/10.2217/Fmb.10.125.

24. Cutting GR. Cystic fibrosis genetics: from molecular understanding to clinical application. Nat Rev Genet. 2015;16(1):45–56. https:// doi.org/10.1038/nrg3849.

25. Brooun A, Liu SH, Lewis K. A dose-response study of antibiotic resistance in Pseudomonas aeruginosa biofilms. Antimicrob Agents Ch. 2000;44(3):640–6. https://doi.org/10.1128/Aac.44.3.640-646. 2000.

26. Xu KD, McFeters GA, Stewart PS. Biofilm resistance to antimicrobial agents. Microbiol. 2000;146:547–9. https://doi.org/10.1099/ 00221287-146-3-547.

27. Cataldi TRI, Bianco G, Frommberger M, Schmitt-Kopplin P. Direct analysis of selected N-acyl-L-homoserine lactones by gas chromatography/mass spectrometry. Rapid Commun Mass Sp. 2004;18(12):1341–4. https://doi.org/10.1002/rcm.1480.

28. Cataldi TRI, Blanco G, Palazzo L, Quaranta V. Occurrence of N-acyl-L-homoserine lactones in extracts of some Gram-negative bacteria evaluated by gas chromatography-mass spectrometry. Anal Biochem. 2007;361(2):226–35. https://doi.org/10.1016/j.ab.2006. 11.037.

29. Cataldi TRI, Bianco G, Abate S. Profiling of N-acyl-homoserine lactones by liquid chromatography coupled with electrospray ionization and a hybrid quadrupole linear ion-trap and Fouriertransform ion-cyclotron-resonance mass spectrometry (LC-ESI-LTQ-FTICR-MS). J Mass Spectrom. 2008;43(1):82–96.

30. Cataldi TR, Bianco G, Abate S. Accurate mass analysis of N-acyl-homoserine-lactones and cognate lactone-opened compounds in bacterial isolates of Pseudomonas aeruginosa PAO1 by LC-ESILTQ-FTICR-MS. J Mass Spectrom. 2009;44(2):182–92. https:// doi.org/10.1002/jms.1479.

31. Hoang TPT, Barthelemy M, Lami R, Stien D, Eparvier V, Touboul D. Annotation and quantification of N-acyl homoserine lactones implied in bacterial quorum sensing by supercritical-fluid chromatography coupled with high-resolution mass spectrometry. Anal Bioanal Chem. 2020.

32. Corrigan JJ. D-amino acids in animals. Science. 1969;164(3876): 142–9. https://doi.org/10.1126/science.164.3876.142.

33. Cline DB. On the physical origin of the homochirality of life. Eur Rev. 2005;13:49–59.

34. Pomini AM, Manfio GP, Araujo WL, Marsaioli AJ. Acyl-homoserine lactones from Erwinia psidii R. IBSBF 435T, a guava phytopathogen (Psidium guajava L.). J Agric Food Chem. 2005;53(16):6262–5. https://doi.org/10.1021/jf050586e.

35. Pomini AM, Paccola-Meirelles LD, Marsaioli AJ. Acyl-homoserine lactones produced by Pantoea sp. isolated from the “maize white spot” foliar disease. J Agric Food Chem. 2007;55(4):1200–4. https://doi.org/10.1021/jf063136a.

36. Gotz C, Fekete A, Gebefuegi I, Forczek ST, Fuksova K, Li X, et al. Uptake, degradation and chiral discrimination of N-acyl-D/Lhomoserine lactones by barley (Hordeum vulgare) and yam bean (Pachyrhizus erosus) plants. Anal Bioanal Chem. 2007;389(5): 1447–57. https://doi.org/10.1007/s00216-007-1579-2.

37. Malik AK, Fekete A, Gebefuegi I, Rothballer M, Schmitt-Kopplin P. Single drop microextraction of homoserine lactones based quorum sensing signal molecules, and the

separation of their enantiomers using gas chromatography mass spectrometry in the presence of biological matrices. Microchim Acta. 2009;166(1–2):101–7. https://doi.org/10.1007/s00604-009-0183-x.

38. Ikeda T, Kajiyama K, Kita T, Takiguchi N, Kuroda A, Kato J, et al. The synthesis of optically pure enantiomers of N-acyl-homoserine lactone autoinducers and their analogues. Chem Lett. 2001;(4): 314–5. https://doi.org/10.1246/Cl.2001.314.

39. Yu L, Zhang Z, You YZ, Hong CY. Synthesis of sequence-controlled polymers via sequential thiol-ene and amino-yne click reactions in one pot. Eur Polym J. 2018;103:80–7.

40. Thakur N, Patil RA, Talebi M, Readel ER, Armstrong DW. Enantiomeric impurities in chiral catalysts, auxiliaries, and synthons used in enantioselective syntheses. Part 5. Chirality. 2019;31(9):688–99. https://doi.org/10.1002/chir.23086.

41. Hofer S, Ronacher A, Horak J, Graalfs H, Lindner W. Static and dynamic binding capacities of human immunoglobulin G on polymethacrylate based mixed-modal, thiophilic and hydrophobic cation exchangers. J Chromatogr A. 2011;1218(49):8925–36. https://doi.org/10.1016/j.chroma.2011.06.012. 42. Ruysbergh E, Stevens CV, De Kimpe N, Mangelinckx S. Synthesis and analysis of stable isotope-labelled N-acyl homoserine lactones. RSC Adv. 2016;6(77):73717–30.

43. Wahab MF, Berthod A, Armstrong DW. Extending the power transform approach for recovering areas of overlapping peaks. J Sep Sci. 2019. https://doi.org/10.1002/jssc.201900799. 2936 Readel E. et al.

44. Wahab MF, Gritti F, O'Haver TC, Hellinghausen G, Armstrong DWJC. Power law approach as a convenient protocol for improving peak shapes and recovering areas from partially resolved peaks. Chromatographia. 2019;82(1):211–20. https://doi.org/10.1007/ s10337-018-3607-0.

45. Rundlett KL, Armstrong DW. Mechanism of signal suppression by an ionic surfactants in capillary electrophoresis electrospray ionization mass spectrometry. Anal Chem. 1996;68(19):3493–7.

46. Xu CD, Guo HY, Breitbach ZS, Armstrong DW. Mechanism and sensitivity of anion detection using rationally designed unsymmetrical dications in paired ion electrospray ionization mass spectrometry. Anal Chem. 2014;86(5):2665–72.

Chapter 4

Production of both L- and D-*N*-acyl-homoserine lactones by *B. cepacia* and *V. fischeri*

4.1 Abstract

Quorum sensing (QS) is a complex process in which signaling molecules, as L-*N*-acyl-homoserine lactones (L-AHLs), are produced as essential signaling molecules allowing bacteria to detect and respond to cell population density by gene regulation. Few studies have considered the natural production and role of the opposite enantiomer, D-AHLs. In this work, production of D,L-AHLs by *B. cepacia* and *V. fisheri* were monitored over time, with significant amounts of D-AHLs detected. Bioluminescence of *V. fischeri* was observed with maximum bioluminescence correlating with the maximum concentrations of both L- and D- octanoyl-homoserine lactones (L- and D-OHL). L-Methionine, a precursor to L-AHLs, was examined via supplementation studies conducted by growing three parallel cultures of *B. cepacia* in M9 minimal media with added L-, D-, or D,L-methionine and observing their effect on *B. cepacia* D,L-AHL production. The results show that addition of any methionine (L-, D-, or D,L-) does not affect the overall ratio of L- to D-AHLs, i.e. D-AHL production was not selectively enhanced by D-methionine addition. However, the overall AHL (L- and D-) concentration does increase with the addition of any methionine supplement. These findings indicate the possibility of a distinct biosynthetic pathway for D-AHL production, possibly exposing a new dimension within bacterial communication.

4.2 Introduction

Bacteria perceive and react to their surroundings by chemical signals (Taga & Bassler, 2003). When faced with environmental stress or changes, bacterial cells can act quickly, adapting, either by changing their structure, physiology, or behavior for survival. Two landmark papers, on bacterial signaling, proposed that bacteria communicate with each other via self-produced signaling molecules (Nealson, Platt & Hastings, 1970; Tomasz, 1965) called autoinducers. This phenomenon, now known as quorum sensing (QS), has been extensively studied and is reasonably well understood (Fuqua, Winans & Greenberg, 1994; Mukherjee & Bassler, 2019; Whiteley, Diggle & Greenberg, 2017). QS is described as the bacteria's ability to sense their population based on the concentration of autoinducers present in their environment. When a critical amount has been reached, the bacteria will jointly express a phenotype. Bioluminescence in Vibrio fischeri or biofilm production in Burkholderia cepacia are examples of two phenotypes that can be expressed (Lewenza, Conway, Greenberg, & Sokol, 1999; Li et al., 2018).

N-acyl-homoserine lactones (AHLs) are a widely studied class of autoinducer molecules in gram-negative bacteria (Fuqua & Greenberg, 2002). The biological precursor for AHLs is S-adenosylmethionine (SAM). Figure 1 shows the general structure of AHLs which consists of a γ-butyrolactone moiety with an acylated α-amino group. The acyl chain length varies from 4 to 14 carbons. However, longer chain lengths up to 18 carbons have been reported (Mohamed et al., 2008). The α-carbon on the lactone ring is a stereogenic center. Chemically, AHLs can exist in either the L- or D- configuration. It is well known that chiral proteogenic amino acids in all organisms are primarily L-amino acids. Until recently, bacteria were believed to produce only the L-form of AHLs for QS. This belief led researchers to conduct studies using, almost exclusively, achiral methods (Liu et al., 2018). Most AHL analyses from bacterial matrices are currently conducted using achiral thin layer chromatography combined with biosensor strains, GC-MS, LC-MS, or SFC-MS (Charlton et al., 2000; Gao et al., 2020; Hoang et al., 2020; Zhou et al., 2020). To the best of our knowledge, only one study has mentioned the presence of D-AHL, i.e., D-decanoyl-homoserine lactone detected in a culture of B. cepacia LA3. The experiment

used a single drop microextraction techniques and chiral GC-MS (Malik et al., 2009). They postulated that bacteria could biosynthesize D-AHL as well as precursor D-methionine derivatives. Other studies have shown the biosynthesis of D-amino acids (Armstrong et al., 1993; Hernández & Cava, 2016; Weatherly et al., 2017).

A thorough investigation on the natural production of all manner of D-AHLs and L-AHLs is necessary to better understand the QS process. In this study, wild-type ¬V. fischeri (ES114) and B. cepacia (25416) were cultured, and the production of both enantiomers of AHLs monitored over time at different nutrient conditions. V. fischeri classically has been a point of reference in QS studies. It plays an active role in oceanic environments, assuming a symbiotic relationship with the bobtail squid (Koehler et al., 2019). Previously, production of L-AHLs from bacterial cultures was monitored over time and compared to bacterial growth (OD¬600) (Fekete et al., 2010; Ravn, Christensen, Molin, Givskov & Gram, 2001). These studies did not apply chiral methods for the analysis of AHLs as it was incorrectly assumed that only L-AHLs were produced. This study will present the first growth versus time studies that focus on the production of both L and D-AHLs from V. fischeri and B. cepacia. Additionally, nutrient conditions are altered, for B. cepacia, by supplementation with L-methionine, D-methionine, or racemic methionine, to investigate whether or not different stereochemical forms of this amino acid affects the production of L and D-AHLs.

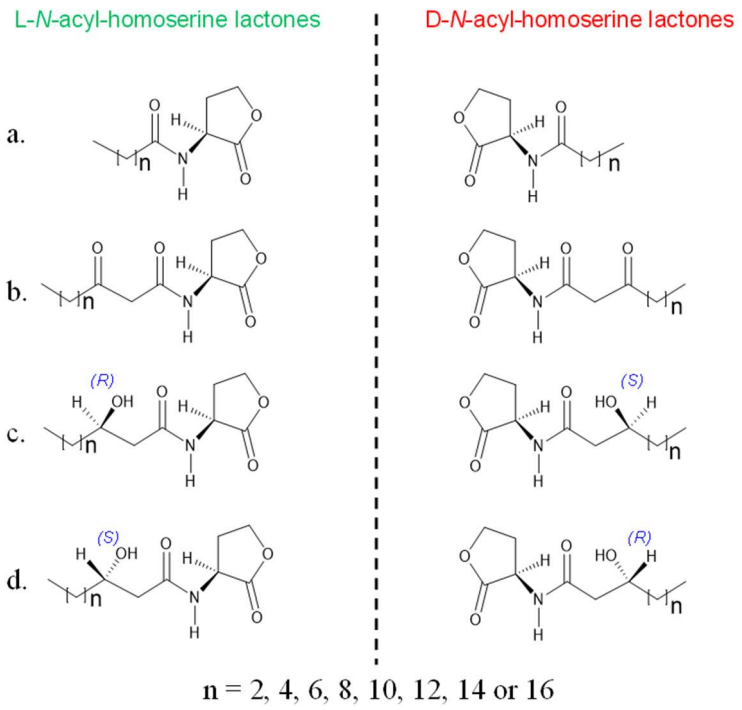

Figure 4-1 Chiral structures of N-acyl-homoserine lactones (AHLs). The structures are for a. acyl, **b.** 3-oxoacyl, and **c.** and **d.** 3-hydroxyacyl. The structures of **c.** and **d.** differ in their stereochemistry on carbon 3 of the acyl chain.

4.3 Materials and Methods

4.3.1 Analytical reagents

Racemic standards of *N*-hexanoyl-homoserine lactone (HHL), *N*-heptanoyl-homoserine lactone (HpHL), *N*-octanoyl-homoserine lactone (OHL), *N*-decanoyl-homoserine lactone (DHL), and *N*-dodecanoyl-homoserine lactone (dDHL), *N*-(3-oxohexanoyl)-homoserine lactone (OHHL), M9 broth, D-(+)-glucose BioReagent grade, magnesium sulfate BioReagent grade, DL-methionine, and all HPLC grade solvents were obtained from Sigma-Aldrich, (St. Louis, Missouri, USA). *N,O*-bis(trimethylsilyl)trifluoroacetamide (BSTFA) with one % v/v trimethylchlorosilane (TMCS), one

gram Supel™-select HLB SPE (HLB) cartridges, and β-DEX™ 225 (25% 2,3-di-*O*-acetyl-6-*O*-TBDMS-β-cyclodextrin in SPB-20 poly(20% phenyl/80% dimethylsiloxane) column, 30 m x 0.25 mm i.d. (film thickness 0.25 µm) were obtained from Millipore Sigma (Supelco, Bellefonte, Pennsylvania, USA). Photobacteria broth was obtained from Carolina biological (Burlington, North Carolina, USA). Deionized water was obtained from in-house Millipore system with 18.2 MΩ•cm.

4.3.2 Strains and growth conditions for bacteria

Two gram-negative bacteria that are known to produce AHLs were selected, *B. cepacia,* 25416, from ATCC (Manassas, VA) and *A. fischeri,* ES114 from Carolina Biological (Burlington, NC). Stock cultures of these strains were stored in their respective media with 25% glycerol at -80°C. Frozen *B. cepacia* strains were inoculated in M9 broth containing 0.4 % D-glucose and two mM magnesium sulfate (creating M9 media) and grown overnight (18 h) at 30°C (200 rpm). The overnight culture was then seeded to fresh M9 media, in duplicate, grown at 30°C (200 rpm) for subsequent studies. Frozen *V. fischeri* strains were inoculated in photobacterium broth (PBB) media at 25°C (200 rpm). The overnight culture was then seeded to fresh PBB media, in four replicates, grown at 25°C (200 rpm) for subsequent studies. The pHs of all growth cultures from the beginning to the end of the experiments were always between 7.2-7.4.

4.3.3 Analysis of standard N-acyl-homoserine lactones by chiral gas chromatography-mass spectrometry (GC-MS)

A 100 µL aliquot of a 10 ppm standard solution of acyl and 3-oxoacyl-HLs in dichloromethane (C4-C12 acyl; C4-C8 3-oxohexanoyl) was placed in a 1 mL sample vial and dried with a gentle stream of ultrahigh purity (UHP) N2. Derivatization of 3-oxoacyl-HLs was conducted as mentioned in the literature (Readel, Portillo, Talebi & Armstrong, 2020). A 100 µL aliquot of BSTFA with 1% TMCS was added to the sample vial with the dried standard solution and sealed with a PTFE lined cap. The sample vial was placed into a 130°C preheated sand bath for 45 min. The sand bath was equilibrated at this temperature for 3 h prior to use in a GC oven. The sample was then removed from the oven and 100 µL of dichloromethane was added to the derivatization

solution and ran on an Aglient 6890N GC with 5975 MSD single quadrupole (Agilent Technologies, Palo Alto, CA, USA) equipped with a β-DEX 225¬TM column. The inlet split ratio was 100:1 (220°C), 1 µL injection introduced, with an oven temperature program starting at 160°C (5-min hold) increased at a rate of 1°C/min to 230°C (25-min hold), constant flow of 1.1 mL/min (40 cm/s). The MS temperature conditions were as follows: MS transfer line at 230°C, ion source temperature of 280°C at 70 eV, and quadrupole temperature of 150°C. The MS was operated in selected ion monitoring (SIM) mode for ion 143 m/z (acyl-homoserine lactones) and 185 m/z (for OHHLs).

4.3.4 Extraction reproducibility of N-acyl-homoserine lactones (AHL) standards from bacterial media

Fresh M9 media and PBB were both spiked with a 2 µg/mL solution of standard AHLs. Only PBB media were spiked with 3-oxohexanoyl-homoserine lactone (OHHL). The spiked media samples were then extracted using one g HLB cartridges which were sequentially conditioned with 5 mL of HPLC grade methanol and 5 mL of DI water. Ten mL of spiked media samples were then loaded on the cartridge bed at a rate of ~ 2 mL/min. Loaded samples were then washed with a solution of 95:5 v/v% water:methanol at a rate of ~ 2 mL/min. Elution was done with twice with 4 mL of HPLC grade acetonitrile. Eluted samples were dried by rotary evaporation on a BUCHI R-100 Rotavapor unit (BUCHI, Flawil, Switzerland) attached to vacuum in a heated water bath (50°C). M9 media samples were reconstituted in 100 µL of dichloromethane and analyzed by GC-MS. PBB samples were processed and analyzed by the above-mentioned method. The method limit of detection (LOD) for acyl was approximately 0.001 µg/mL while for 3-oxoacyl-HLs was 0.006 µg/mL. Good extraction reproducibility of AHLs was seen in M9 minimal (M9) media and photobacterium broth (PBB) media. The %RSD of recovery for the spiked AHLs standards were all lower than 3%. Only L and D-OHHL showed %RSD of recovery at 6.4% in PBB.

4.3.5 Analysis of enantiomeric AHLs from bacterial cultures by chiral GC-MS

N-acyl-homoserine lactones were extracted and analyzed from preliminary 24-h cultures of B. cepacia and V. fischeri by using the above mentioned, culturing, extraction, and GC-MS analysis methods. The 3-oxohexanoyl-homoserine lactone (OHHL) and 3-oxooctanoyl-homoserine lactone (OOHL) concentrations were below the LOD for the GC-MS in bacterial samples. Therefore, OHHL and OOHL in there samples were quantified by LC-MS/MS as previously reported (Readel et al., 2020).

4.3.6 Quantitative analysis

B. cepacia: Internal standard calibration curves were constructed by preparing standard solutions of HHL, OHL, and DHL at concentrations of 0.2, 0.4, 0.8, 2.0, 2.4, 3.6, and 4 µg/mL in triplicate in HPLC grade acetonitrile and spiked with L-dDHL to a concentration of 8 µg/mL and then analyzed by GC-MS.

V. fischeri: internal standard calibration curves were constructed by preparing standard solutions of HHL, OHL, and OHHL at concentrations of 0.80, 0.30, 1.25, 2.0, 2.5, 3.0, 5.0, 8.0, 12.0, 15.0, 22.5, 30.0 µg/mL in triplicate in HPLC grade acetonitrile and spiked with L-HpHL to a concentration of 3 µg/mL. Samples were blown with UHP N2 until dried. Leftover residue was guided through derivatization method as described previously.

4.3.7 Growth and AHL production by B. cepacia

Overnight cultures of B. cepacia and V. fischeri were seeded to fresh M9 media and PBB media respectively and grown at the above mentioned conditions. Quadruplicate samples were evaluated for B. cepacia and V. fischeri. B. cepacia: a 1.5 mL aliquot was taken from the growth cultures at times: 4.5, 15, 20, 30, 45, 54, 69, 93 h, diluted by half with fresh M9 media, and

plaed into polystyrene cuvets. OD600 absorbance measurements were taken to monitor bacterial growth with a Vernier SpectroVisTM Plus spectrophotometer. Two 10 mL samples were taken from growth culture and centrifuged, only supernatant was set aside. The supernatant of each sample was spiked with L-dodecanoyl-homoserine lactone (L-dDHL) to a concentration of 8.0 µg/mL and guided through the SPE method described in Section 2.4. Extractant was rotary evaporated to dryness. The leftover residue was dissolved into 200 µL of dichloromethane and transferred to a two mL sample vial for analysis by GC-MS.

4.3.8 Growth, AHL and bioluminescence production by V. fischeri

A 1.5 mL aliquot was taken from the growth cultures at times: 6, 9, 10, 11, 12, 16, 20, 24, 28, 33.5, 44.5, 52, 60 and 74 h, diluted by half with fresh PBB media, and placed in polystyrene cuvettes. OD600 measurements were taken as described in the previous section. Replicate 10 mL samples were taken per growth culture and processed in the same way as B. cepacia. Supernatant of each sample was spiked with L-heptanoyl-homoserine lactone (L-HpHL) to a concentration of 3 µg/mL and guided through the SPE method. After rotary evaporation, the residue was dissolved in 200 µL of dichloromethane, transferred to a two mL sample vial, and dried by blowing with UHP N2. Leftover residue was guided through the derivatization method described in Section 2.4 and analyzed by GC-MS. The bioluminescence intensities of V. fischeri were analyzed by using Image J from the National Institute of Health, USA (http://imagej.nig.gov.ij). First, the vial image was selected, and a "Plot Profile" option was used to generate an intensity plot of gray values as a function of position on the bioluminescence image. The larger the "gray value," the higher is the intensity of the bioluminescence. Further documentation and calculation of gray values are provided in the software. The highest gray values from the "Plot Profile" are listed in the Results, Section 3.2.

4.3.9 Methionine enantiomers as nutrients for B. cepacia

Overnight cultures of B. cepacia were grown as described previously and supplemented with one of three amounts of methionine: (i) 6.8 mmol of L-methionine (ii) 6.8 mmol of D-methionine and (iii) 3.4 mmol each of L and D-methionine, grown at 30°C (200 rpm). Collection of OD600 and N-acyl-homoserine lactone growth curves was done following the method for B. cepacia in Section 2.7.

4.4 Results

4.4.1 Presence of both enantiomeric forms of AHLs from bacterial cultures

The AHL standards shown in Table 4.1 were selected because of the occurrence of their L-AHLs are well-documented in cultures of B. cepacia and V. fischeri (Kuo et al., 1994; Lewenza et al., 1999; Venturi et al., 2004).

Table 4-1 *N*-acyl-homoserine lactones (AHL) standards analyzed and the ion detected for analysis.

***N*-acyl-homoserine lactones**		
AHL	**Ion detected (m/z,GC,LC)**	**Bacterial Production(B,V)**
HHL	143,-	B,V
HpHL	143,-	B
OHL	143,-	B,V
DHL	143,-	B
dDHL	143,-	-
OHHL	185,102	V

OOHL	-,102	-

GC and LC denote method that ion was used to detect the respective AHL.

B. cepacia (B), *V. fischeri* (V). The dash (-) denotes that production of AHL is not documented for either of the bacteria studied.

N-hexanoyl-homoserine lactone (HHL), *N*-heptanoyl-homoserine lactone (HpHL, internal standard) *N*-octanoyl-homoserine lactone (OHL), *N*-decanoyl-homoserine lactone (DHL), *N*-dodecanoyl-homoserine lactone (dDHL), *N*-(3-oxohexanoyl)-homoserine lactone (OHHL), and *N*-(3-oxooctanoyl)-homoserine lactone.

The focal point of this study is on the stereochemical production of these AHLs over time. An initial 24-h culture of B. cepacia was tested for the presence and identification of any AHLs produced. The detected AHLs were L-HHL, L- and D-OHL, and L-DHL (Figs. 4.2a and 4.2b).

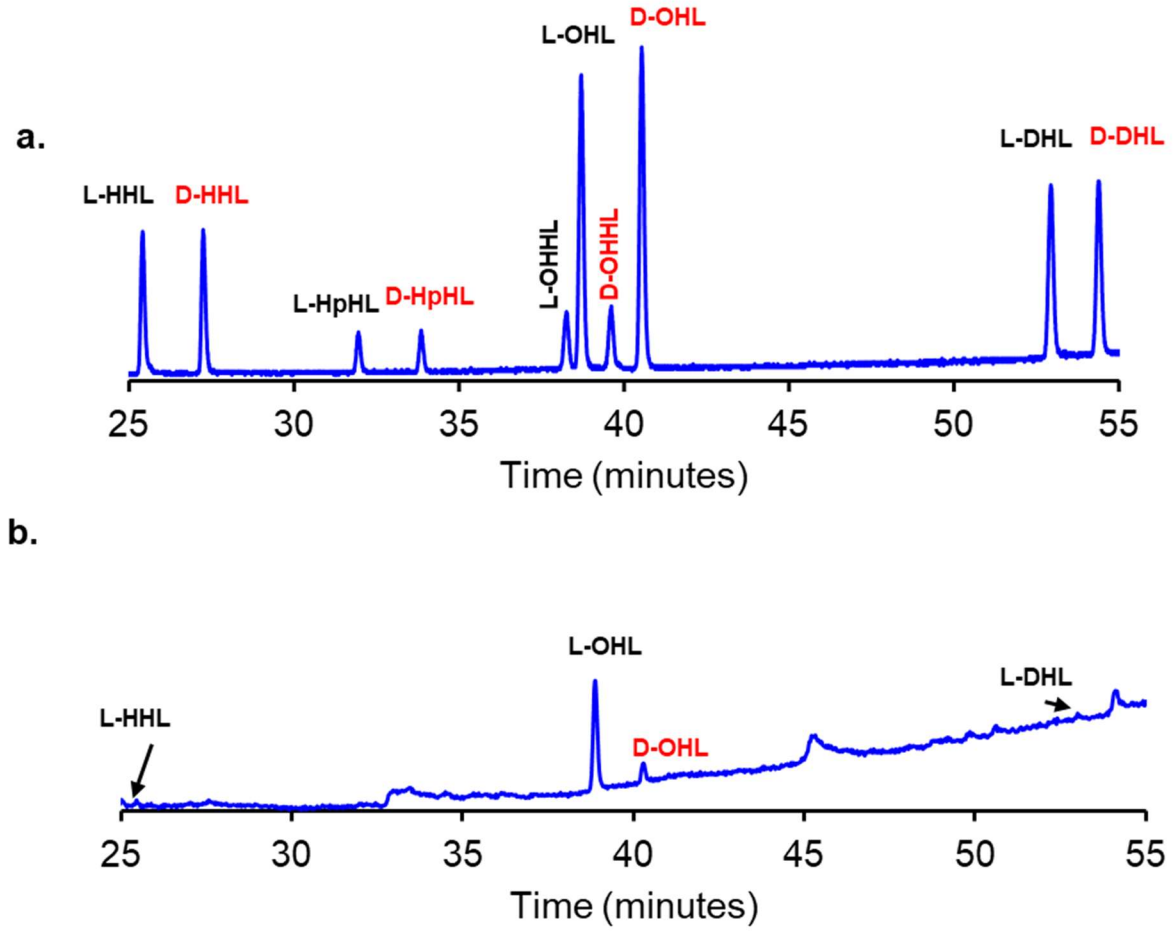

Figure 4-2 **a.** GC-MS chromatogram of a standard solution of D and L hexanoyl (HHL), heptanoyl (HpHL, internal standard), octanoyl (OHL), decanoyl (DHL), 3-oxobutanoyl (OBHL), and **b.** GC-MS chromatogram showing the production of L-HHL, D- and L-OHL, and possibly L-DHL from 24-h growth culture of *Burkholderia cepacia*. (See experimental for GC-MS and extraction methods).

The amounts of L-HHL and L-DHL were near the limit of detection (LOD, Experimental Procedures). In a 24-h prelimimary culture of V. fischeri, the extracts contained substantial amounts of L- and D-HHL and L- and D-OHL (Figs 4.3a and 4.3b).

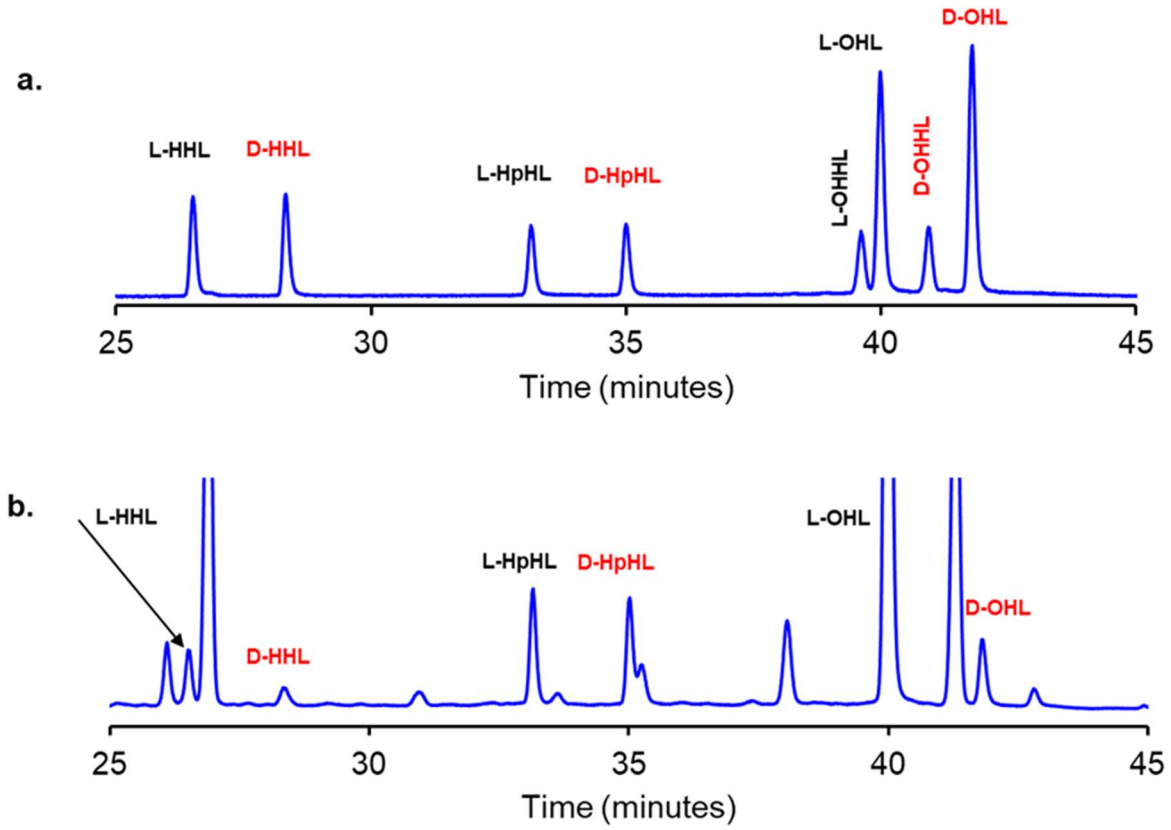

Figure 4-3 **a.** GC-MS chromatogram of a standard solution of DL-hexanoyl (HHL), heptanoyl (HpHL), octanoyl (OHL), and 3-oxohexanoyl homoserine lactones and **b.** GC-MS chromatogram showing the production of D and L isomers of HHL and OHL from 24-h growth culture of *Vibrio fischeri*. 3.0 µg/mL of D and L HpHL was used as an internal standard. Unlabeled peaks are matrix peaks from media. (See experimental for GC-MS and extraction methods)

The 3-oxo-AHLs, OHHL and OOHL, were detected at much smaller amounts for V. fischeri, and only by LC-MS/MS. Table 4.2 summarizes the screening results. The most abundant AHL detected for both bacteria was L-OHL with the next most abundant being D-OHL. The amounts of L-HHL and L-DHL produced by B. cepacia were approximately the same. However, V. fischeri produced approximately three times higher concentrations of L-HHL compared to D-HHL (Figure 4.3b). Other peaks in the extracted samples did not match with any of the standard AHLs used in this study.

Table 4-2 Chiral *N*-acyl-homoserine lactone (AHL) production patterns for *B. cepacia* grown in M9 media, four methionine supplemented *B. cepacia* also grown in M9 media, and *V. fischeri* was grown in photobacteria media. Dots (•) represent detectable homoserine lactones. (See experimental for details)

	Detected *N*-acyl-homoserine lactones											
	L-HHL	D-HHL	L-HpHL	D-HpHL	L-OHL	D-OHL	L-DHL	D-DHL	L-OHHL	D-OHHL	L-OOHL	D-OOHL
B. cepacia	•				•	•	•					
B. cepacia(L-met)	•	•			•	•	•					
B. cepacia (D-met)	•	•			•	•	•					
B. cepacia (D,L-met)	•	•			•	•	•					
V. fischeri	•	•			•	•			•*		•*	

*These were detected only by LC-MS/MS

N-hexanoyl-homoserine lactone (HHL), *N*-heptanoyl-homoserine lactone (HpHL, internal standard) *N*-octanoyl-homoserine lactone (OHL), *N*-decanoyl-homoserine lactone (DHL), *N*-(3-oxohexanoyl)-homoserine lactone (OHHL), and *N*-(3-oxooctanoyl)-homoserine lactone.

4.4.2 Chiral N-acyl-homoserine lactone (AHL) production during bacterial growth

Figure 4.4 shows the OD600 growth curve for B. cepacia. An increase in cell density is observed over time with a maximum reached at ~45 h. Cell density decreased slightly at 54 h and then remained nearly constant through the end of the experiment. Initial production of the dominant L-OHL, was observed at 20 h. The L-OHL production increased until reaching a maximum at ~54 h at a concentration of 0.034 µg/mL. The enantiomer, D-OHL, was initially detected at ~20 h, which was the same time of appearance as L-OHL. The concentration of D-OHL reached a maximum at ~30 h, with a concentration of approximately 0.01 µg/mL, which remained at that level for the duration of the experiment (Figure 4.4).

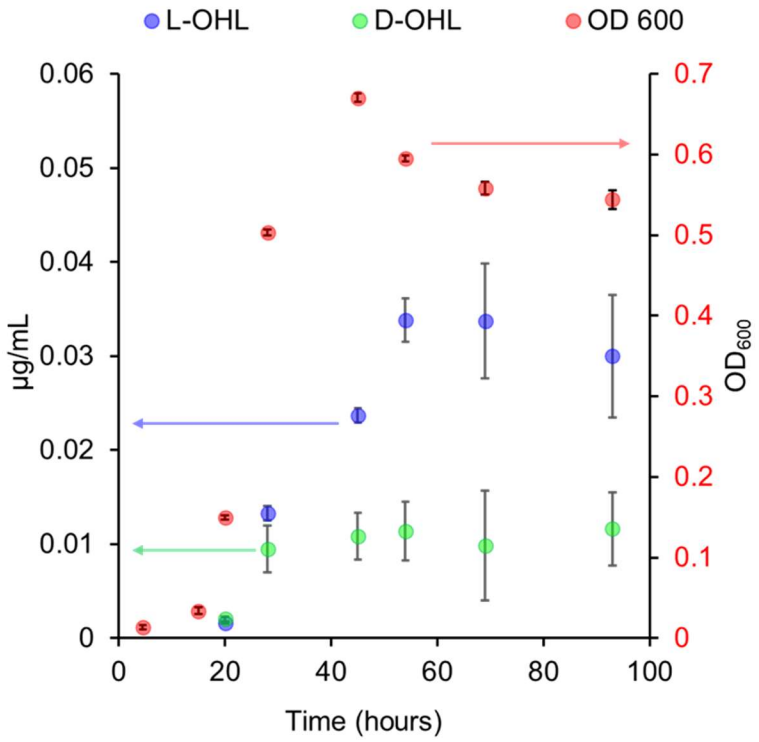

Figure 4-4 Production of DL-octanoyl-homoserine lactone (OHL) with biomass (OD_{600}) curves during growth of *B. cepacia.* Data represent averages with standard deviations calculated from four replicates.

Other AHLs detected were L-HHL and L-DHL. Both were initially detected at 30 h, with a maximum concentration of approximately 0.007 µg/mL for both at ~70 h.

The OD600 growth curve for V. fischeri also showed increasing cell density with a maximum cell density observed at ~44 h. The observed cell density then remained constant through the end of the experiment (Figs. 4.5a and 4.5b).

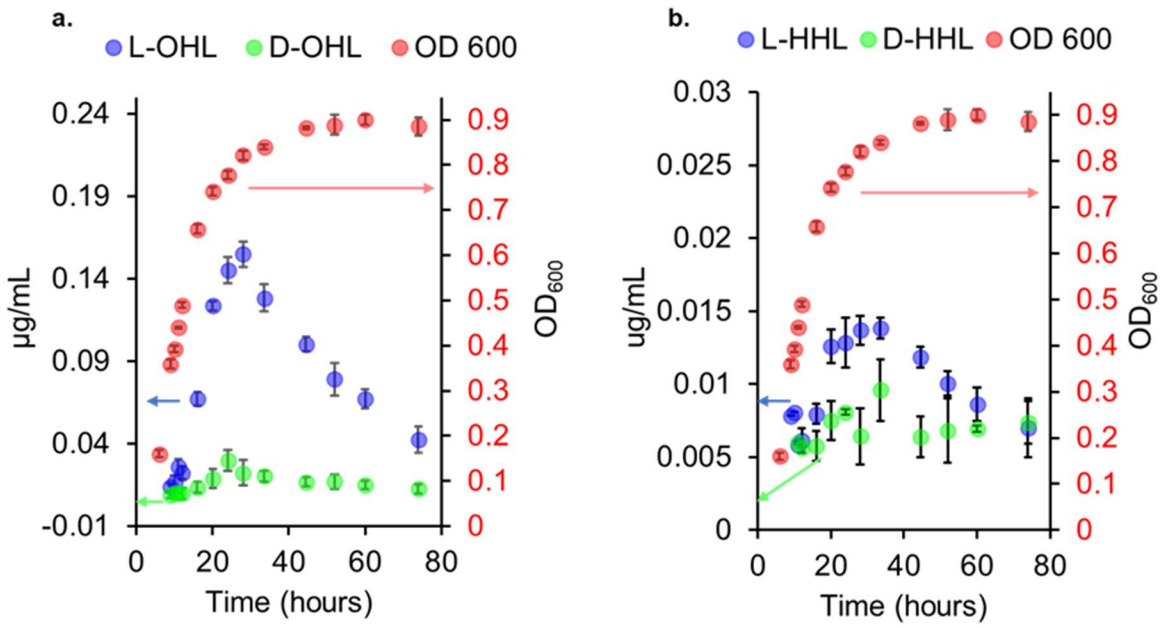

Figure 4-5 Production of a) DL-octanoyl-homoserine lactone (OHL) and b) DL-hexanoyl-homoserine lactone (HHL) with biomass (OD_{600}) curves during growth of *V. fischeri.* Data represent averages with standard deviations calculated from four replicates.

L-OHL concentrations reached a maximum of 0.150 µg/mL at ~28 h. Significant depletion of L-OHL was observed at ~33 h, with its concentration diminishing to 0.043 µg/ml by the end of the experiment (Figure 4.5a). D-OHL was first detected at ~9 h and a maximum concentration of 0.030 µg/mL was reached at ~24 h. There were also signs of slight depletion of D-OHL starting at ~33 h after which the concentration plateaued at 0.010 µg/mL. Both L and D-HHL were observed for V. fischeri with greater amounts observed for the L-enantiomer (Figure 4.5b). The concentration L-HHL steadily increased over time, reaching a level of 0.014 µg/mL at ~33 h. The D-HHL also was produced at slightly lower concentrations, reaching a maximum of 0.009 µg/mL at ~33 h. Much lower amounts of L-3-oxo-HHL (OHHL) and L-3-oxo-OHL (OOHL) were detected

by LC-MS/MS (Readel et al., 2020) at concentrations of approximately 0.0001 µg/mL for both enantiomers.

Bioluminescence was monitored throughout the growth of V. fischeri (Figure 4.6).

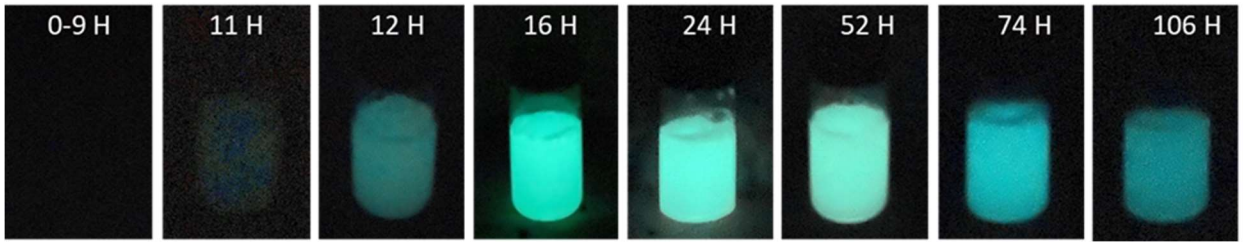

Figure 4-6 Images of bioluminescence of *V. fisheri* over time, cultured in Photobacterium broth (PBB) at 25°C. Relative intensities at the indicated time intervals are: 0 h = 0, 11 h = 24, 12 h = 88, 16 h = 167, 24 h = 193, 52 h = 190, 74 h = 153, 106 h = 100. See Materials and Methods section for experimental details.

The initial observation of bioluminescence by V. fischeri was at 11 h with maximum luminescence (light production) seen at approximately 24 h. A gradual dimming (decreasing light production) was observed starting at 28 h and continued to the end of the experiment (Figure 4.6). The maximum luminescence correlated with the maximum production of D-OHL and L-OHL at ~24-28 h (Figure 4.5a). It is important to note that the most produced AHL was L-OHL and the second most produced was its enantiomer D-OHL. All other L-AHLs were of lower concentration than D-OHL for both B. cepacia and V. fischeri.

4.4.3 Enantiomeric N-acyl-homoserine lactone production by B. cepacia in methionine supplemented M9 media

There has only been one instance where a D-AHL has been reported from a bacterial culture. D-decanoyl-homoserine lactone was detected in a culture of B. cepacia. (Malik et al., 2009) The authors postulated that the production of this molecule "... could be derived from its

biosynthesis since it forms from amino acid derivatives and the bacteria were shown to be able to produce D-methionine derivatives." (Malik et al., 2009). To see if the presence of methionine enantiomers influenced AHL production, parallel, identical, cultures of B. cepacia were individually supplemented with identical amounts of L-Met, D-Met, or racemic Met (D,L-Met). The production of L- and D-OHL was compared to the unsupplemented culture of Figure 4.4. The three supplemented cultures had comparable growth curves, reaching maximum cell densities at ~45 h (Figs. 4.7a and 4.7b).

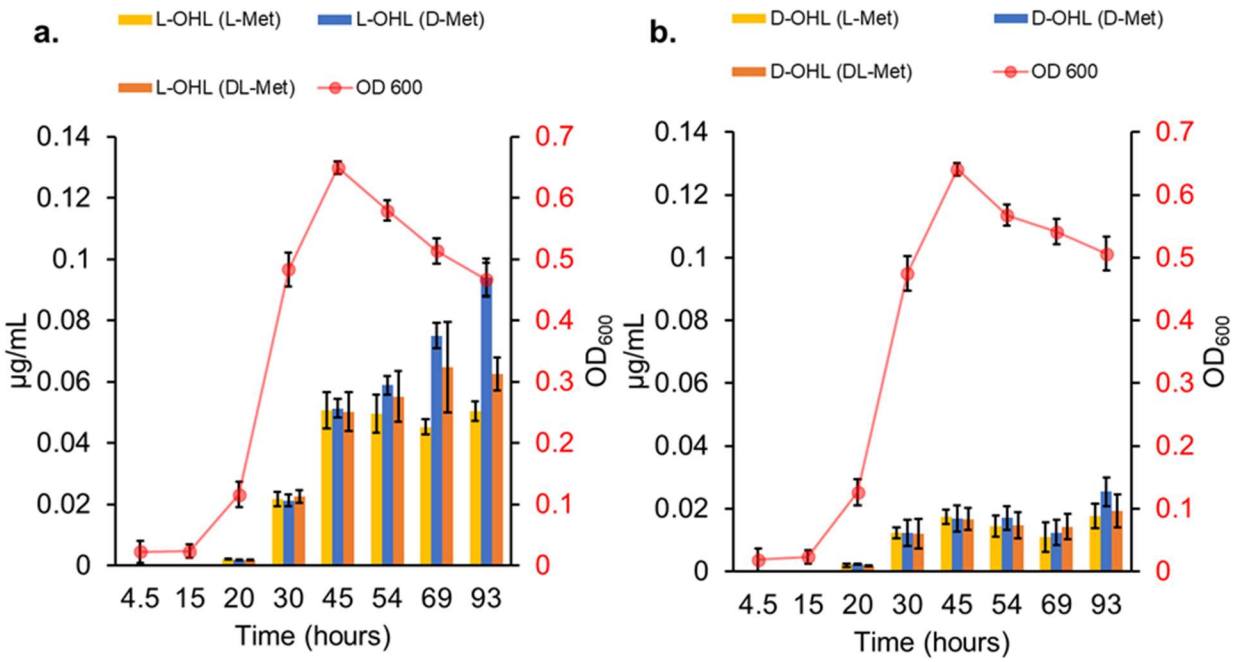

Figure 4-7 Production of **a.** L-octanoyl-homoserine lactone (L-OHL) and **b.** D-octanoyl-homoserine lactone (D-OHL) with biomass (Abs OD 600) curves during growth of *B. cepacia* supplemented with 6.8 mmol of L-methionine (L-Met), 6.8 mmol of D-methionine (D-Met) or supplemented with 3.4 mmol of L-methionine and 3.4 mmol of D-methionine (DL-Met). Data represents averages with standard deviations calculated from four replicates.

Subsequently a slight, but continual, decrease in cell density was found until the end of the experiment (Figure 4.7). Again, it was observed that L-OHL was the dominant AHL produced for all methionine supplemented cultures of B. cepacia (Figure 4.7a). The L-Met supplemented

cultures produced 0.051 µg/mL of L-OHL at 45 h with its concentration staying constant through the end of the growth period. Interestingly, the production of L-OHL for the D-Met supplemented cultures increased continuously to the end of the experiment reaching a concentration of 0.094 µg/mL at ~93 h (Fig 4.7a). For D,L-Met supplemented cultures, production of L-OHL reached a maximum concentration of 0.065 µg/mL at ~70 h (Figure 4.7a). Maximum production of D-OHL was approximately 0.020 µg/mL for all three of the parallel cultures (Figure 4.7b). Production of L-HHL and L-DHL was observed at lower concentrations than the aforementioned AHLs. Their concentrations reached a maximum of approximately 0.008 µg/mL for both AHLs. The production of D-HHL was observed for all parallel, methionine supplemented, cultures, reaching maximum concentrations of approximately 0.006 µg/mL. D-HHL was not previously observed (for unsupplemented B. cepacia cultures) as it was below the detection limit of the method. Comparing the results to those of the unsupplemented culture it is clear that the addition of any form of methionine (L-, D-, or racemic) does not affect the ratio of L- to D-AHL production, that is to say, D-AHL production is not exclusively enhanced by any addition of methionine. However, methionine supplementation does increase the overall AHL concentrations (both L- and D-AHLs).

4.5 Discussion

B. cepacia (25416) and V. fischeri (ES114) were found to produce D-AHLs throughout their growth period. All D-AHLs detected were enantiomers of the expected L-AHLs that are produced by these two species (Fuqua et al., 1994; Kuo et al., 1994; Lewenza et al., 1999; Venturi et al., 2004). It is known that the AHL responsible for regulation of the lux operon and bioluminescence in V. fischeri is OHHL (Fuqua et al., 1994; Kuo et al., 1994). However, the amounts of OHL produced were ~1500 times higher than OHHL for this strain of V. fischeri during this study. It has been observed that ES114 produces OHL at higher amounts than OHHL (Stabb et al., 2008). Nevertheless, biolumincense of V. fischeri correlated with the most produced AHLs, L- and D-OHL. The role of L-OHL in V. fischeri and its involvement in bioluminescence has been explored by others. These studies conclude that the role of L-OHL is as an initial inducer of bioluminescence and regulator of OHHL production in the lux system of

V. fischeri (Collins et al., 2005; Lupp & Ruby, 2004; Miyashiro & Ruby, 2012; Sun, Pan, Gu, & Lin, 2018).

D-OHL was the second most produced AHL both by V. fischeri and by B. cepacia cultured in M9 media (Figure 4.4). All other AHLs were produced in much lower amounts. Although pH mediated chemical hydrolysis could decrease the total AHLs, this would have no effect on the relative amounts of AHL enantiomers which have identical chemical hydrolysis rates. Further, chemical hydrolysis at the pHs encountered in these studies was minimal, pHs 7.2 to 7.4. (see Materials and Methods, Section 2.2). Questions arise as to both the mechanism of production and the possible biological significance of the ubiquitous D-AHLs. One suggested biosynthetic pathway was that D-AHLs are produced via the same process as the L-AHLs, but perhaps with a D-methionine derivative starting material. Another possibility is that, initially, the AHLs produced are of the L-configuration and they are subsequently acted upon by a racemase enzyme. Amino acid racemases, including ones for serine and methionine, are well-known throughout many biological systems (Radkov & Moe, 2014), but no AHL racemases have been reported, to our knowledge.

An examination of parallel cultures of B. cepacia supplemented with methionine (L-, D-, or racemic) produced much higher concentrations of AHLs, L- and D- alike, with the detection of D-HHL now possible. The D-Met supplemented cultures produced the highest concentrations of AHLs, about three times more than the unsupplemented media. D,L-Met and L-Met produced about two times and 1.5 times the amounts of AHLs as compared to the unsupplemented cultures (Figure 4.7 vs Figure 4.4). The ratios of the L-AHLs to their corresponding D-AHL enantiomer did not significantly change regardless of the stereochemical nature of the methionine supplement. It is known that most bacterial species can biosynthesize methionine, meaning it is not an essential amino acid (Ferla & Patrick, 2014). It appears that any added methionine (i.e., L-, D- or D,L-) to the B. cepacia cultures was mainly used as an alternative carbon and nitrogen source in the M9 minimal media. The fact that L-Met supplemented cultures produced lower amounts of all AHLs than D-Met cultures was surprising. Perhaps L-

Met has immediate utility in the organism's other metabolic pathways (Tanaka, Esaki, & Soda, 1985), while D-Met is more broadly useful as a carbon and nitrogen source.

Clearly, D-AHL production was not exclusively enhanced by addition of any of the methionine stereoisomers. In the biosynthesis of L-AHLs, L-methionine is used to make S-adenosylmethioinine, with this metabolite transforming into various L-AHLs when acylated by an acyl-carrier protein. It appears that D-AHLs may not be directly produced by the conventional biosynthetic pathway of L-AHLs. D-methionine does not seem to play a direct role in the production of D-AHLs. Auto-racemization studies have been applied to AHLs, with findings suggesting there is negligible physico-chemical racemization occurring in the bacterial matrix nor during the chromatographic time frame (Hodgkinson et al., 2011; Malik et al., 2009). There are at least two other possibilities for the origin of D-AHLs, another unidentified synthetic pathway, distinct from that of L-AHL synthesis or the aforementioned possibility of chiral interconversion between L- and D-AHLs.

Collins et al. (2005) studied the directed evolution of V. fischeri LuxR as a means to broaden the spectrum and sensitivity to different L-AHLs. They found that broadening a given protein's specificity is the easiest evolutionary path to obtaining higher selectivity to new signaling molecules. However, their focus was on mutations that affected or were affected the nature of the acyl group, but not on the stereochemistry of the homoserine lactone group. This is not to say that an analogous mechanism may not be relevant for D-AHLs, only that it hasn't been considered or studied. D-ACLs are known to have activity as autoinducer molecules (Li et al. 2018). However, it also is possible that they play some other, as yet undetermined, regulatory or feed-back role in quorum sensing.

4.6 Conclusions

This work is the first to detect D-AHLs in the wild-type strain of V. fischeri (ES114) and the first to monitor the production of D-AHLs over time for B. cepacia (25416) and V. fischeri (ES114). The AHL screening and production curve demonstrated that D-OHL and D-HHL are produced in significant amounts by both bacteria. In V. fischeri, maximum bioluminescence correlated with maximum concentrations of both D-OHL and L-OHL. The addition of any enantiomer of methionine, into M9 minimal media, augments the production of all AHLs (L- and D-) by B. cepacia. However, the D- to L- ratios of AHLs are not affected. The supplementation of the B. cepacia growth media with D-Met enhanced the production of both L and D-AHLs to a greater extent than the addition of equivalent amounts of L or D,L-Met. The study indicates that another biosynthetic pathway is likely involved for D-AHL production. Alternatively, the initially produced L-AHL is converted to the D-AHL. The reasons for the ubiquitous presence of D-AHLs are considered, but are not yet well understood.

4.7 References

Armstrong, D. W., Gasper, M. P., Lee, S. H., Ercal, N., & Zukowski, J. (1993). Factors controlling the level and accurate determination of D-amino acids in the urine and plasma of laboratory rodents. Amino Acids, 5, 299-315.

Armstrong D. W., Gasper, M. P., Lee, S. H., Zukowski, J., & Ercal, N. (1993). D-amino acid levels in human physiological fluids. Chirality, 5, 375-378.

Charlton, T. S., De Nys, R., Netting, A., Kumar, N., Hentzer, M., Givskov, M., & Kjelleberg, S. (2000). A novel and sensitive method for the quantification of N-3-oxoacyl homoserine lactones using gas chromatography–mass spectrometry: application to a model bacterial biofilm. Environmental Microbiology, 2 (5), 530-541.

Collins, C. H., Arnold, F. H., & Leadbetter, J. R. (2005). Directed evolution of Vibrio fischeri LuxR for increased sensitivity to a broad spectrum of acyl-homoserine lactones. Molecular Microbiology, 55 (3), 712-723.

Fekete, A., Kuttler, C., Rothballer, M., Hense, B. A., Fischer, D., Buddrus-Schiemann, K., & Hartmann, A. (2010). Dynamic regulation of N-acyl-homoserine lactone production and degradation in Pseudomonas putida IsoF. FEMS Microbiology Ecology, 72 (1), 22-34.

Ferla, M. P., & Patrick, W. M. (2014). Bacterial methionine biosynthesis. Microbiology, 160 (8), 1571-1584.

Fuqua, C., & Greenberg, E. P. (2002). Listening in on bacteria: acyl-homoserine lactone signalling. Nature Reviews Molecular Cell Biology, 3 (9), 685-695.

Fuqua, W. C., Winans, S. C., & Greenberg, E. P. (1994). Quorum sensing in bacteria: the LuxR-LuxI family of cell density-responsive transcriptional regulators. Journal of Bacteriology, 176 (2), 269-275.

Gao, X. Y., Fu, C. A., Hao, L., Gu, X. F., Wang, R., Lin, J. Q., & Lin, J. Q. (2020). The substrate-dependent regulatory effects of the AfeI/R system in Acidithiobacillus ferrooxidans reveals the novel regulation strategy of quorum sensing in acidophiles. Environmental Microbiology, 23 (2), 757-773.

Hernández, S. B., & Cava, F. (2016). Environmental roles of microbial amino acid racemases. Environmental Microbiology, 18 (6), 1673-1685.

Hoang, T. P. T., Barthélemy, M., Lami, R., Stien, D., Eparvier, V., & Touboul, D. (2020). Annotation and quantification of N-acyl homoserine lactones implied in bacterial quorum sensing by supercritical-fluid chromatography coupled with high-resolution mass spectrometry. Analytical and Bioanalytical Chemistry, 412, 1-16.

Hodgkinson, J. T., Galloway, W. R., Casoli, M., Keane, H., Su, X., Salmond, G. P., & Spring, D. R. (2011). Robust routes for the synthesis of N-acylated-L-homoserine lactone (AHL) quorum sensing molecules with high levels of enantiomeric purity. Tetrahedron Letters, 52 (26), 3291-3294.

Koehler, S., Gaedeke, R., Thompson, C., Bongrand, C., Visick, K. L., Ruby, E., & McFall-Ngai, M. (2019). The model squid–vibrio symbiosis provides a window into the impact of strain-and species-level differences during the initial stages of symbiont engagement. Environmental Microbiology, 21 (9), 3269-3283.

Kuo, A., Blough, N. V., & Dunlap, P. V. (1994). Multiple N-acyl-L-homoserine lactone autoinducers of luminescence in the marine symbiotic bacterium Vibrio fischeri. Journal of Bacteriology, 176 (24), 7558-7565.

Lewenza, S., Conway, B., Greenberg, E., & Sokol, P. A. (1999). Quorum sensing in Burkholderia cepacia: identification of the LuxRI homologs CepRI. Journal of Bacteriology, 181 (3), 748-756.

Li, S.-Z., Xu, R., Ahmar, M., Goux-Henry, C., Queneau, Y., & Soulère, L. (2018). Influence of the d/l configuration of N-acyl-homoserine lactones (AHLs) and analogues on their Lux-R dependent quorum sensing activity. Bioorganic Chemistry, 77, 215-222.

Liu, J., Fu, K., Wu, C., Qin, K., Li, F., & Zhou, L. (2018). “In-Group” communication in marine vibrio: a review of N-acyl homoserine lactones-driven quorum sensing. Frontiers in Cellular and Infection Microbiology, 8, 139.

Lupp, C., & Ruby, E. G. (2004). Vibrio fischeri LuxS and AinS: comparative study of two signal synthases. Journal of Bacteriology, 186 (12), 3873-3881.

Malik, A. K., Fekete, A., Gabifuegi, I., Rothballer, M., & Schmitt-Kopplin, P. (2009). Single drop microextraction of homoserine lactones based quorum sensing signal molecules, and the separation of their enantiomers using gas chromatography mass spectrometry in the presence of biological matrices. Microchimica Acta, 166 (1), 101-107.

Miyashiro, T., & Ruby, E. G. (2012). Shedding light on bioluminescence regulation in Vibrio fischeri. Molecular Microbiology, 84 (5), 795-806.

Mohamed, N. M., Cicirelli, E. M., Kan, J., Chen, F., Fuqua, C., & Hill, R. T. (2008). Diversity and quorum-sensing signal production of Proteobacteria associated with marine sponges. Environmental Microbiology, 10 (1), 75-86.

Mukherjee, S., & Bassler, B. L. (2019). Bacterial quorum sensing in complex and dynamically changing environments. Nature Reviews Microbiology, 17 (6), 371-382.

Nealson, K. H., Platt, T., & Hastings, J. W. (1970). Cellular control of the synthesis and activity of the bacterial luminescent system. Journal of Bacteriology, 104 (1), 313-322.

Radkov, A. D., Moe, L. A. (2014) Bacterial synthesis of D-amino acids. Applied Microbiology and Biotechnology, 98, 5363-5374.

Ravn, L., Christensen, A. B., Molin, S., Givskov, M., & Gram, L. (2001). Methods for detecting acylated homoserine lactones produced by Gram-negative bacteria and their application in studies of AHL-production kinetics. Journal of Microbiological Methods, 44 (3), 239-251.

Readel, E., Portillo, A., Talebi, M., & Armstrong, D. W. (2020). Enantiomeric separation of quorum sensing autoinducer homoserine lactones using GC-MS and LC-MS. Analytical and Bioanalytical Chemistry, 412, 2927-2937.

Stabb, E., Schaefer, A., Bose, J., & Ruby, E. (2008). Quorum signaling and symbiosis in the marine luminous bacterium Vibrio fischeri. Eds. Winans, S. C., & Bassler, B. L, Chemical Communication Among Bacteria, Washingon, DC, ASM Press 233-250.

Sun, H., Pan, Y., Gu, Y., & Lin, Z. (2018). Mechanistic explanation of time-dependent cross-phenomenon based on quorum sensing: A case study of the mixture of sulfonamide and quorum sensing inhibitor to bioluminescence of Aliivibrio fischeri. Science of The Total Environment, 630, 11-19.

Taga, M. E., & Bassler, B. L. (2003). Chemical communication among bacteria. Proceedings of the National Academy of Sciences, 100 (suppl 2), 14549-14554.

Tanaka, H., Esaki, N., & Soda, K. (1985). A versatile bacterial enzyme: L-methionine γ-lyase. Enzyme and Microbial Technology, 7 (11), 530-537.

Tomasz, A. (1965). Control of the competent state in Pneumococcus by a hormone-like cell product: an example for a new type of regulatory mechanism in bacteria. Nature, 208 (5006), 155-159.

Venturi, V., Friscina, A., Bertani, I., Devescovi, G., & Aguilar, C. (2004). Quorum sensing in the Burkholderia cepacia complex. Research in Microbiology, 155 (4), 238-244.

Weatherly, C.A., Du, S., Parpia, C., Santos, P.T., Hartman, A.L. and Armstrong, D.W. (2017). D-Amino acid levels in perfused mouse brain tissue and blood: a comparative study. ACS Chem. Neuro. 8, 1251-1261.

Whiteley, M., Diggle, S. P., & Greenberg, E. P. (2017). Progress in and promise of bacterial quorum sensing research. Nature, 551 (7680), 313-320.

Widdel, F. (2007). Theory and measurement of bacterial growth. Didalam Grundpraktikum Mikrobiologie, 4 (11), 1-11.

Zhou, J., Lin, Z. J., Cai, Z. H., Zeng, Y. H., Zhu, J. M., & Du, X. P. (2020). Opportunistic bacteria use quorum sensing to disturb coral symbiotic communities and mediate the occurrence of coral bleaching. Environmental Microbiology, 22 (5), 1944-1962.

Chapter 5

Comprehensive chiral GC-MS/MS and LC-MS/MS methods for identification and determination of N-acyl homoserine lactones

5.1 Abstract

N-acyl homoserine lactones (N-HLs) are signaling molecules synthesized by gram-negative bacteria to communicate in a process called quorum sensing. Common methods for analysis of N-HLs are achiral, examples including biosensors, liquid chromatography with UV detection, gas chromatography coupled with a mass spectrometer (GC-MS) and liquid chromatography coupled with mass spectrometer (LC-MS). Recently, the production of both D,L-N-HLs have been reported in Vibrio fischeri and Burkholderia cepacia using previously published methods. Concentrations of the D-N-HLs were found at the limit of quantification for the employed method. Therefore, for further studies of the role of the D-N-HLs in bacterial physiology, more sensitive, reliable, and selective analytical methods are necessary. The aim of the work is to develop comprehensive chiral analytical methods for the identification and determination of 18 AHLs derivatives using solid phase extraction followed by GC-MS/MS and LC-MS/MS analyses. As a result, the chiral separations of all 18 N-HLs derivatives were accomplished by the complementary GC-MS/MS and LC-MS/MS methods. Generally, the limit of detection for LC-MS/MS method was as low as 1 ppb. The limit of detection for GC-MS/MS method was found to be one order to three orders of magnitude higher than LC-MS/MS method. Due to the high extraction recovery and preconcentration factor of 100, the concentrations of 10 ppt can be detected by LC-MS/MS in biological samples. The presented comprehensive and sensitive methods can aid in studying the role of D-N-HLs in bacterial quorum sensing.

5.2 Introduction

N-Acyl homoserine lactones (N-HLs) (Figure 5-1) are communication/signaling molecules synthesized by gram-negative bacteria for a process known as quorum sensing. N-HLs are biosynthesized from S-adenosyl-L-methionine [1]. It was shown previously that different bacteria, e.g., Vibrio fischeri [2], Burkholderia cepacia [3], Pseudomonas aeruginosa [4, 5, 6], etc. produce specific N-HLs. N-HLs differ in the acyl chain length and in the substitution on the third position of the acyl chain, which can be unsubstituted (AHLs), oxo-substituted (OHLs) or hydroxy-substituted (HHLs), see Figure 5-1.

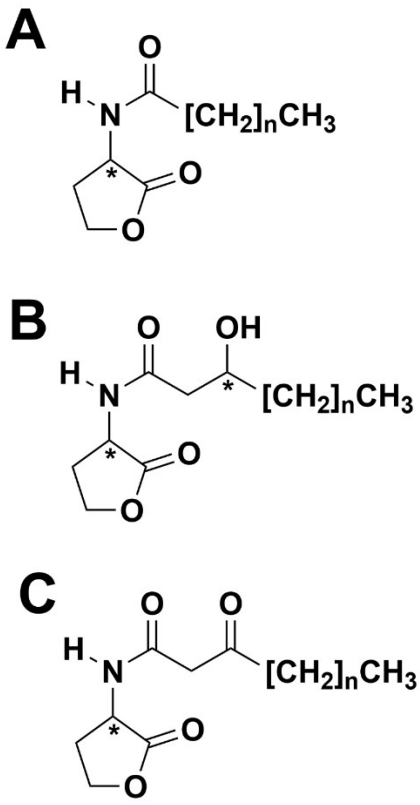

Figure 5-1**. A.** D-/L-*N*-acyl homoserine lactones, **B.** D-/L-*N*-3-hydroxyacyl homoserine lactones and **C.** D-/L-*N*-3-oxoacyl homoserine lactones. Asterisks (*) correspond to chiral centers. For the D-/L-*N*-acyl homoserine lactone structures **n** = 2,4,6,8,10 and 12. For the D-/L-*N*-3-hydroxyacyl and D-/L-N-3-oxoacyl homoserine lactone structures **n** = 2,4,6,8 and 10.

N-HLs are chiral due to the stereogenic center located on the α position of the γ-butyrolactone ring. Since N-HLs are closely related to the amino acid, homoserine, D,L- stereochemical nomenclature is used. HHLs possess another stereogenic center resulting from the hydroxy group located at the third carbon of the acyl chain, yielding two sets of enantiomers

Although quorum sensing pathways employing N-HLs have been well known for more than 40 years, the general assumption was that only L-N-HLs were biosynthesized by bacteria. Therefore, predominantly achiral methods including biosensors [7, 8], GC MS [9], HPLC-UV [10], LC-MS/MS [11], MALDI-MS [12], SFC-MS [13], and LC-ESI-LTQ-FTICR-MS [14] were developed for their identification and determination. Nevertheless, a few and limited chiral methods for the analysis of D enantiomers of N-HLs have been developed using GC-MS [15, 16, 17] and LC-MS [18]. Some chiral separations of N-HLs have recently been reported employing GC-MS and LC-MS on standards [19] and to detect and quantify D N-HLs in bacterial cultures [20]. These methods had moderate sensitivity, at best.

Considering the important role of D-amino acids in bacterial metabolism [21], it is not surprising that D-enantiomers of N-HLs have been reported recently in bacteria [20]. However, until recently, the chirality of N-HLs was usually overlooked. It has become clear that methods to detect trace amounts of N-HLs (e.g., in ppb to ppt range) are necessary. To achieve this low sensitivity, sample preconcentration with very sensitive detection must be utilized.

Previously single drop microextraction [16], liquid-liquid extraction [16] and solid phase extraction (SPE) [20, 22] were used to purify and preconcentrate N-HLs from different matrices. Generally, liquid-liquid extraction is considered unsuitable for trace analysis due to the high volume of extraction solvents, repeated extractions for increasing extraction recoveries, and the lack of a high throughput sample processing procedure. In contrast, SPE cartridges with higher loads (e.g. 1 g of extraction sorbent) can preconcentrate large volumes of sample in a single extraction with high throughput for sample processing.

Highly sensitive detection of AHLs can be achieved by biosensors, LC-MS/MS, and GC-MS/MS. The advantages of using biosensors are their affordable price, fast analysis time, and high sensitivity, which makes them ideal for routine testing and screening of samples. However,

biosensors cannot compete yet with SPE LC-MS/MS methods in accuracy, reproducibility, reliability of results and the capacity for multi-analyte determination [23]. Furthermore, each bacterium used as a biosensor has different receptor proteins (e.g., Chromobacterium violaceum [24], Agrobacterium tumefaciens (TraR) [25] and Pseudomonas aeruginosa (LasR) [26]) responding to a distinct range of N-HLs. Hence the occurrence of false positive results is possible [9] thereby rendering the comprehensive determination of N-HLs with biosensors, unreliable. In contrast, LC or GC connected with selected reaction monitoring (SRM) using a triple quadrupole MS as an ion analyzer is a highly selective and sensitive approach for the detection and quantification of N-HLs in different matrices. Another advantage of using chromatographic techniques coupled with MS/MS is the possibility of chiral separations that enable detection and quantification of all D,L-N-HL in one analysis.

In this paper, the aim is to develop the most sensitive and comprehensive chiral methods for the detection and quantification of trace amounts of six AHLs, six OHLs, and six HHLs using SPE LC-MS/MS and SPE GC-MS/MS. The recovery of the SPE method will be investigated and chromatographic techniques compared in terms of enantioselectivity, enantioresolution, limit of detection (LOD), limit of quantification (LOQ), linearity of calibration curves, and reproducibility. The investigated methods will enable further research on the role that D N-HLs have in quorum sensing.

5.3 Experimental

5.3.1 Chemicals and Materials

ZORBAX SB-C18 (4.6 x 150 mm, 5 µm particle size) columns were purchased from Agilent Technologies, Inc. (Santa Clara, CA). CHIRALPAK® IC-3 (250 x 4.6 mm, 3µm particle size) columns were purchased from Chiral Technologies, Inc. (Ann Arbor, MI). β-DEX™ 225 (30 m × 0.25 mm , 0.25 µm film thickness) and SupelTM-Select HLB SPE cartridges were provided by

MilliporeSigma (Supelco, Bellefonte, PA). LCMS grade acetonitrile (ACN), LCMS grade methanol (MeOH), LCMS grade water, ACS grade dichloromethane (DCM) and ACS grade ethyl acetate (EtOAc) were purchased from Fisher Chemical (Fischer Scientific, Hampton, NH) High purity formic acid (FA) was purchased from VWR (Randor, PA). Racemic standards of N-butanoyl homoserine lactone (A-C4), N-hexanoyl homoserine lactone (A-C6), N-heptanoyl homoserine lactone (A-C7) N-octanoyl homoserine lactone (A-C8), N-decanoyl homoserine lactone (A-C10), N-dodecanoyl homoserine lactone (A-C12), N-tetradecanoyl homoserine lactone (A-C14), N-3-oxohexanoyl homoserine lactone (O-C6), N-3-oxooctanoyl homoserine lactone (O-C8), N-3-oxotetradecanoyl homoserine lactone (O-C14), N-3-hydroxyoctanoyl homoserine lactone (H-C8), N-3-hydroxydecanoyl homoserine lactone (H-C10), and N-3-hydroxytetradecanoyl homoserine lactone (H-C14) were obtained from MilliporeSigma (St. Louis, MO). Racemic standards of N-3-oxobutanoyl homoserine lactone (O-C4), N-3-oxodecanoyl homoserine lactone (O-C10), N-3-hydroxybutanoyl homoserine lactone (H-C4), N-3-hydroxy hexanoyl homoserine lactone (H-C6), and N-3-hydroxy dodecanoyl homoserine lactone (H-C12) and L-N-3-oxododecanoyl homoserine lactone (O-C12) were purchased from Chemodex Ltd. (St. Gallen, Switzerland). All solvents (HPLC and LC-MS grade methanol and acetonitrile, and reagent grade dichloromethane), M9 medium, D-(+)-glucose, and magnesium sulfate were purchased from MilliporeSigma (St. Louis, MO). A Thermo Scientific™ Barnstead™ GenPure™ Pro water purification system was used for preparation of deionized (DI) water.

5.3.2 Preparation of Stock Solutions and Full M9 Medium

Samples of 2 mg of racemic N-HLs were weighed with an analytical balance into 5 mL volumetric flasks. The flasks were filled with acetonitrile to the volume line to yield 400-ppm solutions for each racemic N-HLs, except for 3-oxododecanoyl-homoserine lactone which was a 400-ppm solution for the L-enantiomer. From the 400-ppm AHL stock solutions, 1-ppm and 4 ppm working solutions were prepared for N-HLs standards and internal standard, respectively.

M9 medium was prepared according to instructions and autoclaved to sterilize. Full M9 medium was completed with filter sterilized 20% (w/w) glucose and 1M magnesium sulfate.

5.3.3 Sample Preparation

A 100 µL aliquot of a 1-ppm working solution of AHLs, OHLs and HHLs in acetonitrile (C4-C14 AHLs; C4-C12 OHLs; C4-C14 HHLs) was used for the LC-MS/MS method development. The same working solution was used for the method development in GC-MS/MS with aliquots placed in 2 mL sample vials, dried with a gentle stream of ultrahigh purity N2, and derivatized with the method described below.

The samples for quantification and extraction recovery were prepared using an SPE manifold coupled to a vacuum pump. The SPE cartridges were conditioned with 10 mL each of acetonitrile, methanol, and water respectively. Then, 10 mL of full M9 medium spiked with internal standard (A-C7) working solution and N-HLs working solution was loaded on the SPE cartridge and processed. Subsequently, the cartridge was washed with 10 mL of 95:5 methanol: water and eluted with 11 mL of acetonitrile. The extracts were then evaporated using a rotatory evaporator and transferred in 2 mL of dichloromethane. Transferred samples were evaporated using a gentle stream of ultrahigh purity N2. The evaporated samples were either reconstituted with 100 µL of methanol for the analysis in LC-MS/MS or further derivatized for GC-MS/MS.

5.3.4 Derivatization for GC-MS/MS Analysis

Derivatization of 3-oxo-N-HLs and 3-hydroxy-N-HLs was conducted by adding a 75 µL of BSTFA with 1% TMCS and a 25 µL aliquot of acetonitrile as a co-solvent to the dried standard solution or biological sample and sealed with a PTFE lined cap. The solution was then mixed for 10 seconds and placed into a 130°C preheated sand bath for 45 minutes.

5.3.5 Chromatographic and MS Conditions

5.3.5.1. LC-MS/MS

A Shimadzu LC-MS 8040 system (Shimadzu Scientific Instruments, Columbia MD) with electrospray ionization and a triple quadrupole mass spectrometer was used in the positive ion mode for the LC-MS/MS analysis. The analysis was done in SRM with optimized transitions and collision energies for each enantiomeric standard. The nebulizing gas flow and drying gas flow were 3.0 and 15.0 L/minute respectively. The interface voltage was 4.5 kV and the heat block temperature was 400 °C. A ZORBAX SB-C18 column was used in tandem with a CHIRALPAK IC-3. A flow rate of 0.4 mL/minute was used with a gradient method held at water (0.1% FA):methanol (0.1% FA): (40:60) from 0-25 min, with a ramp from (40:600) to (10:90) from 25-37.5 min. Then a step gradient from (10:90) to (5:95) from 37.50-37.51 min and held at (5:95) from 37.51-50 min was implemented.

5.3.5.2 GC-MS/MS

Samples were run on a Shimadzu GCMS-TQ 8040 (Shimadzu Scientific Instruments, Columbia, MD, USA) equipped with a β-DEX 225¬TM column (30m x 0.25mm x 0.25µm film thickness) (25% 2,3-di-O-acetyl-6-O-TBDMS-β-cyclodextrin in SPB-20 poly[20% phenyl/80% dimethylsiloxane]) (Millipore-Sigma, Burlington, MA, USA). A split-less injection of 1 µL with 2-minute split-time, ending at a split ratio of 20:1 was delivered (220°C). The constant flow of carrier gas (He) was 1.1 mL/minute (40 cm/s), with an oven temperature program starting at 160°C (10-minute hold) increased at a rate of 1°C/minute to 230°C (50-minute hold). A GC-MS interface temperature and MS ion source temperature were set to 230°C and 280°C, respectively. EI was adjusted to 70 eV and the mass spectrometer was operated in SRM mode with optimized collision energies and quadrupole one and quadrupole three voltages.

5.3.6 Extraction Recovery

The extraction recovery was assessed in pentaplicates for a concentration of 100 ppb. Firstly, a 10 mL amount of full M9 medium was spiked with 10 µL of working solution (1 ppm) ("pre spike") and subsequently processed as outlined in the Sample Preparation section above. A 7.5 µL of internal standard working solution (4 ppm) was added to the reconstituted sample (2 mL of dichloromethane) before the last evaporation step. Secondly, a blank 10 mL amount of full M9 medium was processed as outlined in the Sample Preparation section above. Then, 10 µL of working solution (1 ppm) and 7.5 µL of internal standard working solution (4 ppm) were spiked ("post-spike") into the reconstituted sample (2 mL of dichloromethane). All samples were analyzed using LC-MS/MS. Extraction recovery was calculated as the ratio of area corrected with internal standard in "pre-spike" and "post-spike" samples.

5.3.7 Quantitation

The calibration curves were measured in pentaplicates. For LC MS/MS, a 10 mL of full M9 medium was spiked with 1, 2.5, 5, 10, 25, 50, 100 and 200 µL of N-HLs working solution (1 ppm) and 7.5 µL of internal standard working solution (4 ppm). For GC MS/MS, a 10 mL of full M9 medium was spiked with 50, 75, 100, 150 and 200 µL of N-HLs working solution (1 ppm) and 100 µL of internal standard working solution (4 ppm).

5.4 Results and Discussion

The difference in lipophilicity of the 18 N-HLs son their retention behavior makes the identification and quantification of all enantiomers in a single analysis very challenging. Thus, comprehensive methods to identify and quantify N-HLs using offline SPE LC-MS/MS and offline SPE GC-MS/MS were developed.

5.4.1 Solid-Phase Extraction

In a previous study, the extraction recovery of 13 AHLs was tested on polyamidic, ion exchange, primary-secondary amine, endcapped octadecyl silica-bonded, and hydrophilic-lipophilic balanced (HLB) SPE cartridges [22]. The highest recoveries were observed for the HLB sorbent. However, the most hydrophilic N-HLs; H-C4-homoserine lactone, O-C4-homoserine lactone and H-C6-homoserine lactone were not tested. Therefore, a more comprehensive recovery study using the HLB sorbent has been carried out for the 18 N-HLs in this study, including the more challenging polar derivatives.

N-HLs are produced in trace amounts by individual bacterial species, thus a preconcentration factor of 100 is considered optimal during extraction. It is clear that preconcentration will increase the sensitivity of the method, however, the drawback of this approach is the preconcentration of other compounds present in the sample matrix, possible impurities in organic solvents and leachable compounds from the laboratory consumables. The presence of these substances in the electrospray ion source concurrently with N-HLs can cause suppression or enhancement of ionization. If the presence of these compounds in samples varies over time, the reproducibility of method is diminished.

It was found that the initial extractions of standard samples spiked in M9 growth medium were not reproducible (%RSD > 20), with multiple matrix peaks observed throughout the chromatogram. Several experiments were carried out to find the source of these unwanted contaminants, including blanks of preconcentrated organic solvents used during sample preparation and extraction blanks of 10 mL of pure M9 medium. The source of the contaminants was identified as leachable polymers from the SPE cartridge itself. Pretreatment of the cartridge with the elution solvent was applied as an extra step before the conditioning of HLB cartridges to limit leaching during the elution step.

The extraction of polar compounds from polar matrices is known to be challenging. In this case, polar matrix compounds affected the extraction recovery and reproducibility of the early eluting polar N-HLs. To limit or prevent the presence of polar matrix molecules in the final

sample, the evaporated extracts were reconstituted in organic solvent, transferred to another vial, evaporated again and finally reconstituted in the sample solvent. Three different organic solvents were tested (i.e., DCM, EtOAc, and MeOH). In the case of DCM and EtOAc, the matrix molecules eluting near the dead volume were substantially reduced compared to MeOH. Highest recoveries were achieved using DCM.

Introducing the pretreatment of SPE cartridges with the elution solvent, together with using DCM as the transferring solvent, significantly increased the reproducibility of the extraction recovery and reduced the number of matrix peaks. The final extraction recoveries for all N-HLs in the study ranged from 80% to 105% except for H-C4, O-C4 , and A-C14 which were 4%, 10%, and 70%, respectively (Figure 5-2).

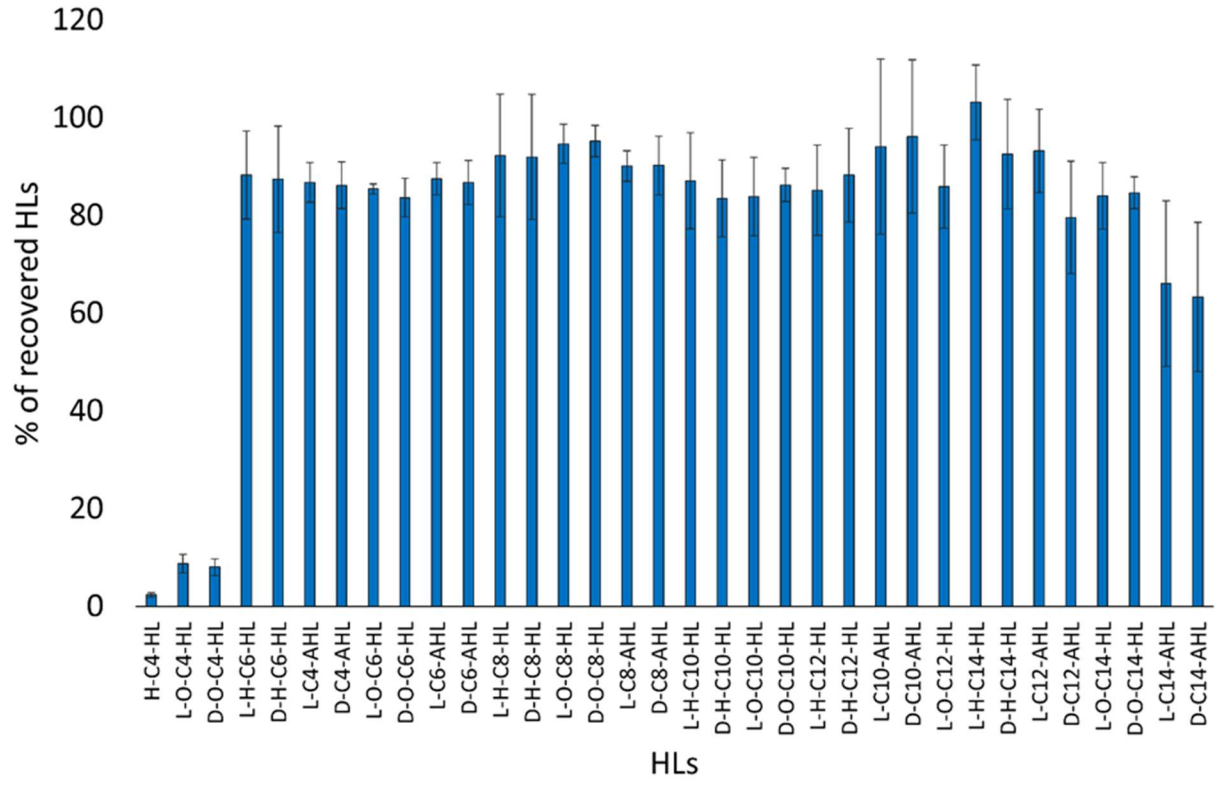

Figure 5-2**.** Acquired percent Recovery for 100 ppb D-/L-*N*-acyl homoserine lactones, D-/L-*N*-3-hydroxyacyl homoserine lactones and D-/L-*N*-3-oxoacyl homoserine lactones. Standards processed by SPE in pentaplicate and analyzed by LC-MS/MS. Method described in Extraction Recovery under the Experimental section.

The low recoveries of H-C4 and O-C4 are the likely reason why these compounds were rarely detected or reported in real bacterial samples.

5.4.2 LC-MS/MS method

The chiral separations of all compounds were achieved using immobilized cellulose tris(3,5-dichlorophenylcarbamate). However, the retention of all N-HLs on this stationary phase is very low, resulting in co-elution of all peaks just after the dead volume of the column. This co-elution leads to inevitable ionization suppression and inaccurate quantification. To overcome this issue, a stationary phase with a different selectivity is needed. A similar problem was encountered and solved earlier by connecting, in-tandem, a C18 column with a chiral column. This approach was briefly presented for the chiral separation of 6 AHLs [19], not including OHLs and HHLs. However, peaks for A-C6, A-C8, and A-C10 still co-eluted and A-C4 was omitted. The connection of the C18 column with cellulose tris(3,5-dichlorophenylcarbamate) enabled homologous separations along with enantioseparations of seven AHLs, six OHLs, and six HHLs (Figure 5-3).

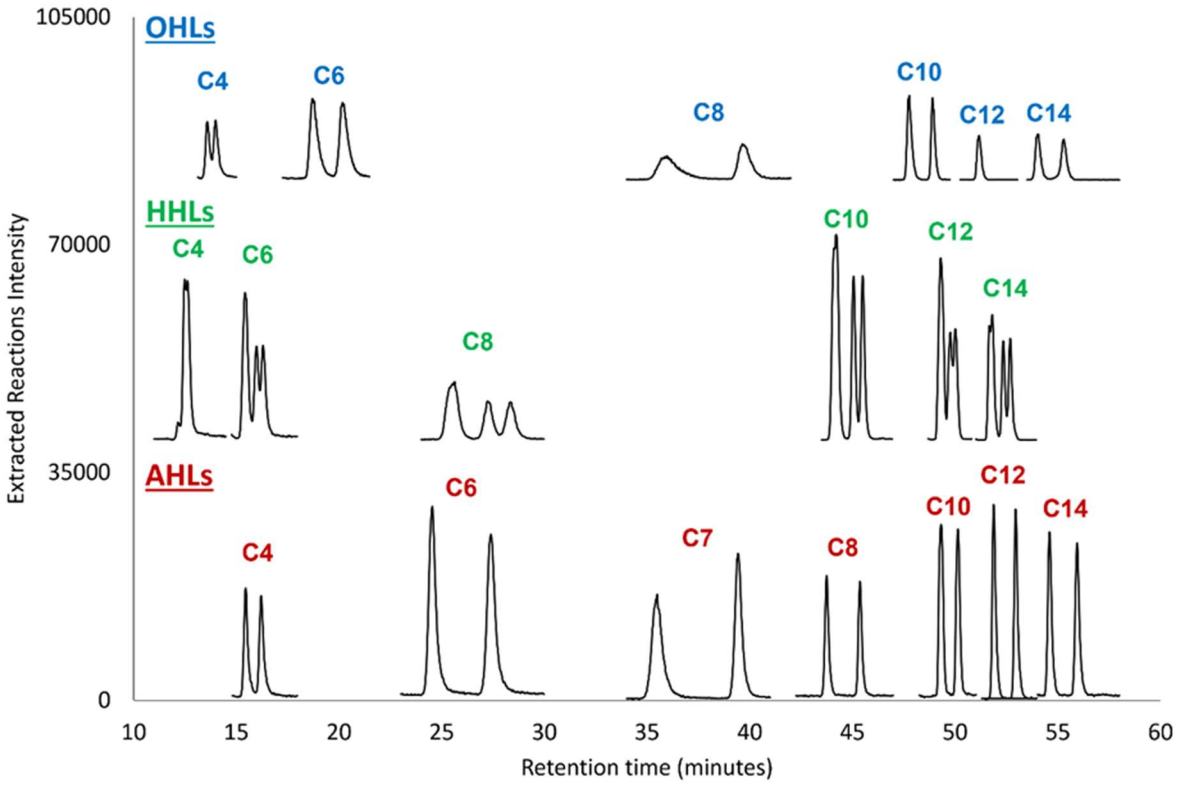

Figure 5-3**.** LC SRM chromatogram for $[M+H]^+$ to 102 m/z for D-/L-*N*-acyl homoserine lactones (AHLs), D-/L-*N*-3-hydroxyacyl homoserine lactones (HHLs) and D-/L-*N*-3-oxoacyl homoserine lactones (OHLs). Chromatographic conditions are outlined in the Chromatographic and MS Conditions. Chromatograms are offset for visual clarity. LC SRM transition are detailed in Supplementary information.

All OHLs and AHLs were baseline separated with L-enantiomers always eluting before D-enantiomers (Table 5.1).

Table 5-1. Optimized chiral separations of L/D-homoserine lactones by LC-MS/MS

Analyte	No. of isomers	$t_{R1\ (min)}$[1]	$t_{R2\ (min)}$[2]	R_s[3]
L, D C4-HSL	2	15.33	16.06	2.00
L, D C6-HSL	2	24.07	26.78	4.12
L, D C8-HSL	2	43.40	45.04	4.87
L, D C10-HSL	2	49.14	50.00	2.20
L, D C12-HSL	2	51.76	52.76	2.62
L, D C14-HSL	2	54.38	55.68	3.44
P_1, P_2, P_3, P_4 [4] 3-hydroxy-C4-HSL*	4	12.45	not separated	0.00
P_1, P_2 3-hydroxy-C6-HSL	2	15.32	not separated	0.00
P_2, P_3 3-hydroxy-C6-HSL	2	15.32	15.84	1.10
P_3, P_4 3-hydroxy-C6-HSL	2	15.84	16.15	0.65
P_1, P_2 3-hydroxy-C8-HSL	2	25.03	not separated	0.00
P_2, P_3 3-hydroxy-C8-HSL	2	25.03	27.66	2.82
P_3, P_4 3-hydroxy-C8-HSL	2	27.66	28.85	1.53
P_1, P_2 3-hydroxy-C10-HSL	2	43.77	43.91	0.08
P_2, P_3 3-hydroxy-C10-HSL	2	43.91	44.75	1.37
P_3, P_4 3-hydroxy-C10-HSL	2	44.75	45.18	1.20
P_1, P_2 3-hydroxy-C12-HSL	2	49.17	not separated	0.00
P_2, P_3 3-hydroxy-C12-HSL	2	49.17	49.61	0.81

P_3, P_4 3-hydroxy-C12-HSL	2	49.61	49.88	0.43
P_1, P_2 3-hydroxy-C14-HSL	2	51.50	51.69	0.33
P_2, P_3 3-hydroxy-C14-HSL	2	51.69	52.18	1.18
P_3, P_4 3-hydroxy-C14-HSL	2	52.18	52.50	0.91
L, D 3-oxo-C4-HSL	2	13.52	13.91	1.00
L, D 3-oxo-C6-HSL	2	18.44	19.87	1.96
L, D 3-oxo-C8-HSL	2	34.90	38.93	3.02
L, D 3-oxo-C10-HSL	2	47.47	48.64	2.98
L, D 3-oxo-C14-HSL	2	53.77	55.02	2.60

[1] Retention time of first peak

[2] Retention time of second peak

[3] Resolution between indicated peaks

[4] P_1, P_2, P_3, P_4 stands for first, second, third, and fourth eluted peak of HHLs, respectively

[*] 3-hydroxy-C4-HSL is eluted as one peak

These results could not be confirmed for the analyte O-C12 due to the lack of a racemic standard or pure D enantiomer. In the case of HHL, four peaks, three peaks, and two peaks were observed for C10 and C14; C6, C8, and C12; and C4 derivatives, respectively. The chiral elution order of HHLs follows the same trend as for other N-HLs derivatives, i.e., L-enantiomers are eluted before D-enantiomers.

The identification of N-HLs was carried out by the conformity of retention time, and three different SRM transitions. To increase the certainty of identification, the ratios of the SRM transitions can be calculated and compared. This identification can be carried out only for peaks that are over the LOD of the chromatographic method (Table 5-2).

Table 5-2 Comparison of enantiomeric quantification of homoserine lactones using LC-MS/MS and GC-MS/MS. Samples extracted by SPE

Analyte	**LC -MS/MS**			**GC – MS/MS**		
	LOD (ppb)	**LOQ (ppb)**	**R^2**	**LOD (ppb)**	**LOQ (ppb)**	**R^2**
L C4-HSL	4	13	0.9981	<LOD	<LOD	<LOD
D C4-HSL	2	7	0.9964	<LOD	<LOD	<LOD
L C6-HSL	2	7	0.9993	382	1160	0.9730
D C6-HSL	3	11	0.9992	242	735	0.9890
L C8-HSL	3	9	0.9994	307	932	0.9824
D C8-HSL	3	9	0.9998	566	1716	0.9426
L C10-HSL	7	23	0.9991	336	1018	0.9635
D C10-HSL	8	27	0.9992	880	2667	0.9425
L C12-HSL	5	16	0.9995	210	637	0.9854
D C12-HSL	2	8	0.9918	63	192	0.9987
L C14-HSL	4	13	0.9979	418	1268	0.9444
D C14-HSL	6	19	0.9965	366	1109	0.9569
3-hydroxy-C4-HSL	Quantitation was not possible because of low extraction recovery.					
P_1 + P_2 [4] 3-hydroxy-C6-HSL	4	13	0.9972	221	671	0.9838
P_3 + P_4 [4] 3-hydroxy-C6-HSL	5	15	0.9977	209	632	0.9586
P_1 + P_2 3-hydroxy-C8-HSL	5	16	0.9976	123	374	0.9949

P_3 + P_4 3-hydroxy-C8-HSL	5	15	0.9980	3588	10872	0.8443
P_1 + P_2 3-hydroxy-C10-HSL	4	14	0.9996	1296	3926	0.8833
P_3 + P_4 3-hydroxy-C10-HSL	3	11	0.9989	1180	3575	0.9725
P_1 + P_2 3-hydroxy-C12-HSL	4	12	0.9982	83	251	0.9977
P_3 + P_4 3-hydroxy-C12-HSL	5	15	0.9951	535	1621	0.9744
P_1 + P_2 3-hydroxy-C14-HSL	2	7	0.9908	417	1264	0.9448
P_3 + P_4 3-hydroxy-C14-HSL	1	5	0.9986	137	414	0.9872
L 3-oxo-C4-HSL	Quantitation was not possible because of low extraction recovery.					
D 3-oxo-C4-HSL	Quantitation was not possible because of low extraction recovery.					
L 3-oxo-C6-HSL	2	8	0.9905	678	2057	0.9159
D 3-oxo-C6-HSL	4	13	0.9900	515	1561	0.9498
L 3-oxo-C8-HSL	2	7	0.9911	<LOD	<LOD	<LOD
D 3-oxo-C8-HSL	2	6	0.9905	<LOD	<LOD	<LOD
L 3-oxo-C10-HSL	4	13	0.9917	<LOD	<LOD	<LOD
D 3-oxo-C10-HSL	2	6	0.9911	446	1338	0.9625
L 3-oxo-C12-HSL	2	7	0.9891	742	2250	0.9081
L 3-oxo-C14-HSL	15	50	0.9917	n.a.	n.a.	n.a.
D 3-oxo-C14-HSL	15	51	0.9866	n.a.	n.a.	n.a.

A previously reported LC-MS method had approximately two orders of magnitude higher LODs which was insufficient for many biological studies [19]. Therefore, this more sensitive LC-MS/MS analysis can be readily used as the scouting method for the identification of D-N-HLs in various matrices, e.g., bacterial medium, nasal lavages, earwashes, wastewater, etc.

The LOQs for all the compounds is below 10 ppb excluding A-C10 and O-C14 (Table 3). The quantitation was carried out using calibration curves for analytes with 6 to 8 concentration levels of pentaplicate standards spiked into full M9 bacterial medium and processed by the sample preparation method described herein (see Experimental). The linearity of calibration curves was higher than 0.99 in all cases (Table 5-3). The precision was calculated as the relative standard deviation and was consistently lower than 20% for AHLs and HHLs and 30% for OHLs. The calculated LODs and LOQs are summarized in Table 5-2. The real lower limit of quantification (LLOQ); i.e., the lowest point on the calibration curve was as low as 5 ppb.

5.4.3 GC-MS/MS Method

A previously developed chiral method using GC coupled with a single quadrupole MS [19] was used for the analysis of 17 N-HLs). The chromatographic method presented herein was coupled with a triple quadrupole MS system allowing for a more sensitive and specific technique compared to the aforementioned method. The enantioseparation of the N-HLs in this study was carried out using a β-DEX 225 GC column (Figure 5-4).

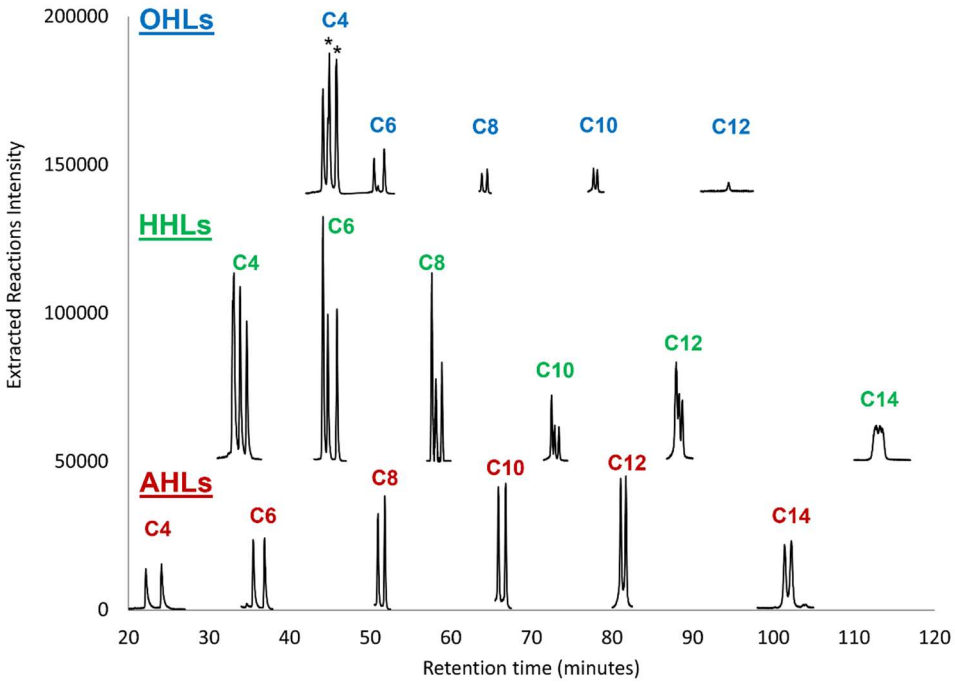

Figure 5-4. GC SRM chromatogram for D-/L-N-acyl homoserine lactones (AHLs), D-/L-N-3-hydroxyacyl homoserine lactones (HHLs) and D-/L-*N*-3-oxoacyl homoserine lactones (OHLs). Chromatographic conditions are outlined in the Chromatographic and MS Conditions. Chromatograms are offset for visual clarity. GC SRM transition are detailed in Supplementary information.

This particular column has an advantage when it comes to separating chiral homologous series due to the presence of both an achiral stationary phase and chiral selector. The 75% of SPB-20 (20 poly[20% phenyl/80% dimethylsiloxane]) enabled the separation of the homologous N-HLs, while concurrently the 25% of 2,3-di-O-acetyl-6-O-TBDMS-β-cyclodextrin, that is dissolved in SPB-20, provided chiral resolution for the N-HLs enantiomers. The AHLs can be analyzed by GC without derivatization. Due to heat lability and low sensitivity, respectively, derivatization of OHLs and HHLs is required. The oxidized carbon on the acyl chain is derivatized by using BSTFA with 1% TMCS as a trimethylsilyl (TMS) donor to the oxygen atom (see Experimental). When OHLs are derivatized, the carbonyl accepts the TMS, with an unsaturated bond forming between carbons 2 and 3 on the acyl chain, no new chiral center is created. When HHLs are derivatized, the hydroxyl moiety is derivatized with TMS and no change in chirality occurs.

For the six N-HLs the best resolution between enantiomers is observed for the A-C4 which is baseline separated in 25 minutes. GC resolution between enantiomeric pairs decreases as the alkyl chain length increases with partial coelution apparent for A-C12 and A-C14. For the five TMS-OHLs the best resolution is observed for TMS-O-C4. A decrease in resolution with increasing chain length is again apparent with partial coelution starting with TMS-O-C10. Separation between enantiomers of TMS-O-C12 was inconclusive because of the unavailability of a racemic standard. HHLs retain their two chiral centers, after derivatized with TMS, thus four stereoisomers will be present. Four distinct peaks are visible for racemic TMS-H-C4. The first two peaks being L-HHLs, which are only partially separated and the last two peaks being D-N-HLs which are baseline separated. The chiral retention order for L- and D-N-HLs remains for TMS-H-C6 through TMS-H-C14, however, the partial separation of the L enantiomers is lost from C6 onward. Resolution between L- and D-TMS-HHLs decreases with increasing chain length with partial coelution apparent at TMS-H-C10 (Figure 5.4).

5.4.4 Comparison of Chiral Separation Methods of N-HLs

Until now, all comprehensive chiral analytical methods involving N-HLs were carried out with GC-MS (single quadrupole). The limit of detection for these methods was around 1 ppm [16, 19, 20]. However, the concentrations of N-HLs in nasal lavages, wastewater, and bacterial medium can be 10 to 1000 times lower. GC coupled with triple-quadrupole was employed and LODs as low as 63 ppb were obtained (Table 5.3).

Table 5-3 Optimized chiral separations of L/D-homoserine lactones by GC-MS/MS

Analyte	**No. of isomers**	$t_{R1\ (min)}$[1]	$t_{R2\ (min)}$[2]	R_s[3]
L, D C4-HSL	2	22.16	24.11	4.65
L, D C6-HSL	2	35.30	36.93	3.44

L, D C8-HSL	2	50.95	51.72	2.48
L, D C10-HSL	2	65.89	66.80	3.17
L, D C12-HSL	2	81.06	81.70	2.03
L, D C14-HSL	2	101.40	102.23	1.45
P_1, P_2 3-hydroxy-C4-HSL	2	33.08	not separated	0.00
P_2, P_3 3-hydroxy-C4-HSL	2	33.08	33.85	1.81
P_3, P_4 3-hydroxy-C4-HSL	2	33.85	34.68	2.52
P_1, P_2 3-hydroxy-C6-HSL	2	44.13	not separated	0.00
P_2, P_3 3-hydroxy-C6-HSL	2	44.13	44.73	1.49
P_3, P_4 3-hydroxy-C6-HSL	2	44.73	45.87	4.03
P_1, P_2 3-hydroxy-C8-HSL	2	58.53	not separated	0.00
P_2, P_3 3-hydroxy-C8-HSL	2	58.53	58.85	1.62
P_3, P_4 3-hydroxy-C8-HSL	2	58.85	59.88	3.86
P_1, P_2 3-hydroxy-C10-HSL	2	72.49	not separated	0.00
P_2, P_3 3-hydroxy-C10-HSL	2	72.49	72.88	1.37
P_3, P_4 3-hydroxy-C10-HSL	2	72.88	73.41	2.01
P_1, P_2 3-hydroxy-C12-HSL	2	87.97	not separated	0.00
P_2, P_3 3-hydroxy-C12-HSL	2	87.97	88.29	0.66
P_3, P_4 3-hydroxy-C12-HSL	2	88.29	88.71	0.93
P_1, P_2 3-hydroxy-C14-HSL	2	112.74	not separated	0.00
P_2, P_3 3-hydroxy-C14-HSL	2	112.74	113.24	0.14
P_3, P_4 3-hydroxy-C14-HSL	2	113.24	113.54	0.11

L, D 3-oxo-C4-HSL	2	44.91	45.81	1.64
L, D 3-oxo-C6-HSL	2	50.68	51.76	3.57
L, D 3-oxo-C8-HSL	2	63.84	64.52	2.83
L, D 3-oxo-C10-HSL	2	77.70	78.16	2.21

[1]Retention time of first peak

[2]Retention time of second peak

[3]Resolution between indicated peaks

[4] P_1, P_2, P_3, P_4 stands for first, second, third, and fourth eluted peak of HHLs, respectively

Even lower LOD and LOQ were obtained using LC-MS/MS. Therefore, both GC-MS/MS (QqQ) and LC-MS/MS (QqQ) methods can be used as complementary approaches for the chiral separation of N-HLs in biological samples. Deciding which technique to use depends on the available instrumentation and the application of the analytical method. The main advantage of LC-MS/MS over GC-MS/MS is the lack of derivatization of HHLs and OHLs, two times faster analysis time, higher sensitivity, and a lower number of artificial peaks from the matrix. Despite these drawbacks, higher resolution of the smaller more hydrophilic N-HLs was obtained in GC-MS/MS. In contrast, higher resolution for more hydrophobic N-HLs was achieved in LC-MS/MS.

The use of the chiral LC-MS/MS method is suggested for scouting and quantification methods. Chiral GC-MS/MS methods developed herein should be used preferably for confirmation of the results obtained by LC-MS/MS. The double confirmation increases specificity towards N-HLs and will ameliorate the sensitivity and reproducibility issue of the results obtained by previous chiral and achiral analytical methods [16, 19, 20].

5.5 Conclusions

Comprehensive analytical approaches for the analysis of N-HLs including sample preparation (SPE), chiral LC-MS/MS and chiral GC-MS/MS were developed. The extraction recovery for the majority of N-HLs ranged from 80% to 105%. The LC-MS/MS method outperforms GC-MS/MS in sensitivity, time of the analysis, and ease of use. Therefore, it is the method of choice with GC-MS/MS being used preferably for the confirmation of results. However, GC-MS/MS provided better stereoisomeric resolution of the smaller, more hydrophilic N-HLs. These newly developed, sensitive methods will aid to unveil the role of not only D-N-HLs in bacteria in vitro but subsequently in vivo.

5.6 References

[1] C. Fuqua, E. Greenberg, Listening in on bacteria: acyl-homoserine lactone signaling, Nat. Rev. Mol. Cell. Biol. 3 (2002) 685–695. https://doi.org/10.1038/nrm907.

[2] J. Liu, K. Fu, C. Wu, K. Qin, F. Li, L. Zhou, “In-Group” Communication in Marine Vibrio: A Review of N-Acyl Homoserine Lactones-Driven Quorum Sensing, Front. Cell. Infect. Microbiol. 8 (2018) 139. https://doi.org/10.3389/fcimb.2018.00139.

[3] A. Suppiger, N. Schmid, C. Aguilar, G. Pessi, A. Eberl, Two quorum sensing systems control biofilm formation and virulence in members of the Burkholderia cepacia complex, Virulence 4 (2013) 400-409. https://doi.org/10.4161/viru.25338.

[4] R.S. Smith, B.H. Iglewski, P. Aeruginosa quorum-sensing systems and virulence, Curr. Opin. Microbiol. 6 (2003) 56-60. https://doi.org/10.1016/s1369-5274(03)00008-0.

[5] P.N. Jimenez, G. Koch, J.A. Thompson, K.B. Xavier, R.H. Cool, W.J. Quax, The Multiple Signaling Systems Regulating Virulence in Pseudomonas aeruginosa, Microbiol. Mol. Biol. Rev. 76 (2012) 46-65. https://doi.org/10.1128/MMBR.05007-11.

[6] M. Schuster, D.J. Sexton, S.P. Diggle, E.P. Greenberg, Acyl-Homoserine Lactone Quorum Sensing: From Evolution to Application, Annu. Rev. Microbiol. 67 (2013) 43–63. https://doi.org/10.1146/annurev-micro-092412-155635.

[7] J.D. Habimana, J. Ji, F. Pi, E. Karangwa, J. Sun, W. Guo, F. Cui, J. Shao, C. Ntakirutimana, X. Sun, A class-specific artificial receptor-based on molecularly imprinted polymer-coated quantum dot centers for the detection of signaling molecules, N-acyl-homoserine lactones present in gram-negative bacteria, Anal. Chim. Acta 1031 (2018) 134-144. https://doi.org/10.1016/j.aca.2018.05.018.

[8] X. Yang, J. Sun, F. Cui, J. Ji, L. Wang, Y. Zhang, X. Sun, An eco-friendly sensor based on CQD@MIPs for detection of N-acylated homoserine lactones and its 3D printing applications, Talanta 219 (2020) 121343. https://doi.org/10.1016/j.talanta.2020.121343.

[9] T.R.I. Cataldi, G. Bianco, L. Palazzo, V. Quaranta, Occurrence of N-acyl-L-homoserine lactones in extracts of some Gram-negative bacteria evaluated by gas chromatography–mass spectrometry, Anal. Biochem. 361 (2007) 226-235. https://doi.org/10.1016/j.ab.2006.11.037.

[10] C. Reimmann, M. Beyeler, A. Latifi, H. Winteler, M. Foglino, A. Lazdunski, D. Haas, The global activator GacA of Pseudomonas aeruginosa PAO positively controls the production of the autoinducer N-butyryl-homoserine lactone and the formation of the virulence factors pyocyanin, cyanide, and lipase, Mol. Microbiol. 24 (1997) 309–319. https://doi.org/10.1046/j.1365-2958.1997.3291701.x.

[11] D. Kušar, K. Šrimpf, P. Isaković, L. Kalšek, J. Hosseini, I. Zdovc, T. Kotnik, M. Vengušt, G. Tavčar-Kalcher, Determination of N-acylhomoserine lactones of Pseudomonas aeruginosa in clinical samples from dogs with otitis externa, BMC Vet. Res. 12 (2016) 233. https://doi.org/10.1186/s12917-016-0843-0.

[12] Y.-W. Kim, C. Sung, S. Lee, K.-J. Kim, Y.-H. Yang, B.-G. Kim, Y.K. Lee, H.W. Ryu, Y.-G. Kim, MALDI-MS-Based Quantitative Analysis for Ketone Containing Homoserine Lactones in Pseudomonas aeruginosa, Anal. Chem. 87 (2015) 858-863. https://doi.org/10.1021/ac5039362.

[13] T.P.T. Hoang, M. Barthélemy, R. Lami, D. Stien, V. Eparvier, D. Touboul, Annotation and quantification of N-acyl homoserine lactones implied in bacterial quorum sensing by supercritical-fluid chromatography coupled with high-resolution mass spectrometry, Anal. Bioanal. Chem. 412 (2020) 2261-2276. https://doi.org/10.1007/s00216-019-02265-4.

[14] T.R.I. Cataldi, G. Bianco, S. Abate, Profiling of N-acyl-homoserine lactones by liquid chromatography coupled with electrospray ionization and a hybrid quadrupole linear ion-trap and Fourier-transform ion-cyclotron-resonance mass spectrometry (LC-ESI-LTQ-FTICR-MS), J. Mass. Spectrom. 43 (2007) 82-96. https://doi.org/10.1002/jms.1275.

[15] A.M. Pomini, G.P. Manfio, W.L. Araújo, A.J. Marsaioli, Acyl-homoserine Lactones from Erwinia psidii R. IBSBF 435T, a Guava Phytopathogen (Psydium guajava L.), J. Agric. Food Chem. 53 (2005) 6262-6265. https://doi.org/10.1021/jf050586e.

[16] A.K. Malik, A. Fekete, I. Gebefuegi, M. Rothballer, P. Schmitt-Kopplin, Single drop microextraction of homoserine lactones based quorum sensing signal molecules, and the separation of their enantiomers using gas chromatography mass spectrometry in the presence of biological matrices, Microchim. Acta 166 (2009) 101-107. https://doi.org/10.1007/s00604-009-0183-x.

[17] C. Götz, A. Fekete, I. Gebefuegi, S.T. Forczek, K. Fuksová, X. Li, M. Englmann, M. Gryndler, A. Hartmann, M. Matucha, P. Schmitt-Kopplin, P. Schröder, Uptake, degradation and chiral discrimination of N-acyl-D/L-homoserine lactones by barley (Hordeum vulgare) and yam bean (Pachyrhizus erosus) plants, Anal. Bioanal. Chem. 389 (2007) 1447-1457. https://doi.org/10.1007/s00216-007-1579-2.

[18] T. Ikeda, K. Kajiyama, T. Kita, N. Takiguchi, A. Kuroda, J. Kato, H. Ohtake, The Synthesis of Optically Pure Enantiomers of N-Acyl-homoserine Lactone Autoinducers and Their Analogues, Chem. Lett. 30 (2001) 314-315. https://doi.org/10.1246/cl.2001.314.

[19] E. Readel, A.E. Portillo, M. Talebi, D.W. Armstrong, Enantiomeric separation of quorum sensing autoinducer homoserine lactones using GC-MS and LC-MS, Anal. Bioanal. Chem. 412 (2020) 2927-2937. https://doi.org/10.1007/s00216-020-02534-7.

[20] A.E. Portillo, E. Readel, D.W. Armstrong, Production of both L- and D- N-acyl-homoserine lactones by Burkholderia cepacia and Vibrio fischeri. MicrobiologyOpen 10 (2021) e1242. https://doi.org/10.1002/mbo3.1242.

[21] T. Miyamoto, H. Homma, D-Amino acid metabolism in bacteria. J. Biochem. 170 (2021) 5 13. https://doi.org/10.1093/jb/mvab043.

[22] J. Wang, L. Ding, K. Li, W. Schmieder, J. Geng, K. Xu, Y. Zhang, H. Ren, Development of an extraction method and LC-MS analysis for N-acylated-L-homoserine lactones (AHLs) in wastewater treatment biofilms, J. Chromatogr. B Analyt. Technol. Biomed. Life Sci. 1041-1042 (2017) 37-44. https://doi.org/10.1016/j.jchromb.2016.11.029.

[23] S. Rodriguez-Mozaz, M.J. Lopez de Alda, D. Barceló, Advantages and limitations of on-line solid phase extraction coupled to liquid chromatography-mass spectrometry technologies versus biosensors for monitoring of emerging contaminants in water, J. Chromatogr. A 1152 (2007) 97-115. https://doi.org/10.1016/j.chroma.2007.01.046.

[24] K.H. McClean, M.K. Winson, L. Fish, A. Taylor, S.R. Chhabra, M. Camara, M. Daykin, S. Swift, B.W. Bycroft, G.S.A.B. Stewart, P. Williams, Quorum sensing and Chromobacterium violaceum: exploitation of violacein production and inhibition for the detection of N-acyl homoserine-lactones, Microbiology (Reading, Engl.) 143 (1997) 3703-3711. https://doi.org/10.1099/00221287-143-12-3703

[25] P.D. Shaw, G. Ping, S.L. Daly, C. Cha, J.E.Jr. Cronan, K.L. Rinehaert, S.K. Farrand, Detecting and characterizing N-acyl-homoserine lactone signal molecules by thin-layer chromatography, Proc. Natl. Acad. Sci. USA 94 (1997) 6036-6041. https://doi.org/10.1073/pnas.94.12.6036.

[26] J.P. Pearson, K.M. Gray, L. Passador, K.D. Tucker, A. Eberhard, B.H. Iglewski, E.P. Greenberg, Structure of the autoinducer required for expression of Pseudomonas aeruginosa virulence genes, Proc. Natl. Acad. Sci. USA 91 (1994) 197-201. https://doi.org/10.1073/pnas.91.1.197

Chapter 6

Comprehensive enantiomeric analysis of D,L-*N*-acyl homoserine lactones in *Pectobacterium atrosepticum* and *Pseudomonas aeruginosa*

6.1 Abstract

Quorum sensing (QS) is a process in which bacterial cells communicate with each other by the means of diffusible signaling molecules. QS aids bacteria to sense their population density and upon reaching a high enough cell density, they collectively exhibit a phenotype. *N*-acyl homoserine lactones (N-HLs) are a type of such signaling molecules synthesized by gram-negative bacteria. Until recently, methods used for detection of N-HLs have not considered the chirality of these molecules and it was assumed that only the L-enantiomer was produced by bacteria. The production and effects of D-N-HLs have rarely been studied. In this work, the temporal production of D-N-HLs in the plant pathogen *Pectobacterium atrosepticum* and the human pathogen *P. aeruginosa* are presented. Both bacteria produced D-N-HLs in significant amounts and in some cases, they had higher concentrations than QS signaling L-N-HLs. Previously unreported D-enantiomers of *N*-3-oxoacyl and *N*-3-hydroxyacyl homoserine lactones were detected in *P. atrosepticum*. Interestingly, L-N-HLs produced in the lowest concentrations had relatively higher amounts of their corresponding D-enantiomers. Potential sources of D-N-HLs and their significance are discussed herein.

6.2 Introduction

Cell-to-cell communication occurs in bacteria through diffusible molecules in a process known as quorum sensing (QS). [1–3] It involves the biosynthesis of autoinducer molecules by bacteria and their release outside the cell. When reaching a critical concentration, the molecules diffuse back into the cell and are responsible for regulating phenotypic expression. This phenomenon enables bacteria to reach a certain population before exhibiting a phenotype. *N*-acyl homoserine lactones (N-HLs) are the autoinducer molecules linked to QS in gram-negative bacteria.[1,2,4] N-HL molecules consist of a fatty acyl chain attached via an amide bond to a γ-butyrolactone ring .[5] Diversity of N-HLs comes from the varying length of the acyl chain and functionality on the third position of the acyl chain. As shown in Figure 6-1, the chain lengths can vary from 4 to 18 carbons and can be substituted with either a hydroxy group or a carbonyl on the third position of the acyl chain. [6]

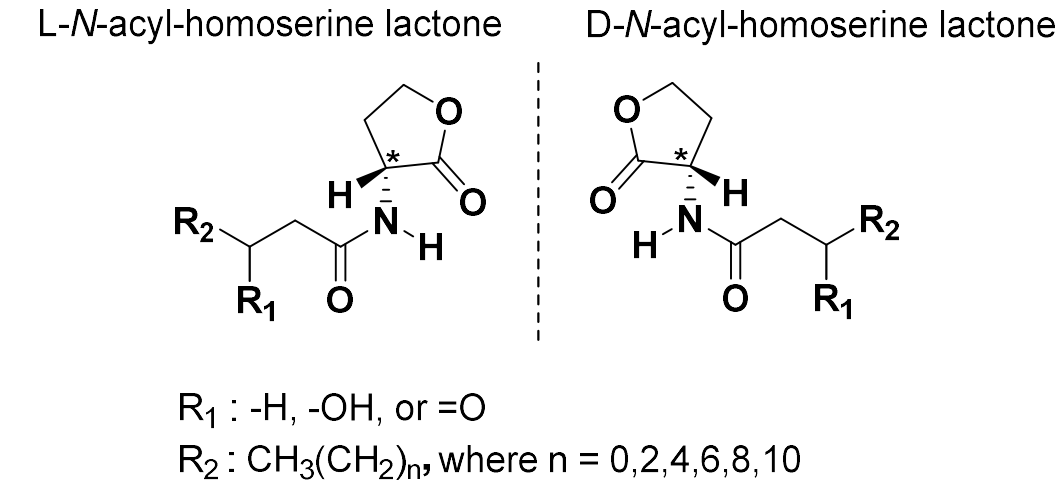

Figure 6-1. Structure of D,L-*N*-acyl homoserine lactones. R_1 represents the substitution on the third position of the acyl chain and R_2 represents the length of the acyl chain.

There is a second chiral center present on the acyl chain of the 3-hydroxy N-HLs. This results in two pairs of enantiomers .[5,7] Different bacteria have been shown to have specific types of N-HLs to facilitate QS.[5,8] To unify varying nomenclature, Table 6.1 exhibits the N-HLs explored in this study and abbreviations thereof. N-HLs indicates all *N*-acyl homoserine lactones, AHLs

Table 6-1. Abbreviations of *N*-acyl homoserine lactones used in this study.

Homoserine lactone	Abbreviation
D,L-*N*-acyl homoserine lactone	D,L-N-HL
Unsubstituted N-HLs	D,L-AHL
D,L-*N*-3-oxoacyl homoserine lactone	D,L-OHL
D,L-*N*-3-hydroxyacyl homoserine lactone	D,L-HHL
D,L-*N*-butanoyl	D,L-A-C4
D,L-*N*-hexanoyl	D,L-A-C6
D,L-*N*-octanoyl	D,L-A-C8
D,L-*N*-decanoyl	D,L-A-C10
D,L-*N*-3-oxobutanoyl	D,L-O-C4
D,L-*N*-3-oxohexanoyl	D,L-O-C6
D,L-*N*-3-oxooctanoyl	D,L-O-C8
D,L-*N*-3-oxodecanoyl	D,L-O-C10
D,L-*N*-3-oxododecanoyl	D,L-O-C12
D,L-*N*-3-oxotetradecanoyl	D,L-O-C14
D,L-*N*-3-hydroxybutanoyl	D,L-H-C4
D,L-*N*-3-hydroxyhexanoyl	D,L-H-C6
D,L-*N*-3-hydroxydecanoyl	D,L-H-C10

represents unsubstituted N-HLs, HHLs represents 3-hydroxy N-HLs and OHLs represents 3-oxo N-HLs. The general notation is D,L-XCY where D,L represents the chirality of the lactone ring, X represents the substitution (A: unsubstituted, H: 3-hydroxyacyl, and O: 3-oxoacyl). Similarly, Y represents the number of carbons on the acyl chain. For HHLs, even though there are two chiral centers, the D,L designation refers to the chirality of the lactone ring. Therefore, there are two L and D diastereomeric pairs respectively.

This study involves two important bacteria: a plant pathogen *Pectobacterium atrosepticum* and a human pathogen *Pseudomonas aeruginosa.* Both bacteria have been shown to have QS mediated virulence factors. *Pectobacterium atrosepticum* causes soft rot in potato tubers and potato blackleg disease. [9,10] QS regulated by O-C6-N-HL in *P. atrosepticum* is responsible for producing various exoenzymes that cause plant cell wall degradation. [11,12] *P. aeruginosa* has been shown to have distinct regulons for its two prominent N-HLs: A-C4 and O-C12. These N-HLs are responsible for triggering virulence factors that aid in biofilm formation, acute infections, and host cell damage.[13,14] *P. aeruginosa* infections are prevalent in cystic fibrosis patients, and many of its strains are resistant to various antibiotics.[15,16] Due to the relevance of virulence factors to QS, it can be an important pathway to target these pathogens. N-HL degrading bacteria have been used to quench the quorum and effectively virulence factors of *P. atrosepticum*.[17–19] Quorum quenching studies have also been done on *P. aeruginosa* using *Bacillus spp*.[20]

So far, biosensors, liquid chromatography coupled to UV and tandem mass spectrometry (HPLC-UV and LC-MS/MS), gas chromatography coupled to tandem mass spectrometry (GC-MS/MS, MALDI-MS, SFC-MS have been used to detect and/or quantify N-HLs. [5,21–23] LC-MS/MS and GC-MS/MS are the most reliable techniques due to the high sensitivity and selectivity that can be achieved using MS/MS. Until recently, the vast majority of methods for detection and quantification of N-HLs have been achiral. [7,8] The chirality of molecules plays a crucial role on their effects in biological systems. Prominent examples have been shown for the effects of D-amino acids on mammalian physiology.[24,25] The first report of D-N-HLs was that of D-A-C10 in *Burkholderia cepacia*.[26] Likewise, D-A-C6 in cultures of *Vibrio fischeri* and D-A-C8 in cultures of both *B. cepacia* and *V. fischeri* have been reported before.[8] Previous chiral analysis

of L-HLs have been done through GC-MS, which makes this study the first instance of a comprehensive chiral analysis of N-HLs in bacterial cultures done with LC-MS/MS. First known cases of D-HHL, and D-OHL in bacterial supernatants are reported herein along with the first instance of D-A-C4. Detection of D-AHL, D-OHL, and D-HHL from the supernatant of a single bacterial species are reported. The production over time of different D-N-HLs in minimal media cultures of *P. aeruginosa* and *P. atrosepticum* were monitored.

6.3 Materials and methods

6.3.1 Chemicals and materials

HPLC grade methanol and acetonitrile, reagent grade dichloromethane, M9 media, D-(+)-glucose, and magnesium sulfate were purchased from MilliporeSigma (St. Louis, MO). A Thermo Scientific™ Barnstead™ GenPure™ Pro water purification system was utilized for deionized (DI) water with 18.2 MΩ-cm resistivity. Racemic standards of O-C4, O-C10, H-C4, H-C6 and H-C12-N-HLs and L-O-C12-N-HL were purchased from Chemodex Ltd. (St. Gallen, Switzerland). Racemic standards of A-C4, A-C6, A-C8, A-C10, A-C12, A-C14, O-C6, O-C8, O-C14, H-C8, H-C10, and H-C14-N-HLs were obtained from MilliporeSigma (St. Louis, MO). ZORBAX SB-C18 (150 mm x 4.6 mm i.d., 5 µm) columns were purchased from Agilent Technologies, Inc. (Santa Clara, CA). ChiralPak® IC-3 (250 mm x 4.6 mm i.d., 3µm) columns were purchased from Chiral Technologies, Inc. (Ann Arbor, MI). β-DEX™ 225 (30 m × 0.25 mm, 0.25 µm film thickness) and Supel™-Select HLB SPE tubes were provided by MilliporeSigma (Supelco, Bellefonte, PA).

6.3.2 Sample preparation

Standards were diluted to a concentration of 400 µg/mL in acetonitrile from which 1 µg/mL working solutions were prepared the calibration curve.M9 media was prepared according to instructions and autoclaved to sterilize. 20% (w/w) glucose and 1M magnesium

sulfate were added to the media. For extraction, an SPE manifold coupled to a vacuum pump was used. The SPE cartridges were conditioned with 10 mL each of acetonitrile, methanol, and water respectively. 10 mL of media was spiked with 7.5 µL of a 4 µg/mL internal standard (D,L-A-C7-N-HL) solution and processed through the SPE cartridge. The column was washed with 10 mL of 95:5 methanol: water and eluted with 11 mL of acetonitrile. The samples were then evaporated using a rotatory evaporator and transferred using dichloromethane. Transferred samples were evaporated using a gentle stream of N_2, and reconstituted with 100 µL of methanol, then transferred to HPLC vials for analysis. For GC-MS/MS, all samples were prepared similarly with the addition of a derivatization step. The samples were first dried using a gentle stream of nitrogen. Then 75 µL of BSTFA with 1% TMCS and 25 µL acetonitrile (co-solvent) was added to the dried sample, mixed for 10 seconds and eventually placed in a 130 °C sand bath for 45 minutes.

6.3.3 Bacterial samples and growth conditions

Samples for *P. aeruginosa* were obtained from Carolina Biological Supply Company (Burlington, NC). *P. atrosepticum* SCRI 1043 samples were purchased from American Type Culture Collection (Manassas, VA). Bacterial samples were spiked into M9 media and allowed to grow in a shaker incubator overnight at 30 °C for *P. aeruginosa* and 25 °C for *P. atrosepticum*. From the overnight growth, 200 µL of sample was inoculated into 200 mL of fresh M9 media in triplicate. Inoculated media were grown using a shaker incubator at respective temperatures. 11.5 mL aliquots were taken at different time intervals. From the aliquots, 1.5 mL was collected and diluted with 1.5 mL of water and OD 600 reading were taken using a Vernier SpectroVis™ Plus spectrophotometer. The samples were centrifuged for 30 mins and supernatants collected. Supernatants were processed using the SPE method described above and analyzed using LC-MS/MS and GC-MS/MS, for which the conditions are outlined below.

6.3.4 Chromatographic conditions

6.3.4.1 LC-MS/MS

Shimadzu LC-MS 8040 system (Shimadzu Scientific Instruments, Columbia MD) with electrospray ionization (ESI) and a triple quadrupole mass spectrometer was used in the positive ion mode for the LC-MS/MS analysis. The analysis was done in multiple reaction monitoring (MRM) mode with optimized MRM transitions and collision energies for each enantiomeric standard. The nebulizing gas flow and drying gas flow were 3.0 and 15.0 L/min respectively. The interface voltage was 4.5 kV, and the heat block temperature was 400 °C. ZORBAX SB-C18 column was used in tandem with a CHIRALPAK IC-3. A flow rate of 0.4 mL/min was used with a gradient starting at 60:40 methanol (0.1% FA): water (0.1% FA) held for 25 mins, then ramped to 90:10 methanol:water over 12.5 minutes and finally stepped up to 95:5 methanol:water at 37.5 minutes and held there until 65 minutes.

6.3.4.2 GC-MS/MS

Shimadzu GCMS-TQ 8040 (Shimadzu Scientific Instruments, Columbia, MD) was used for GC-MS/MS analysis. It was equipped with a β-DEX™ 225 (30 m × 0.25 mm, 0.25 µm film thickness). He was used as a carrier gas with a constant flow of 1.1 mL/min (40 cm/s). The oven temperature was held at 160 °C for 10 minutes and increased at a rate of 1 °C/min to 230 °C and then held for 50 min. The injection mode was splitless with a 1µL injection and 2 min split time with a 20:1 split ratio. The interface temperature was 230 °C and the MS ion source temperature was 280 °C. Electron ionization (EI) was set to 70 eV. MRM mode was used with optimized collision energies and Q1 and Q3 voltages.

6.3.5 Analysis of N-HL standards

Racemic standards of D,L-A-C4-C14, D,L-H-C4-C14, and D,L-O-C4-C14 (excluding C-12) were run on LC-MS/MS and GC-MS/MS. Due to the lack of a racemic standard for O-C12 only L-O-C12 was tested. Identification of N-HLs was done based on matching the retention times and three characteristic product ions. LC chromatograms of N-HLs detected in this study are presented in Figures 6-5 & 6-6. All enantiomeric pairs had 2 peaks except for HHLs. HHLs had three peaks for majority of the standard solutions: the first peak is a combination of the two L diastereomers, and the second and third peak represent the D counterparts, which are designated as D1 and D2 respectively (Figure 6-6). For H-C10 and H-C14, there was some resolution between the L diastereomers. There is ample resolution between homologues for quantitation. All enantiomeric pairs are sufficiently resolved except for O-C6. Peak processing software was used to resolve O-C6 through deconvolution methods and subsequently quantify D-O-C6. Other peaks were observed but eliminated as matrix peaks based on the retention time and mass transitions.

6.3.6 Quantitation

The calibration curve for LC-MS/MS included concentrations of 5, 12.5, 25, 50, 125, 250, 500, and 1000 ng/mL per enantiomer for all standard N-HLs. The calibration curve for GC-MS/MS included concentrations of 500, 750, 1000, 1500, 2000 ng/mL per enantiomer for all standard N-HLs listed above. Samples for both LC-MS/MS and GC-MS/MS were processed in triplicate using the respective methods outlined above. All quantitation was done using the calibration curves for LC-MS/MS.

6.4 Results and discussion

6.4.1 Production of D-OHL and D-HHL in P. atrosepticum

The purpose of this study is to detect different classes of D-N-HLs in gram-negative bacteria using sensitive analytical methods such as chiral LC-MS/MS and GC-MS/MS developed specifically for this purpose. Preliminary studies conducted on *P. atrosepticum* revealed that the production of D-N-HLs was occurring at times >40 h and even up to ~120 h. Hence, a 124 h growth period was selected. Different N-HLs produced during the growth period are summarized in Figure 6-2 along with expected N-HLs for the respective bacteria. Literature refers to N-HLs detected in previous studies.

Literature	○
Detected in this study	△
Not detected/expected	-

HLs / Source	A-C4		A-C6		A-C8	O-C4	O-C6		O-C8	O-C10	H-C6	
	L	D	L	D	L	L	L	D	L	L	L	D
Literature	-	-	○	-	○	-	○	-	○	○	-	-
LC-MS/MS	△	△	△	△	△	△	△	△	△	△	△	△
GC-MS/MS	-	-	-	-	-	△	△	△	-	-	△	△

HLs / Source	A-C4		A-C6		A-C8	A-C10	O-C6	O-C8	O-C10	O-C12	H-C4	H-C10
	L	D	L	D	L	L	L	L	L	L	L	L
Literature	○	-	○	-	○	-	○	○	○	○	○	○
LC-MS/MS	△	△	△	△	△	△	-	-	△	△	△	△
Gc-MS/MS	△	△	-	-	-	△	-	-	-	-	△	△

Figure 6-2. N-HLs detected in by LC-MS/MS and GC-MS/MS compared to N-HLs reported previously in (A) *P. atrosepticum* and (B) *P. aeruginosa.* Sources of previously reported N-HLs mentioned in section 5.

N-HLs detected through LC-MS/MS and GC-MS/MS are distinguished. *P. atrosepticum* produced all classes of N-HLs (AHL, HHL, and OHL) in both enantiomeric forms. The N-HLs detected were D,L-A-C4, D,L-A-C6, D,L-O-C6, and D,L-H-C6. This is the first reported case of D-HHL and D-OHL in bacterial samples. On the contrary, A-C8, O-C4, O-C8, and O-C10 were only detected in the L enantiomeric form. LC-MS/MS chromatograms of standards and bacterial

samples for D,L-A-C4, D,L-A-C6, D,L-O-C6, and D,L-H-C6, L-A-C8 and L-O-C8 are presented in Figure 6-3. H-C6 N-HL has three peaks. The first peak is a combination of the L diastereomers, while the second and third peaks correspond to the D-diastereomers and are designated as D1 and D2 respectively (Figure 6-3). GC-MS/MS was used to confirm the presence of L-O-C4, D,L-O-C6, and D,L-H-C6. Of these N-HLs, L-A-C6, L-A-C8, L-O-C6, L-O-C8, L-O-C10 were expected based on previous studies.[9,19,27,28] However, these N-HLs were reported for a different strain of *P. atrosepticum.* Different strains have been shown to produce distinct N-HLs.[9,19,29] For SCRI 1043, L-O-C6 has been reported as the major N-HL involved in QS. [19,29] This study shows that the D-enantiomer is also produced.

6.4.2 Production of D-AHLs in P. aeruginosa

Similar to *P. atrosepticum,* preliminary studies of *P. aeruginosa* were done to select a growth period of 96 h. N-HLs expected for *P. aeruginosa,* and ones produced in this study are summarized in Figure 6-2. D,L-A-C4 and D,L-A-C6 were detected for *P. aeruginosa*. D-A-C4 has not been reported previously. Only L enantiomers of A-C8, A-C10, O-C10, O-C12, H-C4, and H-C10 were detected. GC-MS/MS was used to confirm the presence of D,L-A-C4, L-A-C10, L-H-C4, and L-H-C10. LC-MS/MS chromatograms of standards and bacterial samples for D,L-A-C4 and D,L-A-C6, L-A-C8, and L-O-C12 are presented in Figure 6-4. Expected N-HLs for *P. aeruginosa* (strain PAO1) include L enantiomers of A-C4, A-C6, A-C8, O-C6, O-C8, O-C10, O-C12, H-C4, and H-C10.[30,31] Of these, O-C6 and O-C8 were not detected in this study. Like *P. atrosepticum*, this could be due to a difference in strain or additionally, the variations in growth conditions. In both bacteria, different classes (AHL, HHL, and OHL) of N-HLs with different chain lengths were detected. Unlike *P. atrosepticum*, *P. aeruginosa* only produced D-AHLs.

A

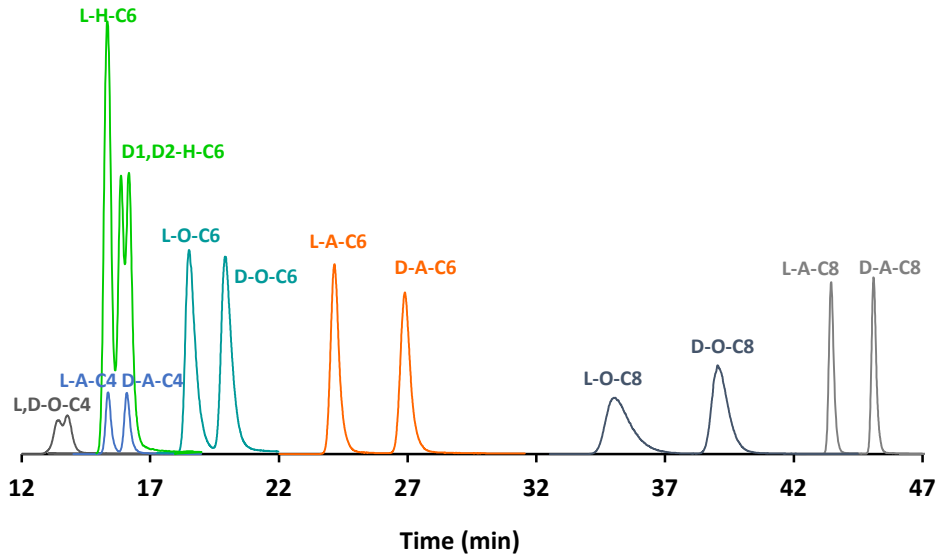

B

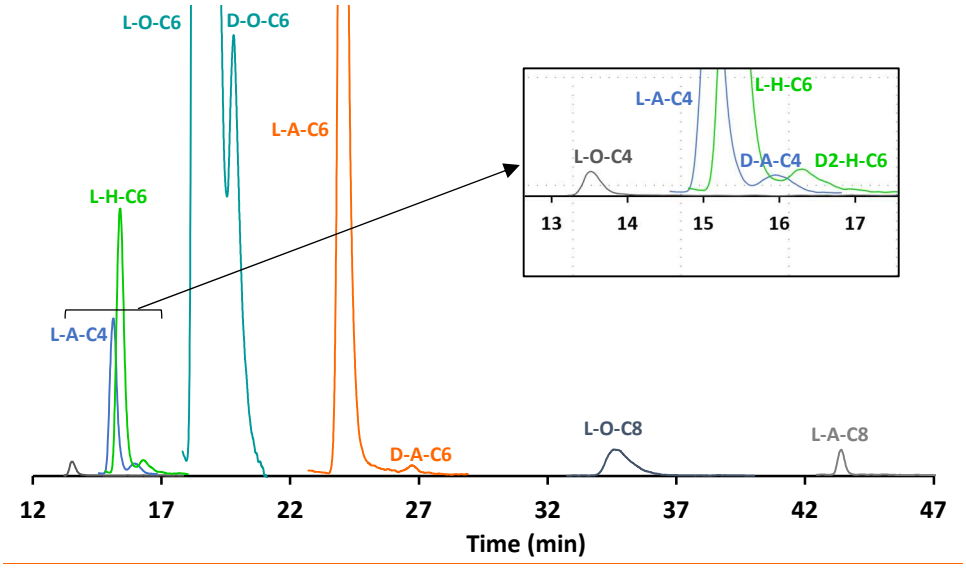

Figure 6-3. LC-MS/MS chromatogram with MRM transition to m/z = 102 showing the separation of most prominent N-HLs in (A) standard solution and (B) 123 h growth culture of *P. atrosepticum*. See method in experimental. Baselines normalized for clarity.

Comparing this to previous findings on *B. cepacia* and *V. fischeri* different bacteria can produce different classes of D-N-HLs [8]. Although different classes of N-HLs with different chain lengths are produced, only some D-N-HLs namely D-A-C4, D-A-C6, D-O-C6, and D-H-C6 were detected.

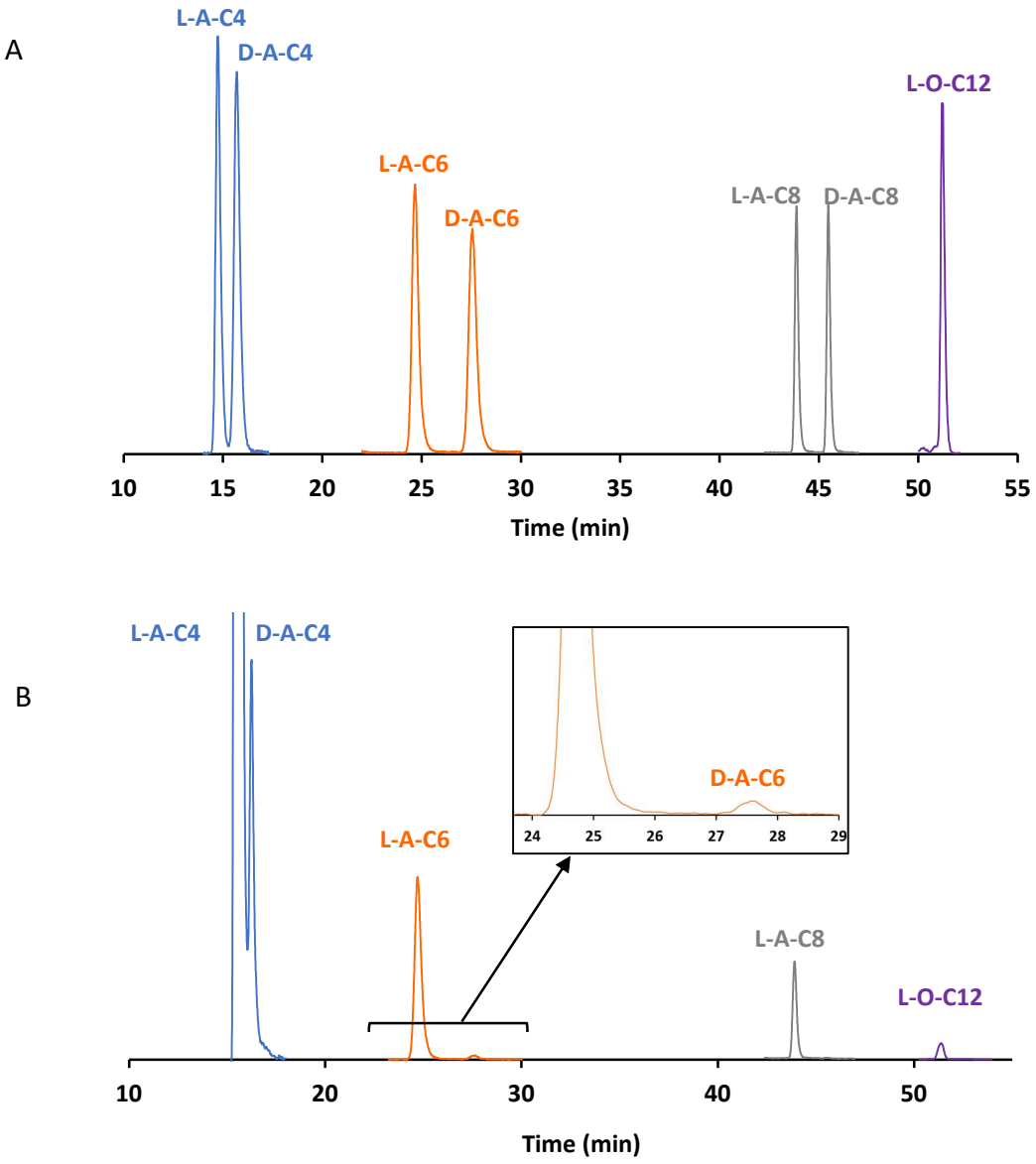

Figure 6-4. LC-MS/MS chromatogram with MRM transition to m/z = 102 showing the separation of most prominent N-HLs in (A) standard solution and (B) growth culture of *P. aeruginosa*. A-C4 and A-C6 were selected from 96 h growth and A-C8 and O-C12 were selected from 36 h growth. See method in experimental. Baselines normalized for clarity.

6.4.3 Enantiomeric production of N-HLs during the growth of P. aeruginosa and P. atrosepticum

Selected growth curves are represented in Figures 6-5 & 6-6 for *P. atrosepticum* and *P. aeruginosa* respectively. O-C6 and H-C6 N-HLs were selected due to novelty of their D-enantiomers.

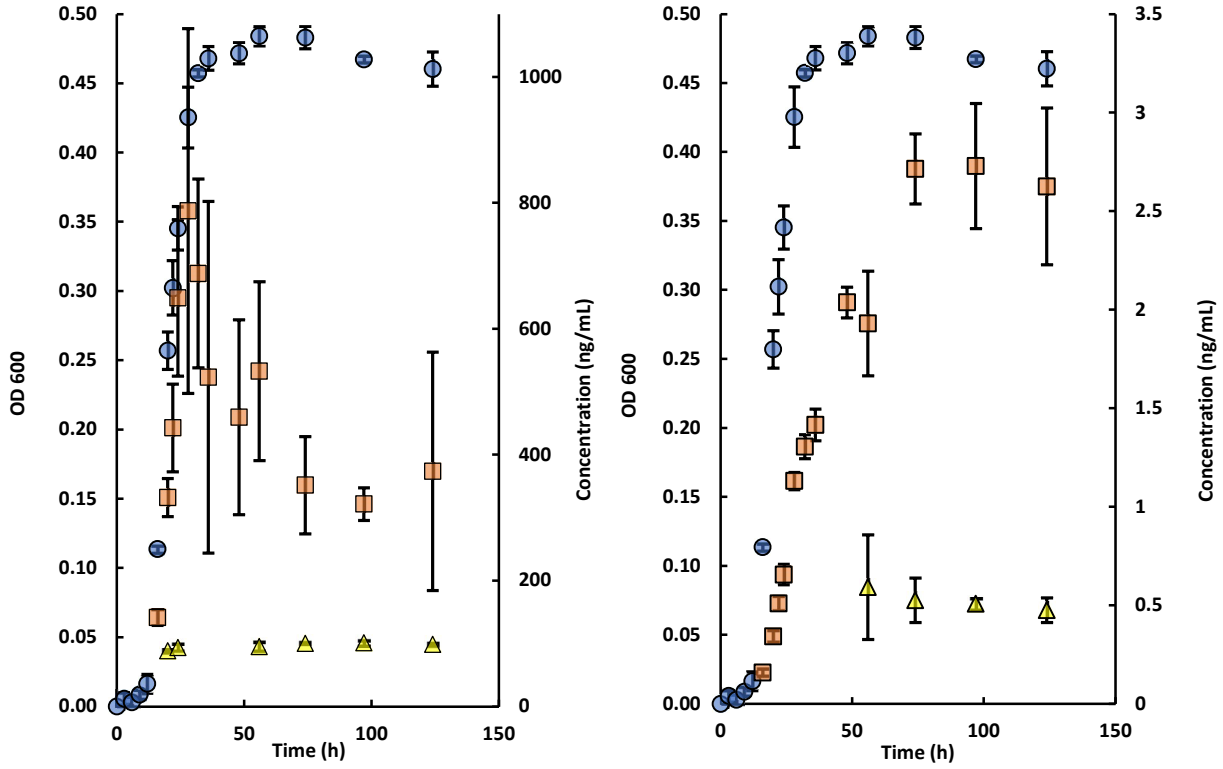

Figure 6-5. Growth curves showing the OD 600 and production of (left) D,L-O-C6 and (right) D,L-H-C6-HLs with respect to time in *P. atrosepticum.* Average of triplicates shown with standard deviations as error bars. ○ indicates the OD 600 reading with the measured values in the left y-axis. □ indicates the concentration of L-O-C6 (left) and L-H-C6 (right) with measured values in the right y-axis. △ indicates the concentration of D-O-C6 (left) and D-H-C6 (right) with measured values in the right y-axis. Concentrations of D-O-C6 was increased by 100 times for clarity.

The growth curves include the OD 600 and concentration of different N-HLs produced during the growth period. For *P. atrosepticum*, the exponential growth started at ~12 h, reached a maximum at ~36 h and remained constant over the next ~100 hours (Figure 6-5). At the maxima, L-O-C6 had a concentration of 800 ± 300 ng/mL and D-O-C6 had a concentration of

1.01 ± 0.04 ng/mL, while L-A-C6 and D-A-C6 had concentrations of 2.7 ± 0.3 and 0.6 ± 0.3 ng/mL respectively; these being the amounts in the growth culture. Peak fitting software was used to quantify D-O-C6 due to insufficient resolution. The resolution of the analytical signals was obtained by iterative curve fitting using exponentially modified Gaussians. Two distinct production patterns were observed for L-O-C6 and L-H-C6. The concentration of L-O-C6 follows the OD 600 growth curve until 28 h and then remains constant. Detectable amounts of D-O-C6 appeared to be constant over the entire growth period. These patterns are different for L-H-C6 which follows the OD600 more closely. D-H-C6 appears at ~56 h and remains constant thereafter.

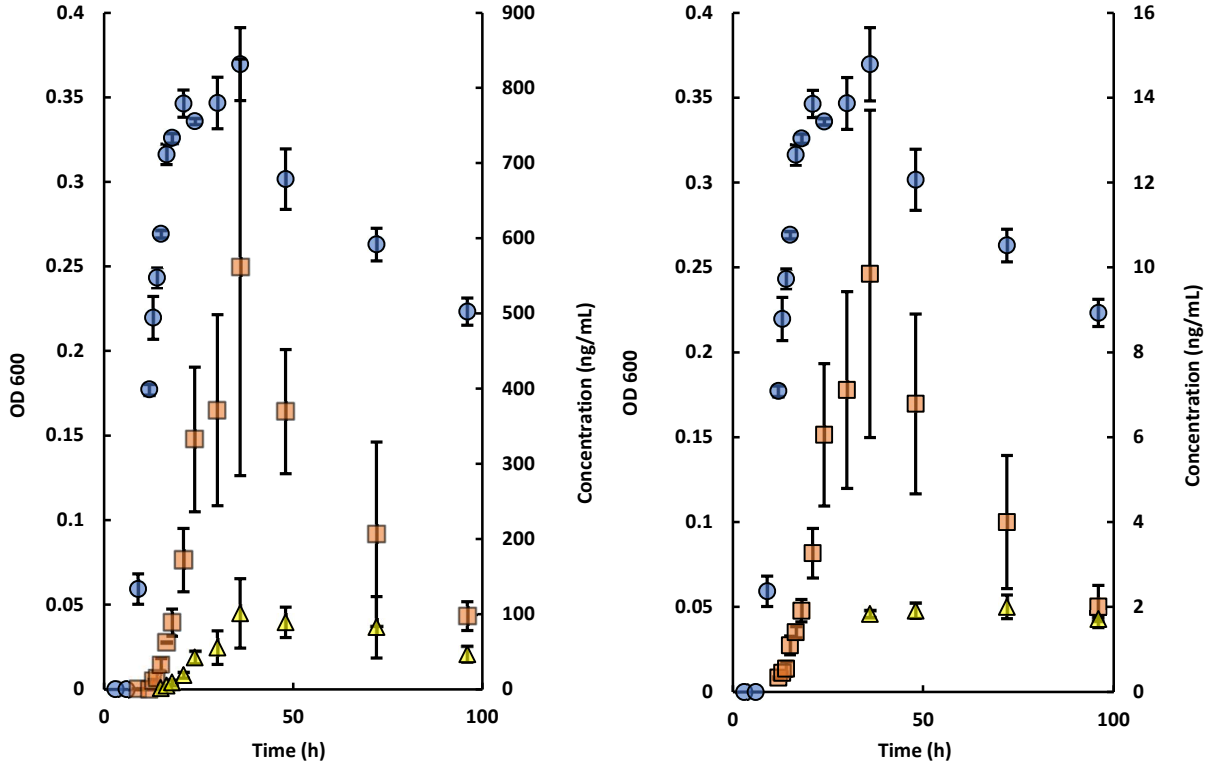

Figure 6-6. Growth curves showing the OD 600 and production of (left) D,L-A-C4 and (right) D,L-A-C6-HLs with respect to time in *P. aeruginosa.* Average of triplicates shown with standard deviations as error bars. ○ indicates the OD 600 reading with the measured values in the left y-axis. □ indicates the concentration of L-A-C4 (left) and L-A-C6 (right) with measured values in the right y-axis. △ indicates the concentration of D-A-C4 (left) and D-A-C6 (right) with measured values in the right y-axis. Concentrations of D-A-C4 and D-A-C6 were increased by 10 times for clarity.

In the case of *P. aeruginosa*, exponential growth started at ~9 h, reached a maximum at ~24 h with the growth decreasing over the next ~100 hours (Figure 6-6). A-C4 and A-C6 were the most produced N-HLs for *P. aeruginosa*. At the maxima, L-A-C4 and D-A-C4 had concentrations of 600±300 and 10±5 ng/mL respectively. L-A-C6 and D-A-C6 had lower concentrations at 10±4 and 2.0±0.3 ng/mL. Contrary to the *P. atrosepticum*, the production of all L-N-HLs in *P. aeruginosa* followed the growth curve. Interestingly, for both L-A-C4 and L-A-C6, the concentration patterns were almost identical. D-A-C4 also followed the growth pattern, while D-A-C6 exhibited less of a change over time as seen in Figure 6-6. For both bacteria, the production patterns and amounts varied between homologues as well as enantiomers.

6.4.4 Comparison of concentrations of L and D N-HLs

Maximum concentrations of N-HLs detected in this study are reported in Table 6.2.

Table 6-2. Maximum concentrations of each N-HL produced during the growth period quantified using LC-MS/MS. The growth period for *P. atrosepticum* and *P. aeruginosa* were 124 h and 96 h respectively. See section 2.5 for quantitation method.

Bacteria	L-N-HLs	Maximum concentration (ng/mL)	D-N-HLs	Maximum concentration (ng/mL)	L/D
P. atrosepticum	L-O-C6	800 ± 300	D-O-C6	1.01 ± 0.04	800 ± 300
	L-A-C6	27 ± 1	D-A-C6	0.29 ± 0.03	90 ± 10
	L-O-C8	5.2 ± 0.2	Not detected	-	-
	L-A-C4	3.4 ± 0.2	D-A-C4	0.15 ± 0.04	26 ± 7
	L-H-C6	2.7 ± 0.3	D2-H-C6	0.6 ± 0.3	5 ± 2
	L-A-C8	0.94 ± 0.05	Not detected	-	-
P. aeruginosa	L-A-C4	600 ± 300	D-A-C4	10 ± 5	60 ± 40
	L-A-C6	10 ± 4	D-A-C6	2.0 ± 0.3	5 ± 2
	L-O-C12	1.8 ± 0.3	Not detected	-	-
	L-A-C8	1.0 ± 0.4	Not detected	-	-

L-H-C10	0.275 ± 0.002	Not detected	-	-

For *P. atrosepticum*, L-O-C6 was the highest produced N-HL, which is consistent with previous findings.[19,27] Most of the L-N-HLs were produced in greater amounts than the highest D-N-HL. The case of O-C8 is particularly interesting because it is the third highest N-HL produced but the LC-MS/MS method was not able to detect any D-enantiomer. L-A-C4 and L-H-C6 were produced in lower quantities than O-C8 and had quantifiable levels of their respective D-enantiomers. Interestingly, of the two D-diastereomers in H-C6, only D2-H-C6 was detected. The order of concentration of L-N-HLs did not match the D-N-HLs. L-H-C6 has the fourth highest concentration among the L-N-HLs, however, D2-H-C6 had second highest concentration among the D-N-HLs. The ratio of maximum produced L to D enantiomers are also presented in Table 6.2. The maximum concentration of L-N-HL was directly proportional to the ratio of maximum concentrations of L to D-N-HL. This indicates that L-N-HLs with lower maximum concentrations had higher relative amounts of their respective D-N-HLs. For example, L-H-C6 had the lowest concentration among the L-N-HLs, but the ratio of L to D enantiomer was ~5:1. Contrarily, L-O-C6 had the highest concentration among L-N-HLs, while its L to D ratio was ~800:1. For *P. aeruginosa*, L-A-C4 is the highest produced N-HL followed by D-A-C4 and L-A-C6, which is different form previously reported trends albeit for different media. Patel et al. reported O-C10 and O-C8 as the second and third highest concentrations respectively, while Ortori et al. reported O-C12 and A-C6 as the as the second and third highest concentrations respectively.[30,31] In all cases, the highest produced N-HL was L-A-C4. The trend for ratio of L to D-N-HL seen in *P. atrosepticum* is also present for *P. aeruginosa*. D-A-C4 along with L-A-C6 have the second highest concentration in this study, which leads to more questions about the role of D-N-HLs in these bacteria.

6.4.5 Potential roles and production mechanisms of D-N-HLs in bacteria

P. aeruginosa has two different QS systems involving LasI and RhlI regulons that are activated by the signaling molecules L-O-C12 and L-A-C4 N-HLs respectively.[13] Both of these QS systems are involved in the production of various virulence factors like exoenzymes alkaline protease, and elastase that induce tissue damage in humans. [13] Interestingly, L-A-C6, which doesn't have a defined QS system in *P. aeruginosa*, had higher concentrations than L-O-C12. Studies done on inhibition and activation of the RhlI synthase in *P. aeruginosa* have revealed that D-A-C4 inhibits this enzyme.[32] In this study, *P. aeruginosa* produced higher concentrations of D-A-C4 than LasI signaling molecule L-O-C12. In, *P.atrosepticum* the highest produced D-N-HL was D-O-C6, which has been shown to activate the RhlI synthase enzyme. [32] D-O-C6 has also been shown to induce bioluminescence by affecting the LuxR dependent QS system found in *V. fischeri*.[33] Both P. atrosepticum and P. aeruginosa produced D-A-C6, which has also been shown to induce bioluminescence through LuxR.[33] Based on these observations, it can be inferred that D-N-HLs can affect the QS systems of their respective L-N-HLs as well as QS systems of other bacteria.[32,33] A study done on cleavage of D,L-O-C12 by fatty acid amide hydrolase enzyme revealed that the D-enantiomer was relatively resistant to hydrolysis.[34] D-N-HLs could also be resistant to other N-HL degrading enzymes.

There have been indications of two pathways for the appearance of D-N-HLs: production through a biosynthetic pathway and post-production racemization.[8] D,L-methionine supplementation studies have been conducted to show that production of D-N-HLs through a biosynthetic pathway is unlikely [8]. In terms of post-production, the racemization could occur through a racemizing agent or racemization during the sample preparation procedure and analysis itself. Significant amounts of auto-racemization during bacterial sampling, sample preparation, and chromatographic analysis has been ruled out previously. [26,35] This is also supported by the lack of a second peak when processing L-O-C12 through our standard sampling procedure. The difference in ratios of L/D concentrations for the N-HLs presented in this study also suggests a lack of racemization during sample preparation and analysis. The possibility of racemization due to pH of the complex biological matrix is also present.

Measurement of supernatant pH was conducted for both bacteria observing pHs around 6.3-7.3, The pH of the growth media did not change significantly throughout the growth period for either bacterium. This observation indicates an absence of either acid or base catalyzed racemization in the growth media. It further implies at the possibility of a racemizing enzyme that is converting the L-N-HLs into D-N-HLs. In any case D-N-HLs are produced in lower concentrations than their L-counterparts. As such, the need for more sensitive and selective chiral analysis methods are always necessary. The LC-MS/MS method used in this study can detect as low as 1 ng/mL of D,L-N-HLs after preconcentration and has been shown to be effective for this purpose.

6.5 Conclusions

Using comprehensive and sensitive LC-MS/MS and GC-MS/MS methods, the presence of D-N-HLs in growth cultures of *P. aeruginosa* and *P. atrosepticum* was confirmed. Confirmation of the presence of previously reported N-HLs with the addition of unexpected N-HLs was done for both bacteria. The first report of D-HHLs and D-OHLs are presented in this study. For *P. atrosepticum,* D-A-C6 and previously unreported D-A-C4, D-O-C6, and D2-H-C6 were detected. Similarly, for *P. aeruginosa*, D-A-C4 and D-A-C6 were detected. In this study, the concentration of D-N-HLs were usually one to two orders of magnitude lower than their L-counterparts. Previously reported analytical methods might have lacked the sensitivity to detect miniscule amounts of D-N-HLs, showing the importance of developing more sensitive techniques for the detection and quantification of N-HLs. The method employed here is sensitive enough to detect down to 1 ng/mL after preconcentration. While LC-MS/MS has been identified as the primary tool in detecting and quantifying N-HLs, GC-MS/MS can be used as an identification confirmation technique when used together with LC-MS/MS. D-N-HLs have been shown to affect various QS systems and can also be resistant to digestion through fatty acid amide hydrolase. Due to these factors along with the relevance of N-HLs in QS mediated virulence, the role of D-N-HLs in bacterial systems should be further explored. If the growing importance of D-amino acids in biological systems is of any indication, the potential of D-N-HLs in biological systems should be investigated.

6.6 References

(1) Nealson, K. H.; Platt, T.; Hastings, J. W. Cellular Control of the Synthesis and Activity of the Bacterial Luminescent System. J. Bacteriol. 1970, 104 (1), 313–322. https://doi.org/10.1128/jb.104.1.313-322.1970.

(2) Tomasz, A. Control of the Competent State in Pneumococcus by a Hormone-like Cell Product: An Example for a New Type of Regulatory Mechanism in Bacteria. Nature 1965, 208 (5006), 155–159. https://doi.org/10.1038/208155a0.

(3) Fuqua, W. C.; Winans, S. C.; Greenberg, E. P. Quorum Sensing in Bacteria: The LuxR-LuxI Family of Cell Density- Responsive Transcriptional Regulators. Journal of Bacteriology. 1994. https://doi.org/10.1128/jb.176.2.269-275.1994.

(4) Fuqua, C.; Greenberg, E. P. Listening in on Bacteria: Acyl-Homoserine Lactone Signalling. Nature Reviews Molecular Cell Biology. 2002. https://doi.org/10.1038/nrm907.

(5) Morin, D.; Grasland, B.; Vallée-Réhel, K.; Dufau, C.; Haras, D. On-Line High-Performance Liquid Chromatography-Mass Spectrometric Detection and Quantification of N-Acylhomoserine Lactones, Quorum Sensing Signal Molecules, in the Presence of Biological Matrices. J. Chromatogr. A 2003, 1002 (1–2), 79–92. https://doi.org/10.1016/S0021-9673(03)00730-1.

(6) Mohamed, N. M.; Cicirelli, E. M.; Kan, J.; Chen, F.; Fuqua, C.; Hill, R. T. Diversity and Quorum-Sensing Signal Production of Proteobacteria Associated with Marine Sponges. Environ. Microbiol. 2008, 10 (1). https://doi.org/10.1111/j.1462-2920.2007.01431.x.

(7) Readel, E.; Portillo, A.; Talebi, M.; Armstrong, D. W. Enantiomeric Separation of Quorum Sensing Autoinducer Homoserine Lactones Using GC-MS and LC-MS. Anal. Bioanal. Chem. 2020, 412 (12), 2927–2937. https://doi.org/10.1007/s00216-020-02534-7.

(8) Portillo, A. E.; Readel, E.; Armstrong, D. W. Production of Both L- and d- N-Acyl-Homoserine Lactones by Burkholderia Cepacia and Vibrio Fischeri. Microbiologyopen 2021, 10 (6), 1–9. https://doi.org/10.1002/mbo3.1242.

(9) Latour, X.; Diallo, S.; Chevalier, S.; Morin, D.; Smadja, B.; Burini, J. F.; Haras, D.; Orange, N. Thermoregulation of N-Acyl Homoserine Lactone-Based Quorum Sensing in the Soft Rot Bacterium Pectobacterium Atrosepticum. Appl. Environ. Microbiol. 2007, 73 (12), 4078–4081. https://doi.org/10.1128/AEM.02681-06.

(10) Smadja, B.; Latour, X.; Faure, D.; Chevalier, S.; Dessaux, Y.; Orange, N. Involvement of N-Acylhomoserine Lactones throughout Plant Infection by Erwinia Carotovora Subsp. Atroseptica (Pectobacterium Atrosepticum). Mol. Plant-Microbe Interact. 2004, 17 (11), 1269–1278. https://doi.org/10.1094/MPMI.2004.17.11.1269.

(11) Whitehead, N. A.; Barnard, A. M. L.; Slater, H.; Simpson, N. J. L.; Salmond, G. P. C. Quorum-Sensing in Gram-Negative Bacteria. FEMS Microbiol. Rev. 2001, 25 (4). https://doi.org/10.1111/j.1574-6976.2001.tb00583.x.

(12) Burr, T.; Barnard, A. M. L.; Corbett, M. J.; Pemberton, C. L.; Simpson, N. J. L.; Salmond, G. P. C. Identification of the Central Quorum Sensing Regulator of Virulence in the Enteric Phytopathogen, Erwinia Carotovora: The VirR Repressor. Mol. Microbiol. 2006, 59 (1). https://doi.org/10.1111/j.1365-2958.2005.04939.x.

(13) Finch, R. G.; Pritchard, D. I.; Bycroft, B. W.; Williams, P.; Stewart, G. S. A. B. Quorum Sensing: A Novel Target for Anti-Infective Therapy. J. Antimicrob. Chemother. 1998, 42 (5), 569–571. https://doi.org/10.1093/jac/42.5.569.

(14) Jurado-Martín, I.; Sainz-Mejías, M.; McClean, S. Pseudomonas Aeruginosa: An Audacious Pathogen with an Adaptable Arsenal of Virulence Factors. Int. J. Mol. Sci. 2021, 22 (6), 1–37. https://doi.org/10.3390/IJMS22063128.

(15) Coutinho, H.; Falcão-Silva, V. S.; Gonçalves, G. Pulmonary Bacterial Pathogens in Cystic Fibrosis Patients and Antibiotic Therapy: A Tool for the Health Workers. Int. Arch. Med. 2008, 1 (1), 24. https://doi.org/10.1186/1755-7682-1-24.

(16) Defez, C.; Fabbro-Peray, P.; Bouziges, N.; Gouby, A.; Mahamat, A.; Daurès, J. P.; Sotto, A. Risk Factors for Multidrug-Resistant Pseudomonas Aeruginosa Nosocomial Infection. J. Hosp. Infect. 2004, 57 (3). https://doi.org/10.1016/j.jhin.2004.03.022.

(17) Mahmoudi, E.; Ahmadi, A.; Sayed-Tabatabaei, B. E.; Ghobadi, C.; Akhavan, A.; Hasanzadeh, N.; Venturi, V. A Novel AHL-Degrading Rhizobacterium Quenches the Virulence of Pectobacterium Atrosepticum on Potato Plant. J. Plant Pathol. 2011, 93 (3).

(18) Crépin, A.; Barbey, C.; Cirou, A.; Tannières, M.; Orange, N.; Feuilloley, M.; Dessaux, Y.; Burini, J. F.; Faure, D.; Latour, X. Biological Control of Pathogen Communication in the Rhizosphere: A Novel Approach Applied to Potato Soft Rot Due to Pectobacterium Atrosepticum. Plant Soil 2012, 358 (1–2), 27–37. https://doi.org/10.1007/s11104-011-1030-5.

(19) Crépin, A.; Beury-Cirou, A.; Barbey, C.; Farmer, C.; Hélias, V.; Burini, J. F.; Faure, D.; Latour, X. N-Acyl Homoserine Lactones in Diverse Pectobacterium and Dickeya Plant Pathogens: Diversity, Abundance, and Involvement in Virulence. Sensors 2012, 12 (3), 3484–3497. https://doi.org/10.3390/s120303484.

(20) Musthafa, K. S.; Saroja, V.; Pandian, S. K.; Ravi, A. V. Antipathogenic Potential of Marine Bacillus Sp. SS4 on N-Acyl-Homoserine- Lactone-Mediated Virulence Factors Production in Pseudomonas Aeruginosa (PAO1). J. Biosci. 2011, 36 (1), 55–67. https://doi.org/10.1007/s12038-011-9011-7.

(21) Cataldi, T. R. I.; Bianco, G.; Palazzo, L.; Quaranta, V. Occurrence of N-Acyl-l-Homoserine Lactones in Extracts of Some Gram-Negative Bacteria Evaluated by Gas Chromatography-Mass Spectrometry. Anal. Biochem. 2007, 361 (2). https://doi.org/10.1016/j.ab.2006.11.037.

(22) Hoang, T. P. T.; Barthélemy, M.; Lami, R.; Stien, D.; Eparvier, V.; Touboul, D. Annotation and Quantification of N-Acyl Homoserine Lactones Implied in Bacterial Quorum Sensing by Supercritical-Fluid Chromatography Coupled with High-Resolution Mass Spectrometry. Anal. Bioanal. Chem. 2020, 412 (10). https://doi.org/10.1007/s00216-019-02265-4.

(23) Yang, X.; Sun, J.; Cui, F.; Ji, J.; Wang, L.; Zhang, Y.; Sun, X. An Eco-Friendly Sensor Based on CQD@MIPs for Detection of N-Acylated Homoserine Lactones and Its 3D Printing Applications. Talanta 2020, 219. https://doi.org/10.1016/j.talanta.2020.121343.

(24) Armstrong, D. W.; Gasper, M.; Lee, S. H.; Zukowski, J.; Ercal, N. D-amino Acid Levels in Human Physiological Fluids. Chirality 1993, 5 (5). https://doi.org/10.1002/chir.530050519.

(25) Armstrong, D. W.; Gasper, M. P.; Lee, S. H.; Ercal, N.; Zukowski, J. Factors Controlling the Level and Determination of D-Amino Acids in the Urine and Plasma of Laboratory Rodents. Amino Acids 1993, 5 (2). https://doi.org/10.1007/BF00805992.

(26) Malik, A. K.; Fekete, A.; Gebefuegi, I.; Rothballer, M.; Schmitt-Kopplin, P. Single Drop Microextraction of Homoserine Lactones Based Quorum Sensing Signal Molecules, and the Separation of Their Enantiomers Using Gas Chromatography Mass Spectrometry in the Presence of Biological Matrices. Microchim. Acta 2009, 166 (1–2). https://doi.org/10.1007/s00604-009-0183-x.

(27) Joshi, J. R.; Khazanov, N.; Khadka, N.; Charkowski, A. O.; Burdman, S.; Carmi, N.; Yedidia, I.; Senderowitz, H. Direct Binding of Salicylic Acid to Pectobacterium N-Acyl-Homoserine Lactone Synthase. ACS Chem. Biol. 2020, 15 (7), 1883–1891. https://doi.org/10.1021/acschembio.0c00185.

(28) Barbey, C.; Crépin, A.; Bergeau, D.; Ouchiha, A.; Mijouin, L.; Taupin, L.; Orange, N.; Feuilloley, M.; Dufour, A.; Burini, J. F.; Latour, X. In Planta Biocontrol of Pectobacterium Atrosepticum by Rhodococcus Erythropolis Involves Silencing of Pathogen Communication by the Rhodococcal Gamma-Lactone Catabolic Pathway. PLoS One 2013, 8 (6), 1–9. https://doi.org/10.1371/journal.pone.0066642.

(29) Chatterjee, A.; Cui, Y.; Hasegawa, H.; Leigh, N.; Dixit, V.; Chatterjee, A. K. Comparative Analysis of Two Classes of Quorum-Sensing Signaling Systems That Control Production of Extracellular Proteins and Secondary Metabolites in Erwinia Carotovora Subspecies. J. Bacteriol. 2005, 187 (23), 8026–8038. https://doi.org/10.1128/JB.187.23.8026-8038.2005.

(30) Patel, N. M.; Moore, J. D.; Blackwell, H. E.; Amador-Noguez, D. Identification of Unanticipatedand Novel N-Acyl L-Homoserine Lactones (AHLs) Using a Sensitive Non-Targeted LC-MS/MS Method. PLoS One 2016, 11 (10), 1–20. https://doi.org/10.1371/journal.pone.0163469.

(31) Ortori, C. A.; Dubern, J. F.; Chhabra, S. R.; Cámara, M.; Hardie, K.; Williams, P.; Barrett, D. A. Simultaneous Quantitative Profiling of N-Acyl-l-Homoserine Lactone and 2-Alkyl-4(1H)-Quinolone Families of Quorum-Sensing Signaling Molecules Using LC-MS/MS. Anal. Bioanal. Chem. 2011, 399 (2), 839–850. https://doi.org/10.1007/s00216-010-4341-0.

(32) Shin, D.; Gorgulla, C.; Boursier, M. E.; Rexrode, N.; Brown, E. C.; Arthanari, H.; Blackwell, H. E.; Nagarajan, R. N-Acyl Homoserine Lactone Analog Modulators of the Pseudomonas Aeruginosa Rhll Quorum Sensing Signal Synthase. ACS Chem. Biol. 2019, 14 (10), 2305–2314. https://doi.org/10.1021/acschembio.9b00671.

(33) Li, S. Z.; Xu, R.; Ahmar, M.; Goux-Henry, C.; Queneau, Y.; Soulère, L. Influence of the D/L Configuration of N-Acyl-Homoserine Lactones (AHLs) and Analogues on Their Lux-R Dependent Quorum Sensing Activity. Bioorg. Chem. 2018, 77. https://doi.org/10.1016/j.bioorg.2018.01.005.

(34) Palmer, A. G.; Senechal, A. C.; Mukherjee, A.; Ané, J. M.; Blackwell, H. E. Plant Responses to Bacterial N-Acyl l-Homoserine Lactones Are Dependent on Enzymatic Degradation to l-Homoserine. ACS Chem. Biol. 2014, 9 (8), 1834–1845. https://doi.org/10.1021/cb500191a.

(35) Hodgkinson, J. T.; Galloway, W. R. J. D.; Casoli, M.; Keane, H.; Su, X.; Salmond, G. P. C.; Welch, M.; Spring, D. R. Robust Routes for the Synthesis of N-Acylated-l-Homoserine Lactone (AHL) Quorum Sensing Molecules with High Levels of Enantiomeric Purity. Tetrahedron Lett. 2011, 52 (26), 3291–3294. https://doi.org/10.1016/j.tetlet.2011.04.059.

Chapter 7

Investigating chirality in quorum sensing by analysis of *Burkholderia cepacia* and *Vibrio fischeri* cultures with comprehensive chiral LC-MS/MS and GC-MS/MS methods

7.1 Abstract

Molecules called N-acyl homoserine lactones (N-HL) are used as signals by gram-negative bacteria in a phenomenon called quorum sensing (QS). Bacteria will detect N-HL as a way of monitoring their population and upon reaching a critical size will express a specific phenotype. An example is the expression of bioluminescence by *Vibrio fischeri*. A limited number of studies have considered the chirality of these molecules with a scarcity of chiral studies which use highly sensitive detections methods. Here, the production of D,L-N-HLs are monitored for *V. fischeri*, *B. cepacia*, *P. fluorescens* and *P. putida*, using highly sensitive tandem mass spectrometry analysis. Novel N-HLs are reported herein for both *V. fischer* and *B. cepacia* including a plethora of novel D-N-HLs. Anomalously, N-HLs were not detected in any cultures of *P. fluorescens* and *P. putida*, which are species known to produce N-HLs. Time studies of *V. fischeri* hint at the possibility that separate synthetic and elimination pathways exist between D- and L-N-HLs. A possible biological process that could be the source of D-N-HL production is synthesis by an enzyme racemase which has been seen to be the case for the production of D-amino acids.

7.2 Introduction

Fungi and bacteria are classical examples of microorganisms that have developed chemical pathways for intraspecies communication (Tomasz, 1965, Nealson *et al.*, 1970, Yashiroda & Yoshida, 2019, He *et al.*, 2022). In gram-negative bacteria one class of chemical signaling molecules is *N*-acyl homoserine lactones (N-HLs). These molecules are biosynthesized from fatty acids that can range from 4 to 20 carbons in length and S-adenosyl-L-methionine (SAM). N-HLs can have hydroxyl (H-Cn), carbonyl (O-Cn) or be non-functionalized (A-Cn) on the third carbon of the acyl chain (Figure 1) (Fuqua *et al.*, 1996). The below scheme outlines the general structures of NHLs. These N-HLs are used in a chemical communication phenomenon referred to as quorum sensing (QS), wherein cells perceive population densities via the concentration of N-HL chemical signaling molecules. As the population of a bacterial species increases, the concentration of N-HLs also increases, inducing a process that ultimately culminates in the expression of a characteristic phenotype. Some manifestations of these phenotypes are bioluminescence by the marine symbiote *Vibrio fischeri* and biofilm production by the opportunistic human pathogen *Burkholderia cepacia*.

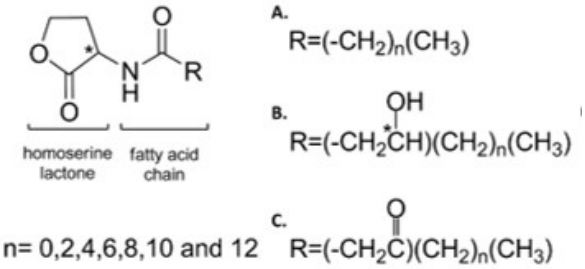

N-HLs are produced in trace amounts by bacteria ranging in concentrations from hundreds of a part per trillion (ppt) up to parts per million (ppm) levels. Some current analytical techniques used for the analysis and quantitation of N-HLs are thin-layer chromatography coupled to biosensor bacterial strains, such as the *Chromabacterium violaceum's* CviI/R system (which allows detection of short to medium chain N-HLs), GC-MS, LC-MS or SFC-MS (Steindler & Venturi, 2007, Hoang *et al.*, 2020, Portillo *et al.*, 2021).The use of biosensor bacteria strains were common early-on for the analysis of N-HLs produced by bacteria, due to ease of implementation and low cost. Limitations of TLC and bioreporter strains have been discussed in the literature (Shaw *et al.*, 1997, Cha *et al.*, 1998, Liu *et al.*, 2007, Diplock *et al.*, 2009). TLC has low selectivity and resolution between various N-HLs as well as other matrix molecules. N-HL standards of the different types, unsubstituted (AHL), 3-hydroxyacyl substituted (HHL) and 3-oxoacyl substituted (OHL), almost always analyzed analyzed separately by TLC to avoid

coelution (Shaw *et al.*, 1997, Cha *et al.*, 1998). This can be a problem when trying to analyze N-HLs by TLC for bacteria that produce more than one type of N-HLs.

The selection of the appropriate bioreporter for the detection of N-HLs also is necessary. Many of these reporters specialize on specific signals (fatty acid chain length range or N-HL type) (Cha *et al.*, 1998, Liu *et al.*, 2007, Poonguzhall *et al.*, 2007). The *A. tumefaciens* reporter strain is a common broad range N-HL detector that can detect N-HLs of the three types. Reports have shown that this bioreporter can detect molecules other than N-HLs (Holden *et al.*, 1999), which could lead to the incidence of false positives (Holden *et al.*, 1999, Pérez-Montaño *et al.*, 2011). In a study, an *A. tumefaciens* reporter strain has been shown to elicit a positive response indicating a specific N-HL, however, other bioreporters specific for that N-HL do not respond (Poonguzhall *et al.*, 2007). In a paper where food spoilage due to QS was studied, TLC and an *A. tumefaciens* reporter strain was used to detect three distinct N-HLs, i.e., O-C6, A-C6 and A-C8, however. However, they were undetected by mass spectrometry (GC-MS) in the same study (Zhu *et al.*, 2015). Another study analyzing the expression of N-HLs in rhizobia bacteria using the *A. tumefaciens* bioreporter approach, countless positive responses were found. However when the same sample was analyzed by LC-MS/MS (hybrid triple-quadrupole-linear trap) no N-HLs were found(Pérez-Montaño *et al.*, 2011). In-lieu of these ambiguous reports using TLC coupled to biosensors for the detection of N-HLs, using higher-end chromatographic methods like GC-MS, LC-MS and SFC-MS would allow for better selectivity, specificity as well as quantitation when analyzing N-HLs in complex biological matrices (Cataldi *et al.*, 2009, Sheng *et al.*, 2017, Hoang *et al.*, 2020).

The vast majority of quorum sensing studies have not considered the chirality of N-HL molecules and so it has been assumed or implied that only L-N-HLs were produced. However recently, the detection of various D-N-HLs in supernatant cultures of *B. cepacia* and *V. fischeri* were reported (Portillo *et al.*, 2021). *N*-octanoyl homoserine lactone was the highest detected N-HL, by GC-MS, for both species in this study with D-*N*-octanoyl homoserine lactone being the second most prevalent N-HL(Portillo *et al.*, 2021). Methionine supplementation of growth media with D-Met, L-Met or racemic Met was tested to study its effects on the production of D-

N-HL in cultures of *B. cepacia*. It was concluded that all sources of methionine supplementation increased the production of both D- and L-N-HL equally. Thus a different pathway for the origin of D-N-HLs must exist. In *V. fischeri* it is well known that 3-oxohexanoyl homoserine lactone regulates the *lux* operon which in turn controls the QS phenotypic expression of bioluminescence (Fuqua *et al.*, 1994, Kuo *et al.*, 1994). It was not until LC-MS/MS was applied in the above mentioned study, (Portillo *et al.*, 2021), that L-3-oxohexanoyl homoserine lactone was detected. However the corresponding D- stereoisomer was not detected in this work. This shows that it is necessary for higher sensitivity detection methods to be utilized in-tandem with comprehensive chiral chromatographic techniques.

Herein, *Vibrio fischeri* ES114, *Burkholderia cepacia* 25416, *Pseudomonas putida* and *Pseudomonas fluorescens* are examined for their production of both D- and L-N-HL with highly sensitive and specific LC-MS/MS and GC-MS/MS methods. Also showcased are previously unknown D-N-HLs from cultures of *B. cepacia* and *V. fischeri* and the first report of D-N-HLs containing oxo and hydroxy functionalities.

7.3 Materials and methods

7.3.1 Analytical materials

Racemic (one-to-one mixture of the D- and L- configurations) analytical standards of N-butanoyl homoserine lactone (A-C4), N-hexanoyl homserine lactone (A-C6), N-heptanoyl homoserine lactone (A-C7), N-octanoyl homoserine lactone (A-C8), N-decanoyl homoserine lactone (A-C10), N-dodecanoyl homoserine lactone (A-C12), N-tetradecanoyl homoserine lactone (A-C14), N-3-oxohexanoyl homoserine lactone (O-C6), N-3-oxooctanoyl homoserine lactone (O-C8), N-3-hydroxyoctanoyl homoserine lactone (H-C8), N-3-hydroxydecanoyl homoserine lactone (H-C10), M9 broth, D-(+)-glucose BioReagent grade and magnesium sulfate BioReagent grade were purchased from MilliporeSigma (St. Louis, MO). N,O-bis(trimethylsilyl)trifluoroacetamide (BSTFA) with 1% v/v of trimethylchlorosilane (TMCS) 1 mL ampules, β-DEX™ 225 (25% 2,3-di-O-acetyl-6-O-TBDMS-β-cyclodextrin in SPB-20 poly(20%

phenyl/80% dimehtylsiloxane) columns (30 m × 0.25 mm , 0.25 µm film thickness) and 1 gram (20 mL) SupelTM-Select HLB SPE cartridges were graciously provided by Len Sidiski (MilliporeSigma, Supelco, Bellefonte, PA). Racemic analytical standards of N-3-oxodecanoyl homoserine lactone (O-C10) and N-3-hydroxyhexanoyl homoserine lactone (H-C6) and L-N-3-oxododecanoyl homoserine lactone (O-C12) were purchased from Chemodex Ltd. (St Gallen, Switzerland). ZORBAX SB-C18 (150 x 4.6mm, 5µm particle size) columns were purchased from Agilent Technologues, Inc. (Santa Clara, CA). CHIRALPAK® IC-3 (250 x 4.6mm, 3µm particle size) columns were purchased from Chiral Technologies, Inc. (Ann Arbor, MI). LCMS grade acetonitrile (ACN), LCMS grade methanol (MeOH), LCMS grade water and ACS grade dichloromethane (DCM) were purchased from Fisheri Chemical (Fischeri Scientific, Hampton, NH) High purity formic acid (FA) was purchased from VWR (Randor, PA). Deionized (DI) water was obtained from an in-house Thermo Scientific DI system producing water of 18.2 MΩ•cm resistivity. Photobacterium broth (PBB) was purchased from Carolina Biological Supply Company (Burlington, NC)

7.3.2 Bacterial strains and growth conditions

Burkholderia cepacia ATCC 25416 and Pseudomonas fluorescens ATCC 13525 was acquired from the American Type Culture Collection (ATCC, Manassas, NC). Vibrio fischeri ES114, Pseudomonas fluorescens and Pseudomonas putida were purchased from Carolina Biological Supply Company (Burlington, NC). All stock cultures were stored in a 1:3 v/v of sterilized glycerol in growth media and placed at -80°C for long-term storage and use.

7.3.3 Preparation of full M9 media and Photobacterium broths

10.5g of dry M9 broth was dissolved into 1L of DI water from the in-house system over a hot plate to insure homogeneity. The prepared M9 solution was then sterilized by autoclave under 15 psi of steam at a chamber temperature of 121°C for 30 minutes. To the autoclaved M9 broth, filter sterilized D-(+)-glucose and magnesium sulfate (MgSO4) solutions were added to an amount of 0.4% and 2 mM in 1L respectively, at this point becoming full M9 media broth

for bacterial growth. For PBB, 66g of dry media was dissolved into 1L of DI water over a hot plate to insure homogeneity. The PBB solution was then sterilized by autoclave under 15 psi of steam at a chamber temperature of 121°C for 30 minutes. The media is complete for bacterial growth once autoclaved.

7.3.4 Preliminary cultures of B. cepacia, V. fischeri, P. fluorescens and P. putida

B. cepacia, P. fluorescens and P. putida from the -80°C storage were inoculated into full M9 media and grown overnight (18 hours). B. cepacia was grown at 30°C with P. fluorescens and P. putida both grown at 25°C in a shaker incubator at 200 rpm. The overnight cultures of B. cepacia, P. fluorescens and P. putida were then reinoculated to sterile full M9 media for subsequent studies. V. fischeri from the -80°C storage was inoculated into PBB and grown overnight (18 hours) at 25°C in a shaker incubator at 200 rpm. The overnight cultures of V. fischeri were then reinoculted to sterile full M9 media for subsequent studies.

7.3.5 Chiral Analysis, standard curve,and calibration for quantitative analysis of N-acyl homoserine lactones

Samples of 2mg racemic N-HLs were weighted by analytical balance in 5mL volumetric flasks and then filled with ACN to the volume line, yielding 200µg/mL solutions per enantiomer in the racemate. The exception was for L-O-C12, due to the lack of a racemic standard for this analyte 2mg of the single enantiomer was weighted by analytical balance in a 5mL volumetric flask. The flask was then filled with ACN to the volume line yielding a 400µg/mL solution for L-O-C12. The stocks were then used to prepare 1µg/mL working solutions for the N-HL standards and a 4µg/mL working solution for the A-C7 internal standard.

7.3.6 Quantitation

The method developed by Horacek, et. al., 2023 was used for the analysis and quantitation of N-HLs by GC-MS/MS and LC-MS/MS with calibration curves prepared as follows.

For the chiral LC separation analysis, a Shimadzu LC-MS 8040 system (Shimadzu Scientific Instruments, Columbia MD) equipped with a ZORBAX-SB C18 tandem to a CHIRALPAK IC-3 columns, electrospray ionization and a triple quadrupole mass analyzer was used in positive ion mode, the LC-MS/MS method is outlined in the literature (Ondrej, et. al). For the chiral GC separation analysis, a Shimadzu GCMS-TQ8040 (Shimadzu Scientific Instruments, Columbia, MD) equipped with a β-DEX 225™ column, electron ionization and triple quadruople mass analyizer, the GC-MS/MS method is outlined in the literature (Ondrej, et. al.). Pentaplicate samples ranging from 5-8 concentration levels were prepared. The calibration curve for LC-MS/MS was created as so; 10 mL of full M9 media was spiked with 1, 2.5, 5, 10, 25, 50, 100 and 200µL of N-HL working solutions (1µg/mL) and spiked with 7.5µL A-C7 internal standard solution. For working with GC-MS/MS full M9 media was spiked with 50, 75, 100, 150 and 200µL of N-HL working solutions (1µg/mL) and spiked with 100µL of A-C7 internal standard solution. These spiked samples were then processed by an SPE extraction method outlined in the literature (Ondrej, et. al.). A final 11 mL of ACN was used to elute the samples from the SPE cartridges. Following extraction, the solvent was rotary evaporated under a vacuum of 60 torr in a 50°C water bath. The leftover dried residue was reconstituted into 2 mL of dichloromethane and transferred to dry working vials. These were subsequential dried using a gentle stream of ultrahigh purity N2. For analysis by LC-MS/MS, the samples were finally reconstituted into 100µL of methanol creating concentration levels of 10, 25, 50, 100, 250, 500, 1000 and 2000ppb of N-HL standards and 75ppb of internal standard concentration for quantitation. For analysis by GC-MS/MS an extra derivatization step was applied to standard solutions to convert HHL and OHL into their TMS derivatives due to their heat lability in their native state. To extracted and dried N-HL standards, 75µl of BSTFA with 1% TMCS and 25µL of ACN co-solvent was added and vial sealed with a PTFE lined cap. The solution was then mixed for 10 seconds and placed into a 130°C preheated sand bath for 45 minutes creating the concentration levels of 500, 750, 1000, 1500 and 2000ppb of N-HL standards and 1000ppb of internal standard concentration.

7.3.7 Detection of N-acyl homoserine lactones from B. cepacia and V. fischeri

Initial working bacterial cultures of B. cepacia and V. fischeri, seeded from the preliminary cultures mentioned in the Preliminary cultures of B. cepacia and V. fischeri section were grown in respective media for 24 hours. Aliquots of 10 mL of each bacteria supernatant was centrifuged at 4000 rpm, decanting cell free supernatants to clean vials. Cell-free supernatant was extracted and processed for analysis by LC-MS/MS and GC-MS/MS by the method outlined in the literature (Ondrej, et. al.) to scout for possible produced N-HLs.

7.3.8 OD600 Growth and N-acyl homoserine lactone production over time for B. cepacia

In triplicate, 1L sterile conical growth flasks were charged with 200mL of sterile full M9 media using sterile 50mL serological pipets. Aliquots of 200µL of preliminary growth culture of B. cepacia were aseptically transferred to the 1L conical flask using sterile 1mL micropipette tips under the flame of a torch. Samples of 1.5 mL of growth culture were taken for each flask at times: 6, 12, 18, 24, 25, 26, 27, 30, 33, 36, 39, 48.5, 60, 72, 98 and 123 hours. These samples were then diluted with 1.5mL of DI water and placed into polystyrene cuvettes for OD600 measurements with a Vernier SpectroVis™ Plus spectrophotometer. Samples of 10 mL was taken from each flask at the mentioned times and processed by the above-mentioned method. The 10 mL samples were spiked with 7.5µL of the 4µg/mL working solution and processed through the extraction and sample processing method mentioned in the above section for analysis by LC-MS/MS and GC-MS/MS.

7.3.9 OD600 Growth and N-acyl homoserine lactone production over time for V. fischeri

Triplicate, 1L sterile conical growth flasks were charged with 200mL of sterile PBB media using sterile 50mL serological pipets. Aliquots of 200µL of preliminary growth culture of V. fischeri were aseptically transferred to the 1L conical flask using sterile 1mL micropipette tips under the flame of a torch. Samples of 1.5 mL of growth culture were taken for each flask at times: 6, 12, 16, 17, 18, 20, 22, 24, 26, 29, 33, 40, 48, 72, 95 and 120 hours. These samples were then diluted with 1.5mL of DI water and placed into polystyrene cuvettes for OD600 measurements with a Vernier SpectroVis™ Plus spectrophotometer. Samples of 10 mL was

taken from each flask at the mentioned times and processed by the above-mentioned method. The 10 mL samples were spiked with 7.5µL of the 4µg/mL internal standard working solution and processed through the extraction and sample processing method mentioned in the above section for analysis by LC-MS/MS. A spike of 100µL of the 4µg/mL internal standard solution was used for analysis by GC-MS/MS.

7.3.10 Measurement of pH for growth over time cultures

For growth over time cultures of B. cepacia pH was always in the range of 7.0-7.2 and for V. fischeri pH ranged from 7.0-7.4.

7.4 Results

7.4.1 Novel D- and L- N-HLs produced by B. cepacia 25416

An initial 24-hour culture of *B. cepacia* 25416 was processed and analyzed for the presence of N-HLs. The N-HLs detected in this preliminary sample were L-H-C6, L-A-C6, L-H-C8, L-A-C8, D-A-C8, L-A-C10, L-H-C10 and L-A-C12 (Supporting Figure 7.S1). Table 7.1 indicate all N-HLs identified in a 120 hours culture of B cepacia categorized by the method of detection (i.e., LC-MS/MS or GC-MS.MS). In addition, all N-HLs previously reported in the literature are indicated. Several N-HLs were detected in this culture that have not been reported in the literature. These were L-O-C8, L-H-C6, L-H-C8 and L-H-C10. There was one N-HL that was not detected, but was reported in the literature as produced by *B. cepacia*, this was L-O-C6. Time studies were conducted for the production of N-HLs from *B. cepacia*. These studies confirm the presence of the novel N-HLs detected in the preliminary 24 hours growth with data shown in supplementary material.

7.4.2 Novel D- and L-N-acyl homoserine lactones produced by Vibrio fischeri ES114

An initial 24-hour grown culture of *V. fisheri* ES114 was processed and analyzed as previously mentioned and evaluated for N-HLs. Many D,L-N-HLs pairs were detected by LC-MS/MS, including L- and D-A-C4, L- and D-A-C6, L- and D-A-C8, L- and D-A-C10, L- and D-O-C6, L-, D1 and D2-H-C8, and L- and D1-H-C10 (Supporting Figure 7.S2). Using GC-MS/MS, the N-HLs detected were L-A-C4, L- and D-A-C6, L- and D-A-C8 and L-A-C10. Of the eight D-N-HLs detected, six have not been reported in the literature previously (see Table7.2). Four of the D-N-HLs detected are from the OHL and HHL classes (Table 7.2 and Figure 7.S2). Two L-N-HLs detected in the *V. fischeri* ES114 culture have not been reported in the literature previously, these were L-A-C12 and L-H-C6 (Table 7.2).

Table 7.1 *N*-acyl homoserine lactones expected* from other studied and reported from current study for B. cepacia 25416

AHLs / Source	A-C4	A-C6		A-C8		A-C10		A-C12	O-C8	H-C6	H-C8	H-C10
	L	L	D	L	D	L	D	L	L	L	L	L
Literature	o	o	o	o	o	o	-	o	-	-	-	-
Current LC-MS/MS	o	o	o	o	o	o	o	o	o	o	o	o
Current GC-MS/MS	-	o	-	o	o	-	-	-	o	o	-	o

Detected	o
Not detected	-

*Expected: Reported in the literature previously

Table 7.2 *N*-acyl homoserine lactones expected* from other studies and reported from current study for *V. fischeri* ES114

AHLs / Source	A-C4		A-C6		A-C8		A-C10		A-C12	O-C6		O-C8	H-C6	H-C8			H-C10	
	L	D	L	D	L	D	L	D	L	L	D	L	L	L	D1	D2	L	D1
Literature	o	-	o	o	o	o	o	-	-	o	-	o	-	o	-	-	o	-
Current LC-MS/MS	o	o	o	o	o	o	o	o	o	o	o	o	o	o	o	o	o	o
Current GC-MS/MS	o	-	o	o	o	o	o	-	-	-	-	o	-	-	-	-	-	-

*Expected: Reported in the literature previously

7.4.3 Enantiomeric production of N-HLs over-time for Vibrio fischeri ES114

Plots of enantiomeric N-HL production versus time for novel D,L-N-HL pairs along with the OD_{600} biomass growth were done for *V. fischeri*. The D,L-N-HLs plotted are A-C10 and H-C10 (Figure 7.4), O-C6 and A-C4 (Figure 7.5) and H-C8 (Figure 7.6). The maximum detected concentration of L-N-HLs and D-N-HLs are presented in Table 7.3. Concentration of L-N-HLs increase with time, reaching maximum concentrations between 20 and 40 hours and then gradually decrease over the rest of the growth period. The concentration of D-N-HLs also increased with time, reaching maximum concentrations between ~30-60 hours and then plateau over the rest of the growth time. The shape of the OD_{600} growth curve resembles the D-N-HLs curves in there experiments (Figures 7.1, 7.2 and 7.3). Production curves of previously reported for N-HLs are also shown in the Supporting Figures 7.S3 and Figure 7.S4. A comprehensive list of the quantitated amounts of all N-HLs produced by *V. fischeri* ES114 are given in Table 3.

Table 7.3. Quantified maximum amounts of D- and L-HL (ng/mL) from bacterial supernatants of *V. fischeri* and *B. cepacia*. L/D ratios are calculated by dividing the maximum L-enantiomer amount by the maximum D-enantiomer amount. A dash (-) means the particular N-HL was not quantified due to falling below the method LOD. Data represent averages with standard deviations calculated from three replicates.

V. fischeri	L	D1*	D2*	L/D ratio	*B. cepacia*	L	D1*	D2*	L/D ratio
A-C4	6.3 ± 2	0.042 ± 0.003	-	150	A-C4	-	-		-
H-C6	-	-	-	-	H-C6	0.16 ± 0.03			
O-C6	4.9 ± 0.9	0.83 ± 0.02	-	6	O-C6	-	-		-
A-C6	42 ± 2	0.51 ± 0.02	-	84	A-C6	2.1 ± 0.3	-		-
H-C8	39 ± 3	0.594 ± 0.009	5 ± 2	7	H-C8	2.4 ± 0.2	-		-
O-C8	2.1 ± 0.4	-	-	-	O-C8	-	-		-
A-C8	1400 ± 50	16 ± 2	-	88	A-C8	110 ± 30	0.5 ± 0.1		210
H-C10	2.5 ± 0.1	0.054 ± 0.003	-	46	H-C10	0.06 ± 0.01	-		-
A-C10	7 ± 1	0.06 ± 0.02	-	120	A-C10	0.4 ± 0.1	-		-
A-C12	0.032 ± 0.003	-	-	-	A-C12	0.16 ± 0.06	-		-

*D1 and D2 are denoted for HL that have two D- stereoisomers, i.e., the 3-hydroxyacyl homoserine lactones.

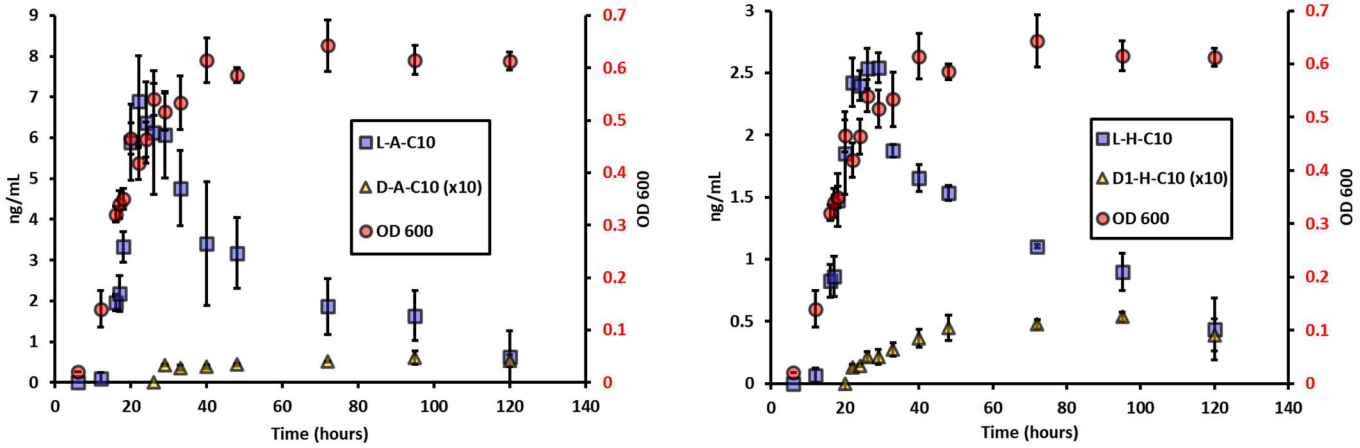

Figure 7.1. Production of **Left:** D,L-decanoyl-homoserine lactone (A-C10) and **Right:** D,L-3-hydroxydecanoyl homoserine lactone (H-C10) with biomass (OD_{600}) curves during growth of *V. fischeri.* The concentrations of D-A-C10 and D1-H-C10 were multiplied by 10 for clarity in the growth curve plot. Data represent averages with standard deviations for three replicates

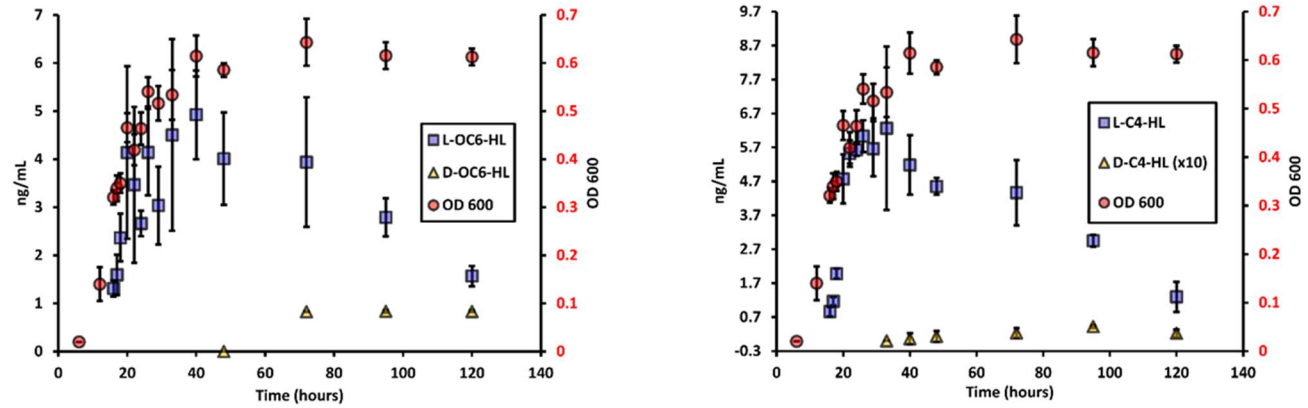

Figure 7.2. Production of **Left:** D,L-3-oxohexanoyl homoserine lactone (D,L-O-C6) and **Right:** D,L-butyryl homoserine lactone (A-C4) with biomass (OD_{600},) curves during growth of *V.* fischeri. The concentration of D-A-C4 was multiplied by 10 for clarity in the time curve plot.Data represent averages with standard deviations calculated from three replicates.

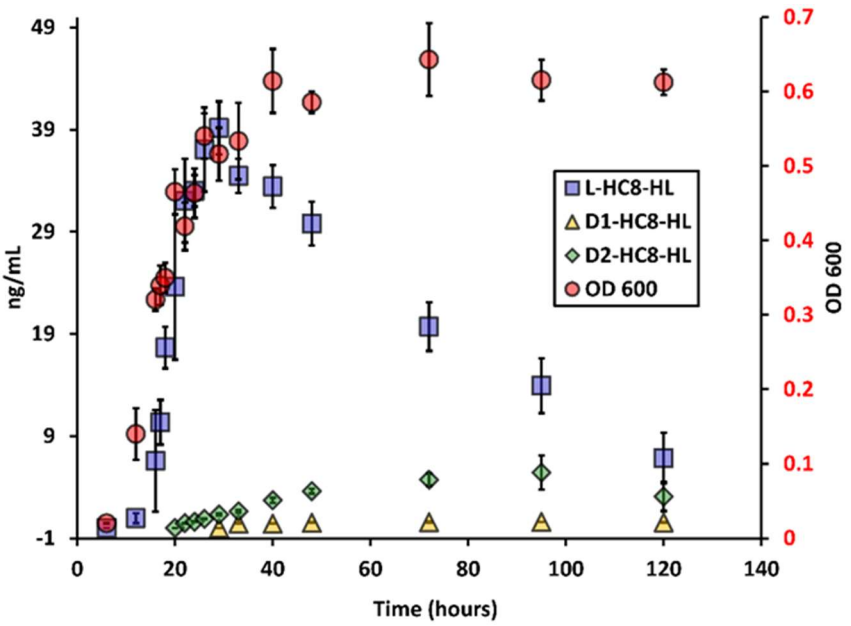

Figure 7.3. Production of D,L-3-hydroxyoctanoyl homoserine lactone (H-C8) with biomass (OD_{600}) curves during growth of *V.* fischeri. Data represent averages with standard deviations calculated from three replicates.

7.4.4 N-acyl homoserine lactones from Pseudomonas fluorescens and Pseudomonas putida

P. fluorescens and *P. putida* were cultured for 24 hours (see Experimental) but no N-HLs were detected in their preliminary studies. Therefore, a second, 95 hour growth study was conducted however, once again no N-HLs were detected (Data not shown) despite previous reports that these bacteria produce N-HLs.

7.5 Discussion

7.5.1 Detection of novel D- and L-N-acyl homoserine lactones from 24-hour growths of B. cepacia 25416

A total of four L-N-HLs were detected that were previously not reported in the literature namely H-C6, H-C8, H-C10 and O-C8 (Table 7.1). The LC-MS/MS method implemented in this study is possibly the most comprehensive, sensitive, and selective approach for the analysis of N-HLs (Horaceck *et al.*, 2022). This could explain why previously unreported N-HLs were detected. The most frequently reported N-HL for *B. cepacia* (L-A-C8) in the literature also was the most produced in our study (Lutter *et al.*, 2001, Conway *et al.*, 2002). Comparing the novel N-HLs found in this study to L-A-C8, L-H-C8 was detected at two orders of magnitude lower, H-C6 at three orders of magnitude lower, H-C10 at four orders of magnitude lower and finally L-O-C8 was detected just above the lower limit of detection for our method (Table 3). One N-HL, L-O-C6, was not detected in this study despite its report in a strain of *B. cepacia* (Conway *et al.*, 2002). Even though the same species was studied, the strains are different. It is possible that different strains of the same species can produce different N-HL profiles. A total of three D-N-HLs were detected in this study however only one, D-A-C8, was produced at quantifiable amounts (Table 3 Supporting Figure 7.S1). The production of two D-N-HL have been reported previously for *B. cepacia* 25416, D-A-C8 and D-A-C6 (Portillo *et al.*, 2021). The concentration of D-A-C8 and D-A-C6 were lower in the current study which used a different methodology and an older strain of bacteria. D-A-C10 was detected for the first time in *B. cepacia* 25416 however, it was just above the lower limit of detection. Interestingly, D-A-C10 has previously been reported in a different strain of *B. cepacia* (strain LA_3) (Malik *et al.*, 2009), which helps support the findings of our study.

Recently, N-HL analogues were studied for their ability to activate the RhlI system, which is regulated by A-C4, in *P. aeruginosa*. Upon testing D-N-HL they observed no activation or inhibition for D-A-C4, however, D-O-C6 showed activation of RhlI and interestingly inhibition was observed for D-O-C8 (Shin *et al.*, 2019). In a report where attenuation of QS of *Acinetobacter baumanii* is tested by chiral N-HL analogues, it was shown in one case that a D-N-

HL analogue was as potent at inhibiting QS as it's opposite enantiomer (Stacy *et al.*, 2012). A different D-N-HL analogue showed one-and-a-half times more potency for inhibition than its corresponding L-N-HL (Stacy *et al.*, 2012). Bacteria are known to produce anti-microbial molecules that allow them to compete with other species of bacteria (Kawai *et al.*, 2007, Liu *et al.*, 2013, Pacheco & Segrè, 2019). It appears that the D- chirality of N-HLs in some cases inhibits QS signaling which alludes to a possible role of D-N-HLs in competition between species of bacteria.

7.5.2 Vibrio fischeri ES114

A myriad of N-HLs were detected with one previously unreported N-HL, L-A-C12 (Table 7.2). Most interesting was the large number of D-N-HLs detected and for the first time the detection of D-HHLs and a D-OHL in *V. fischeri* ES114 (Table 2 and Supporting Figure S7.2). A total of eight D-N-HLs were detected in this strain of *V. fischeri* and all of them quantified by LC-MS/MS (Table 7.3). Two of the eight D-HLs have previously been reported (Portillo *et al.*, 2021), D-A-C8 and D-A-C6 and have been confirmed herein (Portillo *et al.*, 2021). However, two novel D-AHL were detected as well, D-A-C4 and D-A-C10 (Table 7.2). The novel D-HHLs detected and quantified are D1-H-C8, D2-H-C8 and D1-H-C10. Only one D-OHL was detected and quantified which was D-O-C6 (Table 7.2 and Table 7.3). One of the most frequently reported N-HLs in cultures of *V. fischeri* is A-C8 (Kimbrough & Stabb, 2013, Purohit *et al.*, 2013, Kimbrough & Stabb, 2016). and this was the most produced N-HL in our study (Kimbrough & Stabb, 2013, Purohit *et al.*, 2013, Kimbrough & Stabb, 2016). L-A-C12 was quantified at amounts five orders of magnitude lower than L-A-C8 (Table 7.3). D-A-C8 was the most abundant D-N-HL in this study. In a recent report both D- and L-O-C6 were tested for the activity of the *lux* operon which is responsible for QS regulated bioluminescence in *V. fischeri* (Li *et al.*, 2018). By testing D-O-C6 for induction of bioluminescence they found that it is not directly involved in activating the *lux* operon, but clearly is not an inhibitor for this process. Agonistic effects were observed for another D-N-HL(D-A-C6) but its activity was similar to D-O-C6 (Li *et al.*, 2018).

The hypothesis that bacteria produce both N-HL enantiomers as "natural" signaling molecule is not new. Myxobacteria, *S. aurntiaca* was found to produce a different chiral

extracellular signaling molecule, 8-hydroxy-2,5,8-trimethyl-4-nonanone (Morikawa *et al.*, 1998). In this case it was found that both enantiomers were produced naturally. The study also showed similar amounts of activity for both enantiomers.

In a previous report, a strain of *Pseudomonas putida* IsoF was shown to produce L-O-C10 and follow a similar production trend to the L-N-HLs in this study (Fekete *et al.*, 2010). A lactonase enzyme was proposed suggesting that N-HL degradation is an integral part of the QS signaling circuit in *P. putida* IsoF (Fekete *et al.*, 2010). It is well-understood that many enzymes are substrate-specific as well as having a degree of enantioselectivity (Schoffers *et al.*, 1996, Sukumaran & Hanefeld, 2005, Mohr *et al.*, 2009). It is possible that an enzyme with enantioselectivity for the L-N-HLs tends to leave the D-N-HLs intact (Figures 7.1, 7.2 and 7.3). It also appears that the ability to "degrade" L-N-HLs is not significantly affected by substitution on the N-HL acyl chain. Whether the L-N-HL was unsubstituted (Figure 7.1-Left and Figure 7.2-Right), carbonyl substituted (Figure 7.2-Left) or hydroxy substituted (Figure 7.1-Right and Figure 7.3), they all reached maximal concentrations at ~30 hours and decreased afterwards. Another interesting study reported on the effectiveness of a plant hydrolase for degradation of N-HLs (Palmer *et al.*, 2014). It was found that when testing L- and D-O-C12 with this hydrolase the D-O-C12 was 30% less susceptible to hydrolysis. It appears that D-N-HLs are more resistant to decomposition by biological processes. Questions remain as to the role of the ubiquitously produced, D-N-HLs, as well as to their origins. Interest in the research of D-amino acids and their involvement in biological systems has increased in the past few years (Armstrong *et al.*, 1993, Armstrong *et al.*, 1993, Ercal *et al.*, 1996, Weatherly *et al.*, 2017). It is known that the majority of D-amino acids originate via amino acid racemases (Wolosker *et al.*, 1999, Tanner, 2002, Radkov & Moe, 2014, Weatherly *et al.*, 2017, Du *et al.*, 2019, Du *et al.*, 2020). The possibility that some type of racemase could be producing D-N-HLs should be considered.

7.5.3 Lack of N-acyl homoserine lactones, Bioreporters and Possible False Positives

An unexpected result in this study was the absence of any N-HLs in samples from cultures of *P. fluorescens* and *P. putida*. A study reported A-C8 in cultures of *P. fluorescens* and of A-C12 in *P. putida* (Bai & Rai, 2011). It was posited that these N-HLs were responsible for the

regulation of proteolytic activity leading to the spoilage of rainbow trout (Bai & Rai, 2011). In a work where *P. putida* T2-2 is isolated from tongue microbiota, A-C12 is detected using an *A. tumefaciens* NTL4 bioreporter strain and Q-TOF MS/MS (Chen *et al.*, 2013). Another study mentions the detection of both A-C4 and O-C8 in a strain of *P. fluorescens* that was isolated from milk. This research used thin-layer chromatography with bioreporter detection coupled with LC-ESI-MS to indicate their presence (Liu *et al.*, 2007). In a study conducted on *P. putida* IsoF using FT-ICR-MS on extracted samples, various N-HLs were detected with the most prominent being O-C10 followed by O-C12 and O-C8 (Fekete *et al.*, 2010). It was also reported the detection of A-C8 in *P. fluorescens* ATCC 13525 using a CV026 bioreporter coupled with GC-MS (Li *et al.*, 2018). The strain of the bacterium cannot be overlooked when viewing N-HL profiles from the same species. For example the *B. cepacia* complex are a consortium of nine closely related species with very similar genetics that exhibit similar functions, however their profiles of N-HL are known to differ between some of their species (Venturi *et al.*, 2004). The question arises as to why there are discrepancies in N-HL profiles for the same strain in different studies. In our study a minimal media was used while the aforementioned study using an all-purpose media. Also, growth conditions were slightly different in that 25°C was used in our study while 28°C was used in the previous study. It has been shown that different temperatures can affect the amount of N-HL produced in strains of *V. fischeri*, however, the temperature differences in that study were 10 to almost 20 degrees and not two to three degrees (Purohit *et al.*, 2013). The question then arises as to the dependability (i.e., selectivity) of bioreporter strains when used for analysis and indication of N-HL in bacterial matrices. As mentioned previously (see Introduction) the bioreporter assay must be used with caution when applied to N-HL detection, given reports of unknown molecules present that activate said bioreporters (Shaw *et al.*, 1997, Liu *et al.*, 2007, Steindler & Venturi, 2007). In one study it was shown that the activation of the LuxR-based bioreporter was being activated, not by an N-HL but by different molecules, specifically diketopiperazines and cyclodipeptides (Holden *et al.*, 1999). It was also shown that in the *Delisea* plant a furanone N-HL mimic exists that induces premature promotion of QS systems in *P. aeruginosa* by binding to their QS receptors (Bauer & Mathesius, 2004). It is evident that great care must be taken when bioreporters are used for

detection and identification of N-HL; contamination, foreign, or endogenous molecules could lead to false positive results. However, their roles as auxiliary methods, in a comprehensive analytical method, do give them some merit with respect to their relatively quick turn-over and ease of use for preliminary detection studies.

7.6 Conclusions

The presence of novel N-HLs in cultures of *B. cepacia* 25416 and *V. fischeri* ES114 are reported. The first oxygen containing D-HHLs and a D-OHL was found in cultures of *V. fischeri*. Quantitation by a sensitive LC-MS/MS analysis reveals that the novel N-HLs reported herein were detected at much lower concentrations than the most prevalent N-HLs for their respective bacterial species. Time studies on the production of N-HLs by *V. fischeri* hints at a separate synthetic pathway for the production of L-N-HLs compared to D-N-HLs as well as possible enantioselective elimination pathways. An intriguing possibility is that a racemase could be involved in D-N-HL production as they are in the production of D-amino acids in biological systems.

Table S7.1 SRM transitions monitored when analyzing N-HL by LC-MS/MS and GC-MS/MS

N-acyl homserine lactone	GC-MS/MS* (m/z>m/z)	LC-MS/MS (m/z>m/z)
D,L-A-C4	143.00>125.10	172.00>102.10
D,L-A-C6	143.00>125.10	200.05>102.10
D,L-A-C7	143.00>125.10	214.00>102.10
D,L-A-C8	143.00>125.10	228.20>102.10
D,L-A-C10	143.00>125.10	256.25>102.10
D,L-A-C12	143.00>125.10	284.10>102.10
D,L-A-C14	143.00>125.10	312.25>102.10
D,L-H-C4	244.00>119.10	186.00>102.10
D,L-H-C6	272.00>200.10	216.00>102.10
D,L-H-C8	300.10>200.10	244.00>102.10
D,L-H-C10	328.10>200.10	272.10>102.10
D,L-H-C12	356.10>200.10	300.10>102.10
D,L-H-C14	384.10>200.10	328.25>102.10
D,L-O-C4	157.00>75.10	186.00>102.10
D,L-O-C6	183.00>75.10	214.05>102.10
D,L-O-C8	213.00>75.10	242.20>102.10
D,L-O-C10	241.00>75.10	270.10>102.10
L-O-C12	269.00>75.10	298.10>102.10
D,L-O-C14	n.a.#	326.10>102.10

*** OHL and HHL transitions are for their trimethyl silyl derivatized form.**

 # D,L-O-C14 was not analyzed by GC-MS/MS

Table S7.2 Comparinson of enantiomeric quantification of homoserine lactones using LC-MS/MS and GC-MS/MS. Samples extracted by SPE

Analyte	LC -MS/MS			GC – MS/MS		
	LOD (ppb)	LOQ (ppb)	R^2	LOD (ppb)	LOQ (ppb)	R^2
L C4-HSL	4	13	0.9981	<LOD	<LOD	<LOD
D C4-HSL	2	7	0.9964	<LOD	<LOD	<LOD
L C6-HSL	2	7	0.9993	382	1160	0.9730
D C6-HSL	3	11	0.9992	242	735	0.9890
L C8-HSL	3	9	0.9994	307	932	0.9824
D C8-HSL	3	9	0.9998	566	1716	0.9426
L C10-HSL	7	23	0.9991	336	1018	0.9635
D C10-HSL	8	27	0.9992	880	2667	0.9425
L C12-HSL	5	16	0.9995	210	637	0.9854
D C12-HSL	2	8	0.9918	63	192	0.9987
L C14-HSL	4	13	0.9979	418	1268	0.9444
D C14-HSL	6	19	0.9965	366	1109	0.9569
3-hydroxy-C4-HSL	Quantitation was not possible because of low extraction recovery.					
P_1 + P_2[4] 3-hydroxy-C6-HSL	4	13	0.9972	221	671	0.9838
P_3 + P_4[4] 3-hydroxy-C6-HSL	5	15	0.9977	209	632	0.9586
P_1 + P_2 3-hydroxy-C8-HSL	5	16	0.9976	123	374	0.9949
P_3 + P_4 3-hydroxy-C8-HSL	5	15	0.9980	3588	10872	0.8443
P_1 + P_2 3-hydroxy-C10-HSL	4	14	0.9996	1296	3926	0.8833
P_3 + P_4 3-hydroxy-C10-HSL	3	11	0.9989	1180	3575	0.9725
P_1 + P_2 3-hydroxy-C12-HSL	4	12	0.9982	83	251	0.9977
P_3 + P_4 3-hydroxy-C12-HSL	5	15	0.9951	535	1621	0.9744
P_1 + P_2 3-hydroxy-C14-HSL	2	7	0.9908	417	1264	0.9448
P_3 + P_4 3-hydroxy-C14-HSL	1	5	0.9986	137	414	0.9872
L 3-oxo-C4-HSL	Quantitation was not possible because of low extraction recovery.					
D 3-oxo-C4-HSL	Quantitation was not possible because of low extraction recovery.					
L 3-oxo-C6-HSL	2	8	0.9905	678	2057	0.9159
D 3-oxo-C6-HSL	4	13	0.9900	515	1561	0.9498
L 3-oxo-C8-HSL	2	7	0.9911	<LOD	<LOD	<LOD
D 3-oxo-C8-HSL	2	6	0.9905	<LOD	<LOD	<LOD
L 3-oxo-C10-HSL	4	13	0.9917	<LOD	<LOD	<LOD
D 3-oxo-C10-HSL	2	6	0.9911	446	1338	0.9625
L 3-oxo-C12-HSL	2	7	0.9891	742	2250	0.9081
L 3-oxo-C14-HSL	15	50	0.9917	n.a.	n.a.	n.a.
D 3-oxo-C14-HSL	15	51	0.9866	n.a.	n.a.	n.a.

n.a. = not applicable (this analyte was not analyzed with GC-MS/MS)

[4] P_1, P_2, P_3, P_4 stands for first, second, third, and fourth eluted peak of HHLs, respectively

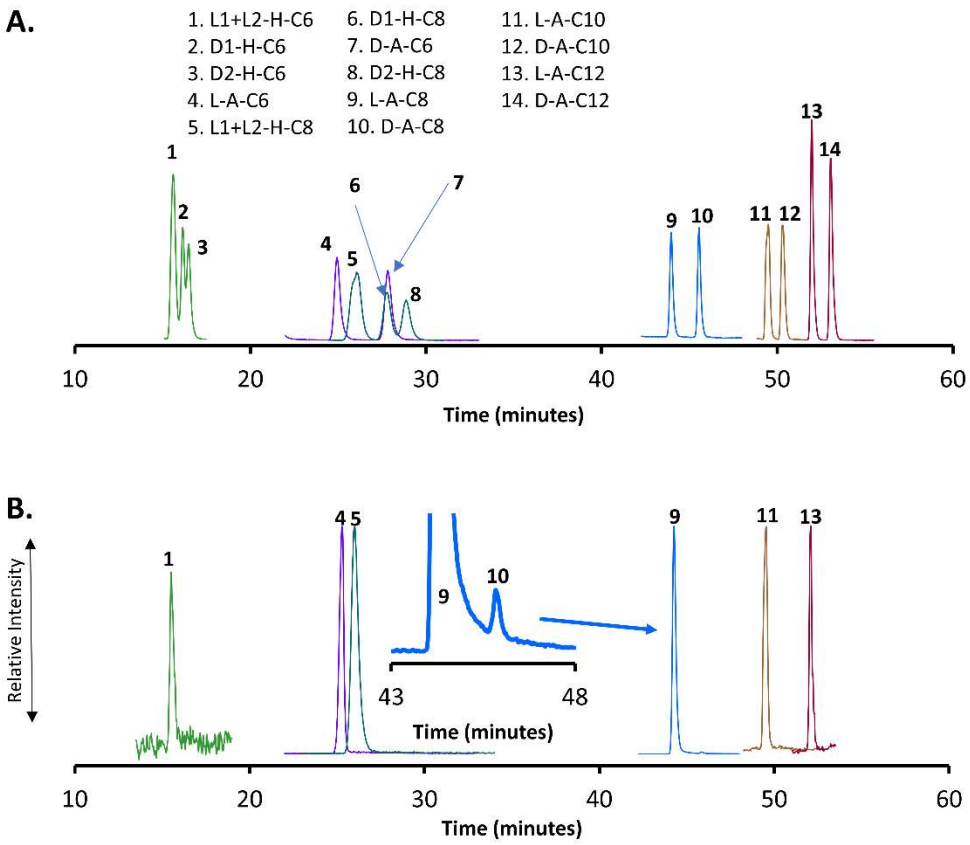

Figure S7.1. Part **A.** MRM extracted chromatogram of standard HLs **B.** MRM extracted chromatogram of HLs detected from *B. cepacia*, relative intensity of the peaks are used for clarity **B. Inset:** Blow-up of D- and L-A-C8. Selected HL chromatograms are shown for visual clarity. MRM data is found in Supplemental Material (Table S1)

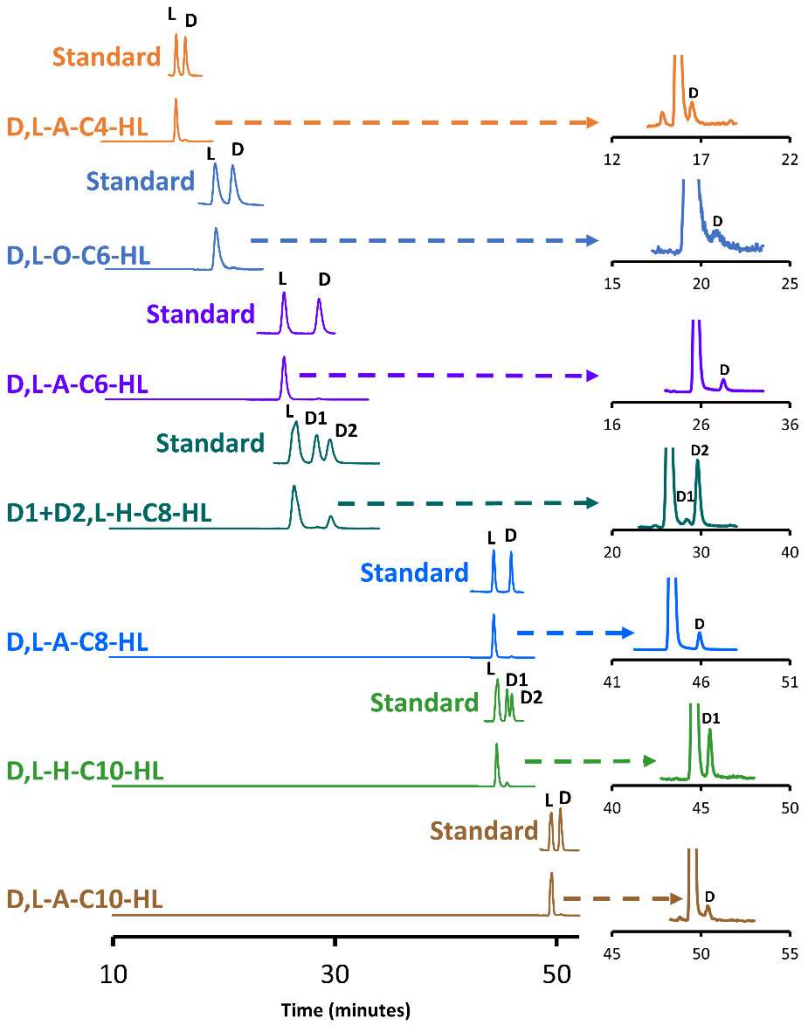

Figure S7.2. **Left:** MRM chromatograms of standards (top) and extracted samples of *V. fischeri* (bottom). **Right:** Close up of MRM chromatograms of HLs detected from extracted samples of *V. fischeri*. MRM data is found in Supplemental Material (Table S2).

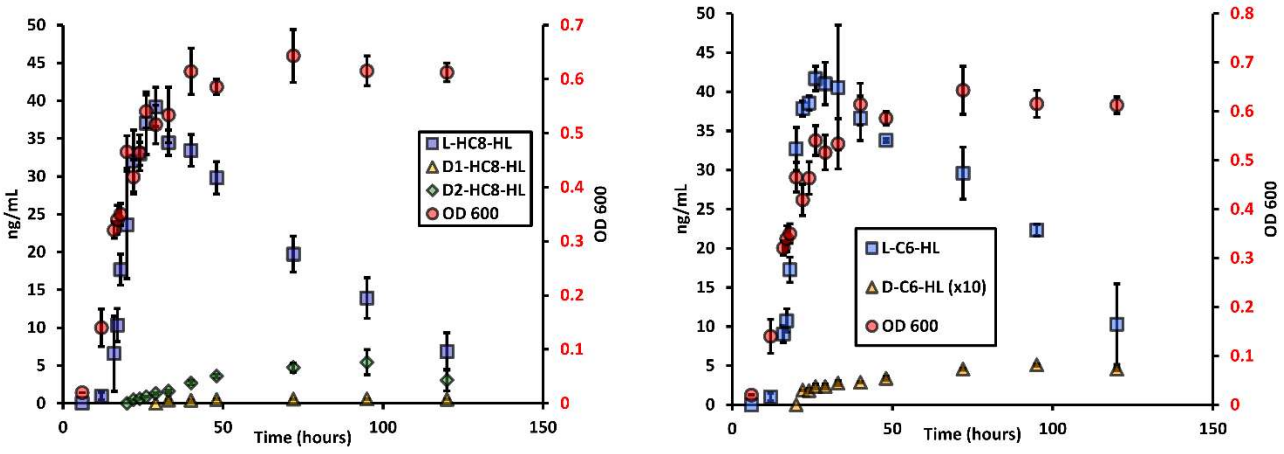

Figure S7.3. Production of **Left:** D, L-3-hydroxyoctanoyl homoserine lactone (H-C8) and **Right**: D, L-hexanoyl homoserine lactone with biomass (OD_{600}) curves during growth of *V. fisheri.* Data represents averages with standard deviations calculated from three replicas.

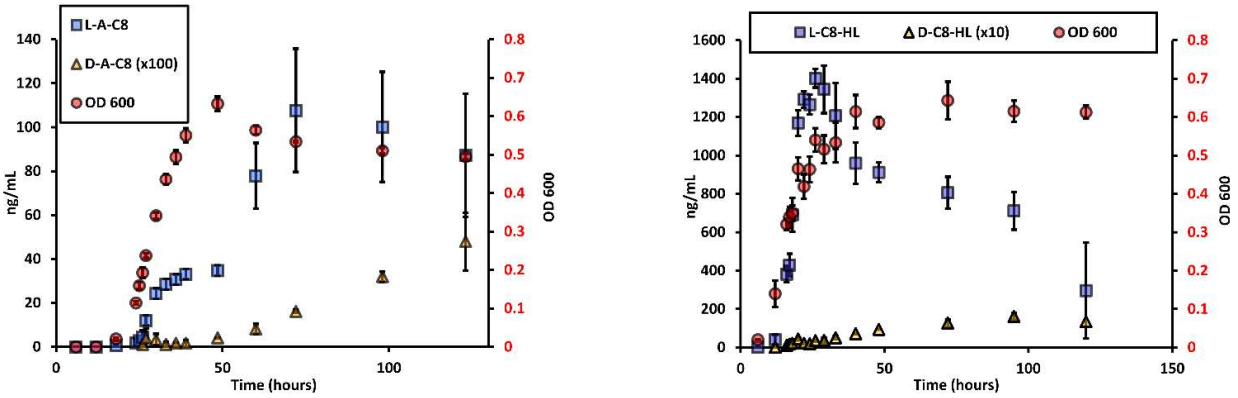

Figure S7.4. Production of D, L-octanoyl homoserine lactone (A-C8) with biomass (OD_{600}) curves during growth of **Left:** *B*. *cepacia* and **Right:** *V*. *fisheri*. Data represents averages with standard deviations calculated from three replicates.

7.8 References

Armstrong D, Gasper M, Lee S, Ercal N & Zukowski J (1993) Factors controlling the level and determination of D-amino acids in the urine and plasma of laboratory rodents. *Amino Acids* **5**: 299-315.

Armstrong DW, Gasper M, Lee SH, Zukowski J & Ercal N (1993) D-amino acid levels in human physiological fluids. *Chirality* **5**: 375-378.

Bai AJ & Rai VR (2011) Bacterial quorum sensing and food industry. *Comprehensive Reviews in Food Science and Food Safety* **10**: 183-193.

Bauer WD & Mathesius U (2004) Plant responses to bacterial quorum sensing signals. *Current opinion in plant biology* **7**: 429-433.

Cataldi TR, Bianco G & Abate S (2009) Accurate mass analysis of N-acyl-homoserine-lactones and cognate lactone-opened compounds in bacterial isolates of Pseudomonas aeruginosa PAO1 by LC-ESI-LTQ-FTICR-MS. *Journal of mass spectrometry* **44**: 182-192.

Cha C, Gao P, Chen Y-C, Shaw PD & Farrand SK (1998) Production of acyl-homoserine lactone quorum-sensing signals by gram-negative plant-associated bacteria. *Molecular Plant-Microbe Interactions* **11**: 1119-1129.

Chen J-W, Chin S, Tee KK, Yin W-F, Choo YM & Chan K-G (2013) N-acyl homoserine lactone-producing Pseudomonas putida strain T2-2 from human tongue surface. *Sensors* **13**: 13192-13203.

Conway B-AD, Venu V & Speert DP (2002) Biofilm Formation and Acyl Homoserine Lactone Production in the Burkholderia cepacia Complex. *Journal of Bacteriology* **184**: 5678-5685.

Diplock E, Alhadrami H & Paton G (2009) Application of microbial bioreporters in environmental microbiology and bioremediation. *Whole cell sensing system II* 189-209.

Du S, Wang Y, Alatrash N, Weatherly CA, Roy D, MacDonnell FM & Armstrong DW (2019) Altered profiles and metabolism of l-and d-amino acids in cultured human breast cancer cells vs. non-tumorigenic human breast epithelial cells. *Journal of pharmaceutical and biomedical analysis* **164**: 421-429.

Du S, Sung Y-S, Wey M, Wang Y, Alatrash N, Berthod A, MacDonnell FM & Armstrong DW (2020) Roles of N-methyl-D-aspartate receptors and D-amino acids in cancer cell viability. *Molecular Biology Reports* **47**: 6749-6758.

Ercal N, Luo X, Matthews RH & Armstrong DW (1996) In vitro study of the metabolic effects of D-amino acids. *Chirality* **8**: 24-29.

Fekete A, Kuttler C, Rothballer M, Hense BA, Fischer D, Buddrus-Schiemann K, Lucio M, Müller J, Schmitt-Kopplin P & Hartmann A (2010) Dynamic regulation of N-acyl-homoserine lactone production and degradation in Pseudomonas putida IsoF. *FEMS Microbiology Ecology* **72**: 22-34.

Fuqua C, Winans SC & Greenberg EP (1996) Census and consensus in bacterial ecosystems: the LuxR-LuxI family of quorum-sensing transcriptional regulators. *Annual review of microbiology* **50**: 727-752.

Fuqua WC, Winans SC & Greenberg EP (1994) Quorum sensing in bacteria: the LuxR-LuxI family of cell density-responsive transcriptional regulators. *Journal of bacteriology* **176**: 269-275.

He Y-W, Deng Y, Miao Y, Chatterjee S, Tran TM, Tian J & Lindow S (2022) DSF-family quorum sensing signal-mediated intraspecies, interspecies, and inter-kingdom communication. *Trends in Microbiology*.

Hoang TPT, Barthélemy M, Lami R, Stien D, Eparvier Vr & Touboul D (2020) Annotation and quantification of N-acyl homoserine lactones implied in bacterial quorum sensing by supercritical-fluid chromatography coupled with high-resolution mass spectrometry. *Analytical and bioanalytical chemistry* **412**: 2261-2276.

Holden MTG, Ram Chhabra S, De Nys R*, et al.* (1999) Quorum-sensing cross talk: isolation and chemical characterization of cyclic dipeptides from Pseudomonas aeruginosa and other Gram-negative bacteria. *Molecular Microbiology* **33**: 1254-1266.

Kawai K, Wang G, Okamoto S & Ochi K (2007) The rare earth, scandium, causes antibiotic overproduction in Streptomyces spp. *FEMS microbiology letters* **274**: 311-315.

Kimbrough JH & Stabb EV (2013) Substrate Specificity and Function of the Pheromone Receptor AinR in Vibrio fischeri ES114. *Journal of Bacteriology* **195**: 5223-5232.

Kimbrough JH & Stabb EV (2016) Antisocial luxO Mutants Provide a Stationary-Phase Survival Advantage in Vibrio fischeri ES114. *Journal of Bacteriology* **198**: 673-687.

Kuo A, Blough NV & Dunlap PV (1994) Multiple N-acyl-L-homoserine lactone autoinducers of luminescence in the marine symbiotic bacterium Vibrio fischeri. *Journal of Bacteriology* **176**: 7558-7565.

Li S-Z, Xu R, Ahmar M, Goux-Henry C, Queneau Y & Soulère L (2018) Influence of the d/l configuration of N-acyl-homoserine lactones (AHLs) and analogues on their Lux-R dependent quorum sensing activity. *Bioorganic Chemistry* **77**: 215-222.

Li T, Wang D, Liu N, Ma Y, Ding T, Mei Y & Li J (2018) Inhibition of quorum sensing-controlled virulence factors and biofilm formation in Pseudomonas fluorescens by cinnamaldehyde. *International journal of food microbiology* **269**: 98-106.

Liu M, Wang H & Griffiths M (2007) Regulation of alkaline metalloprotease promoter by N-acyl homoserine lactone quorum sensing in Pseudomonas fluorescens. *Journal of applied microbiology* **103**: 2174-2184.

Liu Z, Wang W, Zhu Y, Gong Q, Yu W & Lu X (2013) Antibiotics at subinhibitory concentrations improve the quorum sensing behavior of Chromobacterium violaceum. *FEMS Microbiology letters* **341**: 37-44.

Lutter E, Lewenza S, Dennis JJ, Visser MB & Sokol PA (2001) Distribution of Quorum-Sensing Genes in the Burkholderia cepacia Complex. *Infection and Immunity* **69**: 4661-4666.

Malik AK, Fekete A, Gebefuegi I, Rothballer M & Schmitt-Kopplin P (2009) Single drop microextraction of homoserine lactones based quorum sensing signal molecules, and the separation of their enantiomers using gas chromatography mass spectrometry in the presence of biological matrices. *Microchimica Acta* **166**: 101-107.

Mohr JT, Hong AY & Stoltz BM (2009) Enantioselective protonation. *Nature chemistry* **1**: 359-369.

Morikawa Y, Takayama S, Fudo R, Yamanaka S, Mori K & Isogai A (1998) Absolute chemical structure of the myxobacterial pheromone of Stigmatella aurantiaca that induces the formation of its fruiting body. *FEMS Microbiology Letters* **165**: 29-34.

Nealson KH, Platt T & Hastings JW (1970) Cellular control of the synthesis and activity of the bacterial luminescent system. *Journal of bacteriology* **104**: 313-322.

Horacek, O, Portillo AE, Dhaubhadel U, Sung Y-S, Readel E, Armstrong, DW (2022) Comprehensive chiral GC-MS/MS and LC-MS/MS methods for the identification and determination of *N*-acyl homoserine lactones. *Talanta* (accepted)

Pacheco AR & Segrè D (2019) A multidimensional perspective on microbial interactions. *FEMS Microbiology Letters* **366**: fnz125.

Palmer AG, Senechal AC, Mukherjee A, Ané J-M & Blackwell HE (2014) Plant responses to bacterial N-acyl L-homoserine lactones are dependent on enzymatic degradation to L-homoserine. *ACS chemical biology* **9**: 1834-1845.

Pérez-Montaño F, Guasch-Vidal B, González-Barroso S, López-Baena FJ, Cubo T, Ollero FJ, Gil-Serrano AM, Rodríguez-Carvajal MÁ, Bellogín RA & Espuny MR (2011) Nodulation-gene-inducing flavonoids increase overall production of autoinducers and expression of N-acyl homoserine lactone synthesis genes in rhizobia. *Research in microbiology* **162**: 715-723.

Poonguzhall P, Selvaraj S, Madhaiyan M & Sa T (2007) Production of acyl-homoserine lactone quorum-sensing signals is wide-spread in gram-negative Methylobacterium. *Journal of microbiology and biotechnology* **17**: 226-233.

Portillo AE, Readel E & Armstrong DW (2021) Production of both l-and d-N-acyl-homoserine lactones by Burkholderia cepacia and Vibrio fischeri. *MicrobiologyOpen* **10**: e1242.

Purohit AA, Johansen JA, Hansen H, Leiros H-KS, Kashulin A, Karlsen C, Smalås A, Haugen P & Willassen NP (2013) Presence of acyl-homoserine lactones in 57 members of the Vibrionaceae family. *Journal of Applied Microbiology* **115**: 835-847.

Radkov AD & Moe LA (2014) Bacterial synthesis of D-amino acids. *Applied microbiology and biotechnology* **98**: 5363-5374.

Schoffers E, Golebiowski A & Johnson CR (1996) Enantioselective synthesis through enzymatic asymmetrization. *Tetrahedron* **52**: 3769-3826.

Shaw PD, Ping G, Daly SL, Cha C, Cronan Jr JE, Rinehart KL & Farrand SK (1997) Detecting and characterizing N-acyl-homoserine lactone signal molecules by thin-layer chromatography. *Proceedings of the National Academy of Sciences* **94**: 6036-6041.

Sheng H, Song Y, Bian Y, Wu W, Xiang L, Liu G, Jiang X & Wang F (2017) Determination of N-acyl homoserine lactones in soil using accelerated solvent extraction combined with solid-phase extraction and gas chromatography-mass spectrometry. *Analytical Methods* **9**: 688-696.

Shin D, Gorgulla C, Boursier ME, Rexrode N, Brown EC, Arthanari H, Blackwell HE & Nagarajan R (2019) N-acyl homoserine lactone analog modulators of the Pseudomonas aeruginosa Rhll quorum sensing signal synthase. *ACS chemical biology* **14**: 2305-2314.

Stacy DM, Welsh MA, Rather PN & Blackwell HE (2012) Attenuation of quorum sensing in the pathogen Acinetobacter baumannii using non-native N-Acyl homoserine lactones. *ACS chemical biology* **7**: 1719-1728.

Steindler L & Venturi V (2007) Detection of quorum-sensing N-acyl homoserine lactone signal molecules by bacterial biosensors. *FEMS microbiology letters* **266**: 1-9.

Sukumaran J & Hanefeld U (2005) Enantioselective C–C bond synthesis catalysed by enzymes. *Chemical Society Reviews* **34**: 530-542.

Tanner ME (2002) Understanding nature's strategies for enzyme-catalyzed racemization and epimerization. *Accounts of chemical research* **35**: 237-246.

Tomasz A (1965) Control of the competent state in Pneumococcus by a hormone-like cell product: an example for a new type of regulatory mechanism in bacteria. *Nature* **208**: 155-159.

Venturi V, Friscina A, Bertani I, Devescovi G & Aguilar C (2004) Quorum sensing in the Burkholderia cepacia complex. *Research in microbiology* **155**: 238-244.

Weatherly CA, Du S, Parpia C, Santos PT, Hartman AL & Armstrong DW (2017) D-amino acid levels in perfused mouse brain tissue and blood: a comparative study. *ACS chemical neuroscience* **8**: 1251-1261.

Wolosker H, Sheth KN, Takahashi M, Mothet J-P, Brady Jr RO, Ferris CD & Snyder SH (1999) Purification of serine racemase: biosynthesis of the neuromodulator D-serine. *Proceedings of the National Academy of Sciences* **96**: 721-725.

Yashiroda Y & Yoshida M (2019) Intraspecies cell–cell communication in yeast. *FEMS Yeast Research* **19**: foz071.

Zhu S, Wu H, Zeng M, Liu Z & Wang Y (2015) The involvement of bacterial quorum sensing in the spoilage of refrigerated Litopenaeus vannamei. *International journal of food microbiology* **192**: 26-33.

Chapter 8

General Summary

In chapter 2 the thermodynamics and kinetics of the racemization of (L)-*N*-acetyl homocysteine thiolactone were described. Chiral GC methods were developed and utilized to produce chromatographic data used for obtaining enantiomerization constants. Batch-wise experiments were conducted by monitoring enantiomerization over-time in three different vial types, untreated, silanized and Teflon coated. It was showed that the kinetics of racemization at 150°C behaves independent of vial composition. Rate constants were determined for the reverse and forward enantiomerization using dynamic chiral GC on B-DP, G-DP and G-BP chiral stationary phases. Mechanisms for racemization were described by quantum chemical modeling that agree with the batch-wise experiments conducted.

Chapter 3 portrays chiral methods developed on GC-MS and LC-MS for the analysis of a wide range of *N*-acyl homoserine lactones and *N*-acyl homocysteine thiolactones. The developed LC methods developed proved to be MS compatible with the ability to analyze and identify N-acyl homoserine lactones of different classes. Here a chiral GC method was developed that can separate all homologues of N-acyl-homoserine lactone as well as separation of the L- and D- enantiomers with the caveat that hydroxylated and oxo derivatized acyl chains be substituted with a trimethylsilyl group.

Chapter 4 describes a work in which the first D-N-HL was detected in a strain of *V. fischeri* (ES114) as well as the first instance to monitor the production of D-N-HL over time. Chiral GC-MS was used in tandem with hydrophilc-lipophilic balanced solid phase extraction to extract and purify the N-HL in question from their respective bacterial matrices. Good method LOD were obtained for this method with 0.001 µg/mL for unsubstituted N-HL and 0.006 µg/mL for OHL (3-oxo-acyl homoserine lactones). The quorums sensing of *V. fischeri* was studied by measuring the production of one of its major N-HL, D,L-A-C8 and comparing it to its bioluminescence production over a period of 120 hours. Methionine supplementation of M9

media used to grow *B. cepacia* revealed that any addition of methionine (L-methionine, D-methionine and racemic methionine) augmented the production of both L- and D-N-HL equally, suggesting the possibility of a distinct mechanism for the biosynthesis of D-N-HL

Chapter 5 involves the development of a comprehensive analytical approach for the analysis of N-HL by using chiral LC-MS/MS and GC-MS/MS. Applying these methods to extraction recovery studies of N-HL from media it was shown that the majority of important N-HL were recovered in the range of 80% to 105% with LOD reaching 0.001 ng/mL. It was here where it was observed that LC-MS/MS outperforms GC-MS/MS in the realm of sensitivity, analysis time and ease of use. GC-MS/MS has its merits displayed as better chromatographic performance for smaller chained and more hydrophilic N-HLs. These methods in combination allow a more sensitive, selective and specific approach for the analysis of D-N-HL *in vitro* and *in vivo* thereafter.

Chapters 6 and 7 focus was on the application of the previously mentioned highly sensitive, selective and specific LC-MS/MS and GC-MS/MS in combination with HLB-SPE for the chiral analysis of L- and D-*N*-acyl homoserine lactones from the bacterial matrices of *Pseudomonas aeruginosa*, *Pectobacterium atroscepticum*, *Pseudomonas putida*, *Pseudomonas fluorescens*, *Burkholderia cepacia* and *Vibrio fisheri*. It was here that it was shown the ubiquity of D-N-HL in various species of gram-negative bacteria. This showed not only the utility but the necessity of this chiral method for future studies of quorum sensing and its related fields.

This dissertation concentrated on the extensive development and application of extraction techniques coupled with highly sensitive chiral LC-MS/MS and GC-MS/MS for the quantitative analysis of *N*-acyl homoserine lactones in bacterial matrices. These methods have proved to have excellent recovery and robustness when it comes to separation of homologues and L- and D-enatiomer of N-HL. These methods can now be used for future studies in the further understanding of gram-negative bacterial communication in quorum sensing. From *B. cepacia* infections in cystic fibrosis patients to agricultural pathogenesis by *Pectobacterium atroscepticum* we hope that these methods will aid in the advancement of knowledge in these cases as well as other related fields.

Appendix A

Publication Information and Contributing Authors

Chapter 2. manuscript published in Journal of Chromatography A. Peter Simon, Jan Krupcik, Abiud E. Portillo, Pavel Majek, Ivan Spanik, Daniel W. Armstrong, 2021, 1653, 462381. DOI: https://doi.org/10.1016/j.chroma.2021.462381

Chapter 3. manuscript published in Analytical and Bioanalytical Chemistry. Elizabeth Readel, Abiud Portillo, Mohsen Talebi & Daniel W. Armstrong, 2020, 412, 2927-2937. DOI: https://doi.org/10.1007/s00216-020-02534-7

Chapter 4. manuscript published in MicrobiologyOpen. Abiud E. Portillo, Elizabeth Readel, Daniel W. Armstrong. 2021, 10:6, e1242. DOI: https://doi.org/10.1002/mbo3.1242

Chapter 5. manuscript submitted to Talanta. Ondrej Horacek, Abiud E. Portillo, Umang Dhaubhadel, Y-S. Sung, Elizabeth Readel, Radim Kucera, Daniel W. Armstrong, 2022

Chapter 6. manuscript submitted to ACS Biological Chemistry. Umang Dhauhbadel, Abiud E. Portillo, Ondrej Horacek, Yu-Sheng Sung, Daniel W. Armstrong, 2022

Chapter 7. manuscript submitted to FEMS Microbiology Ecology. Abiud E. Portillo, Umang Dhaubhadel, Ondrej Horacek, Yu-Sheng Sung, Daniel W. Armstrong, 2022

Appendix B

Copyright and Permissions

ELSEVIER LICENSE
TERMS AND CONDITIONS
Sep 16, 2022

This Agreement between The University of Texas at Arlington -- Abiud Portillo ("You") and Elsevier ("Elsevier") consists of your license details and the terms and conditions provided by Elsevier and Copyright Clearance Center.

The publisher has provided special terms related to this request that can be found at the end of the Publisher's Terms and Conditions.

License Number	5387700114462
License date	Sep 14, 2022
Licensed Content Publisher	Elsevier
Licensed Content Publication	Journal of Chromatography A
Licensed Content Title	Headspace study of chiral interconversion of N-acetyl-homocysteine thiolactones
Licensed Content Author	Peter Šimon,Ján Krupčík,Abiud E. Portillo,Pavel Májek,Ivan Špánik,Daniel W. Armstrong
Licensed Content Date	Sep 13, 2021
Licensed Content Volume	1653
Licensed Content Issue	n/a
Licensed Content Pages	1
Start Page	462381
End Page	
Type of Use	reuse in a thesis/dissertation
Portion	full article
Circulation	30
Format	both print and electronic
Are you the author of this Elsevier article?	No
Will you be translating?	No
Title	Development of specific and sensitive chiral selective methods for the enantiomeric analysis of n-acyl homoserine lactones in bacterial matrices
Institution name	The University of Texas at Arlington

Expected presentation date	Sep 2022
Order reference number	0821
	The University of Texas at Arlington 700 Planetarium Pl.
Requestor Location	
	ARLINGTON, TX 76019 United States Attn: The University of Texas at Arlington
Publisher Tax ID	98-0397604

SPRINGER NATURE LICENSE
TERMS AND CONDITIONS
Sep 13, 2022

This Agreement between The University of Texas at Arlington -- Abiud Portillo ("You") and Springer Nature ("Springer Nature") consists of your license details and the terms and conditions provided by Springer Nature and Copyright Clearance Center.

License Number	5387180180369
License date	Sep 13, 2022
Licensed Content Publisher	Springer Nature
Licensed Content Publication	Analytical and Bioanalytical Chemistry
Licensed Content Title	Enantiomeric separation of quorum sensing autoinducer homoserine lactones using GC-MS and LC-MS
Licensed Content Author	Elizabeth Readel et al
Licensed Content Date	Mar 20, 2020
Type of Use	Thesis/Dissertation
Requestor type	academic/university or research institute
Format	print and electronic
Portion	full article/chapter
Will you be translating?	no
Circulation/distribution	1 - 29
Author of this Springer Nature content	yes
Title	Development of specific and sensitive chiral selective methods for the enantiomeric analysis of n-acyl homoserine lactones in bacterial matrices
Institution name	The University of Texas at Arlington
Expected presentation date	Sep 2022
Order reference number	0821
Requestor Location	The University of Texas at Arlington 700 Planetarium Pl. ARLINGTON, TX 76019 United States Attn: The University of Texas at Arlington

Biographical Information

Abiud E. Portillo obtained a dual major Bachelor of Science in Biochemistry and Microbiology from the University of Texas at Arlington in Spring of 2015. In Fall of 2017, he joined the chemistry graduate program at the University of Texas at Alrington and joined Professor Daniel W. Armstrong's laboratory that same semester. He obtained his Doctor of Philosophy degree in Analytical Chemistry in the Fall of 2022. Abiud's graduate research centered on the development of comprehensive and highly sensitive chromatographic methods in line to tandem mass spectrometry detection for the analysis of *N*-acyl homoserine lactones. His research focuses were on standard analyte synthesis, extraction reproducibility and recovery, method development and optimization, trace analysis detection and quantitation with a focus on the application of said developed methods to complex biological matrices.